Dexterous Serial Comanipulation for Minimally Invasive Surgery

Ali Hassan Zahraee

UNIVERSITÉ DE PIERRE ET MARIE CURIE - PARIS 6

ÉCOLE DOCTORALE SMAE

T H È S E

pour obtenir le titre de Docteur de l'UPMC en Robotique

Présentée et soutenue par
Ali Hassan Zahraee

Comanipulation Série Dextre pour la Chirurgie Mini Invasive

soutenue le 4 janvier 2012

Jury :

D. MESTRE	-	Professeur à l'Université de la Méditerranée	*Rapporteur*
T. REDARCE	-	Professeur à l'INSA Lyon	*Rapporteur*
J. SZEWCZYK	-	Professeur à l'UPMC	*Directeur*
P. GARDA	-	Professeur à l'UPMC	*Examinateur*
G. MOREL	-	Professeur à l'UPMC	*Examinateur*
J.L. VERCHER	-	Professeur à l'Université de la Méditerranée	*Invité*
B. HERMAN	-	Chercheur à l'Université Catholique de Louvain	*Invité*

Reséumé

Une chirurgie minimalement invasive (CMI), qui implique gnralement une camra endoscopique et des instruments de laparoscopie, peut sembler tre la procdure chirurgicale idale pour ses avantages apparents. Toutefois, en comparaison la chirurgie ouverte, les limites spatiales et outils mcaniques poss sur les chirurgiens sont si levs que, souvent, la CMI est abandonn pour des cas complexes et mme quand elle est possible, la procdure ncessite une grande dextrit, calibre et exprience du chirurgien.

Cette recherche a t motive par la ncessit d'habiles instruments chirurgicaux qui offrent un contrle intuitif et une interface ergonomique, avec l'objectif final de dvelopper un instrument robotis adapt aux interventions par laparoscopie.

La recherche a t base sur l'valuation comparative des diffrentes interfaces, modes de contrle et cinmatiques, en utilisant un simulateur de ralit virtuelle, dveloppe spcialement cet effet. Les rsultats montrent que:

1. l'interface optimale a un mode de contrle WYSIWYD (ce que vous voyez est ce que vous faites) et est exploit par les doigt. 2. les mobilits distales motorises de l'effecteur doivent produire deux degrs de libert (DDL) indpendants pour la flexion et la rotation de l'effecteur. Ce qui est suffisant pour des gestes SIG complexes. 3. ajouter une libre articulation la poigne de linstrument permet au chirurgien d'avoir une posture ergonomique. 4. un trocart actif permettrait la rotation de l'arbre de linstrument avec un joint libre.

Cette recherche a galement permis le dveloppement d'un prototype de validation de concept. Le prototype a t test avec succs, in vitro et in vivo sur un modle porcin.

Abstract

A minimally invasive surgery, which typically involves endoscopic camera and laparoscopic instruments, may seem to be the ideal surgical procedure for its apparent benefits. However, in comparison to open surgeries, the spatial and mechanical tool limitations posed on surgeons are so high that often MIS is foregone for complex cases and even when it is possible, the procedure requires a high dexterity, caliber and experience from the surgeon.

This research was motivated by the need for dexterous surgical instruments that offer an intuitive control and an ergonomic interface, with the final objective of developing a suitable robotic hand-held surgical device for laparoscopic interventions.

The research was based on comparative evaluation of different interfaces, control modes and kinematics, using a virtual reality simulator, developed specially for this purpose. The results show that:

1. The optimal interface has a WYSIWYD (what you see is what you do) control mode and is finger-operated.

2. The optimal distal motorized mobilities of the end-effector produce two independent DOF for flexion and rotation of the end-effector which are sufficient for complex MIS gestures.

3. Adding a free articulation to the instrument's handle allows the surgeon to have an ergonomic posture.

4. An active trocar makes the rotation of the shaft with a free joint possible.

This research also resulted in the development of a proof-of-concept prototype. The prototype was tested successfully, in vitro and in vivo on a porcine model.

Contents

List of Figures

Introduction

0.1 Minimally Invasive Surgery

The recent increase in the practice of laparoscopic surgery and other forms of Minimally Invasive Surgery (MIS)[1] has introduced a new era of surgical treatment which has profound effects on surgical management across various specialties. Although the new approach was initiated by adult general surgeons and gynecologists, there is increasing interest in performing laparoscopic procedures in other specialties, such as pediatric surgery, urology, orthopedic surgery, cardiovascular surgery, neurosurgery and plastic surgery.

Laparoscopy or laparoscopic surgery is the performance of surgical procedures with the assistance of a video camera and several thin and rigid instruments —introduced through the abdominal wall—in the peritoneal cavity after creation of a pneumoperitoneum[2]. A tube like port called trocar is placed in each incision for the instrument to pass through and to maintain the gas pressure inside the abdomen.

Using two manipulating instruments and an endoscopic camera is typical. While an assistant holds the camera, the surgeon holds the instruments and manipulates them watching the intracorporeal image on a screen.

In laparoscopic surgery, established surgical procedures are executed in a way which leads to the reduction of the trauma of access and thereby accelerates the recovery of the patient. Surgical procedures are conducted by remote manipulation and dissection within the closed confines of the abdominal cavity or extra peritoneal space under visual control via endoscopic video cameras and television screens.

0.1.1 History

The idea of MIS is not new; the use of tube and speculum in medicine dates from the earliest days of civilization in Mesopotamia and ancient Greece.

[1] Other names such as Minimal Access Surgery or keyhole surgery are also common in the literature. Laparoscopic Surgery is a branch of Minimally Invasive Surgery, dealing with operations in the peritoneal cavity. In this thesis, both MIS or laparoscopy are used to refer to Laparoscopic Surgery unless otherwise specified.

[2] Inflation of the peritoneal cavity with gas.

Modern endoscopy started in 1 805, when Bozzini, an obstetrician from Frankfurt, using candlelight through a tube attempted to examine urethra and vagina in patients. Laparoscopic techniques continued to develop until the introduction of fiber optic light, and the development of the rod lens system by the British physicist Hopkins in 1952, led to dramatic worldwide increase in the use of telescopes in general and laparoscopes in particular.

The origin of modern laparoscopic surgery is derived from the Kiel School in Germany headed by Semm, a gynecologist. This center developed and refined many instruments and established most laparoscopic gynecological procedures currently in practice. Semm and his group described the technique of a laparoscopic appendicectomy without recourse to minilaparotomy in 1983.

The latest highly significant advance was the introduction of the computer chip video camera in 1986 which ignited the development of today's laparoscopic surgery. The first published report of the current multi puncture cholecystectomy was in Paris, France in 1989. Since then, the practice of laparoscopic surgical procedures has mushroomed across the various specialties. There can be little doubt that many aspects of the current technology and instrumentation can and will be improved in the near future, thereby increasing the ease of performance and scope of this type of MIS [Najmaldin 1998].

0.1.2 Advantages of Laparoscopy

In addition to avoiding large, painful access wounds of conventional surgery, laparoscopy allows the operation to be carried out with minimal parietal trauma, avoiding exposure, cooling, desiccation, handling, and forced retraction of abdominal tissues and organs. Thus the overall traumatic assault on the patient is reduced drastically, and as a result of this:

- Postoperative wound complications such as infection and dehiscence are reduced and recovery is accelerated.
- Abdominal adhesion formation, which may become the source of recurrent pain, intestinal obstruction and female infertility, is reduced.
- Surgically induced immunosuppression, which may have important implications particularly in cancer surgery, is decreased.
- Postoperative chest complications are reduced.
- Cosmetic results are greatly improved.

- The greatly reduced contact with patient's blood and body fluid has important implications for both patient and surgeon in relation to the transmission of viral diseases [Schneider 2003].

- Reduced blood loss [Ravi 2004]

0.2 Surgeon-Related Difficulties of MIS

The introduction of endoscopes and accompanying tools has brought about increased technical complexity for the surgeon, making procedures that were simple as open procedures, difficult as laparoscopic procedures, and making procedures that were complex as open procedures, unapproachable as laparoscopic procedures. Complexity in laparoscopic procedures using endoscopes originates in four sources [Najmaldin 1998]:

i. introduction of the endoscope forces the surgeon to work looking at a video instead of working looking at his own hands, breaking the surgeon's hand-eye coordination (see Fig. 1).

Figure 1: Standard setup in laparoscopic surgery

ii. the tools used for manipulating tissue inside the body work through ports at the body's wall. A port acts as pivot, making the direction of the tool tip motion reversed from that of the tool's handle in side to side

movements (fulcrum effect), making hand-eye coordination even more difficult for the surgeon (Fig. 2).

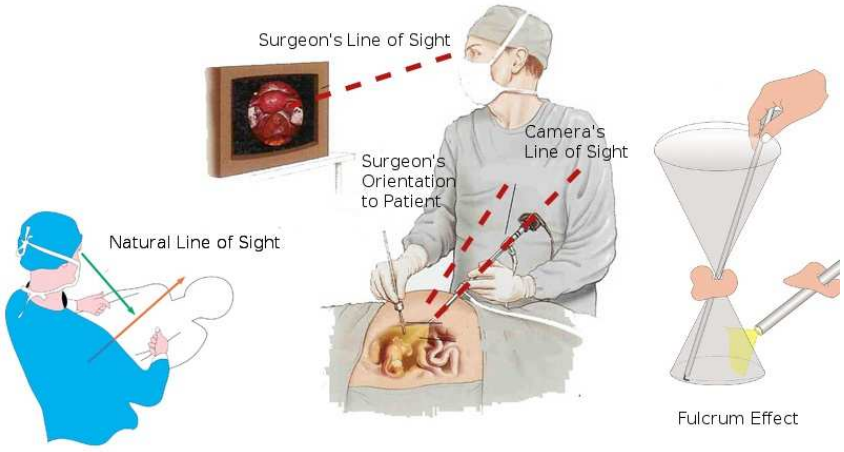

Figure 2: Indirect vision and fulcrum effect in laparoscopy [Lai 2000]

iii. the port at the body wall constraints the motion of the tools in two directions, so that the tip of the tool has fewer DOF, typically reduced from the six DOF of unconstrained position and orientation to four DOF [Buess 1989] (Fig. 3):

   1. translation along the instrument's shaft. The instrument can be inserted in the abdominal cavity or taken out from it.
   2. rotation around the translational axis. This is done either by rotating the hand or by rotating an axial knob on the shaft using the index finger.
   3. limited inclination of the shaft pivoted through the incision in two directions [Lai 2000]. The surgeon can incline the instrument in his frontal or sagittal plane, although the motion is limited by the abdominal wall.

iv. Conventional endoscopes use two-dimensional vision, removing some depth cues of normal binocular vision. Some stereoscopic endoscopes exist, but their performance has been limited in resolution and contrast, both in the endoscope itself and in the display technology.

Due to these difficulties, laparoscopic procedures require more technical expertise and take longer, at least initially, than open procedures.

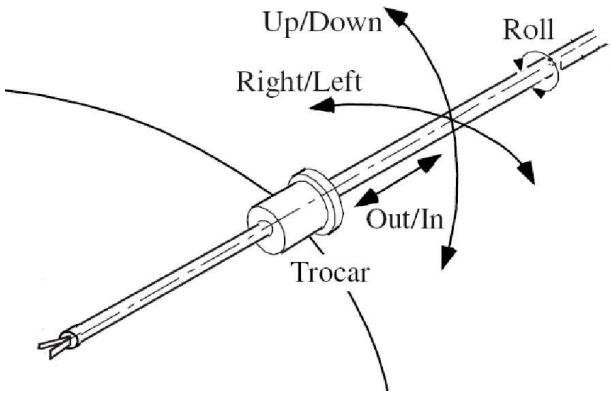

Figure 3: Conventional laparoscopic instruments and its 4 DOF [Jinno 2002]

0.3 Solutions Provided by Comanipulation and Robotics

Comanipulation and robotics can provide solutions for at least some of the problems presented in the previous section. Robotic systems that have multi DOF instruments have been reported as alternatives to conventional ones and new applications that are feasible only with robotic devices have been reported [Hashizume 2002, Hubens 2003, Ballantyne 2004]. These devices have intracorporeal DOF that are actuated with electrical actuators and controlled by the surgeon. The added number of DOF allows the surgeon to perform complex gestures in a limited workspace.

Based on the relation between the human and the robotic system, we are going to study these systems under two categories:

1. teleoperators
2. comanipulators

Telemanipulation is the manipulation of objects from distance using a master-slave system. In telesurgery, the master console, installed away from the patient, controls robotic slave arms, which are installed around the patient and carry out the task. The master console offers a comfortable workspace and intuitive control to the surgeons that is not available in conventional laparoscopy (see Fig. 4). The multi DOF manipulators have dexterous instruments to perform the task.

Teleoperation systems offer an unprecedented gesture quality to the surgeon. The mapping between the movements of the hand and those of the

instrument is not constrained in teleoperation and can be chosen arbitrarily. This mapping is adapted to the position and the orientation of the endoscope, in a way to restore the intuitive hand-eye coordination for the surgeon and eliminate the fulcrum effect from the surgeon's point of view.

The instruments can have additional DOF without bringing in the problem of controlling them, as they can be controlled in the Cartesian space intuitively.

Figure 4: Telesurgery with the da Vinci®Surgical System

Despite the advantages that teleoperation systems offer, they have their own shortcomings. These systems lack force feedback, an important source of information for surgeons during laparoscopy. Contact forces have to be estimated mostly by visual observation of tissue deformation and color change.

The distance between the surgeon and the patient in telesurgery that prevents direct contact can also be a problem. Most of the information that the surgeon gathers from the proximity of the patient is lost in telesurgery.

Security risks also arise from the distance. In telesurgery, the surgeon works on a non sterilized console and can not change the intervention to an open surgery immediately in case it is needed. This could be dangerous for the patient in case of an unpredicted or sudden hemorrhage.

Telesurgery systems also have other disadvantages:

- Bulky telesurgery systems take a lot of the space available in the operation room (OR).

- Long set up time to install the robotic arms over the operating bed and cover them with sterile plastic covers.
- Robotic arms limit access by the anesthetist to the patient.
- An assistant surgeon is needed by the operating table to change the end effectors.
- High operating and maintenance costs

0.4 Comanipulation

Comanipulation is defined as the cooperative manipulation of an object by a human and a robot manipulator. In parallel comanipulation, the link between the robot and the human arm is usually the end effector. One could say that the robot and the human arm make a parallel manipulator together. As a result, the force applied by the end effector is the sum of the forces applied by the human arm and the robot. A cobot is the term commonly used to refer to a robot used in parallel comanipulation.

Parallel comanipulation has been used in MIS to guide the surgeon in his motions. The guidance system can constrain or modify the surgeon's motions in useful ways. Though constrained by the guidance system, the surgeon could directly control tool motion, orientation, and force (see Fig. 5).

The end effector of a parallel comanipulation system keeps its original manual DOF and does not include additional robotic DOF. So parallel comanipulation would not solve the problem of dexterity in laparoscopy.

Most of the other instruments used in laparoscopy fall into the category of serial comanipulators. In serial comanipulation, the human user holds the manipulator by its handle, which acts as a middle link between the robot and the human hand so that the instrument is an extension of the arm. One could say that the robot and the arm make a serial manipulator together. As a result, the movement of the end effector is the sum of the movements of the human arm and the robot (see Fig. 6). A hand-held instrument is the term commonly used to refer to a serial comanipulator.

Robotic hand-held instruments for laparoscopy have been the subject of many research works during the last decades. The research is based on the fact that adding more DOF to the conventional instrument will make it more dexterous, while avoiding the different problems that telemanipulation causes, particularly the distance between the surgeon and the patient and the loss

Figure 5: Acrobot®, a Parallel Comanipulation System for Orthopedic Surgery

of haptic feedback. A number of hand-held surgical instruments have been developed with a multi DOF at the end of the instrument controlled either manually or electronically. A few manual instruments, such as RealHand HD (high dexterity) and Autonomy Laparo-Angle, have been commercialized and used in several surgeries.

0.5 Challenges Facing Serial Comanipulation for Laparoscopy

Many hand-held instruments have already been developed for laparoscopy. But they have different problems preventing them from being used effectively, regularly, or at all in the OR, and the next generation of hand-held instruments faces several challenges:

1. Controlling the end effector: the problem of choosing a precise and intuitive handle and control mode.

   Due to the fulcrum effect, the indirect vision and the two dimensional presentation of the scene in laparoscopy, the coordination between the visual perception of the scene and the movements of the hand becomes a complex task, to the point that the most basic task of moving the

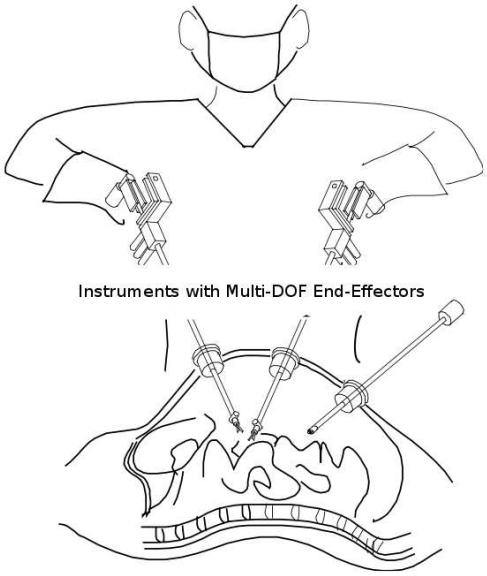

Figure 6: Serial comanipulation with a multi DOF surgical instrument [Jinno 2008]

instrument on a straight line between two desired points becomes difficult. For a hand-held instrument with an articulated end effector, the tasks of positioning and orienting challenge the brain even more, as the number of degrees of freedom (DOF) to control has increased. In this case, the choice of the human machine interface of the instrument and its control mode has a direct effect on the complexity of the hand-eye coordination task.

2. Dexterity: the problem of choosing the suitable kinematics for a dexterous instrument.

   Conventional instruments used in laparoscopy have four DOF and their movements are considerably limited. The result is that some tasks are very difficult to perform and some can not be done at all. An example is sagittal suturing, a difficult yet important task in many laparoscopic interventions. A serial comanipulation system with additional DOF is more dexterous than the conventional four DOF laparoscopic instrument. But the question is how many additional DOF are needed and how they are supposed to be arranged.

3. Ergonomics: the problem of making the instrument as comfortable and ergonomic as possible for the surgeon.

Several studies have shown that laparoscopy puts much more stress on the surgeons' back, neck and arm muscles compared to open surgery. This extra stress is related to the static posture of the surgeon during operation and the non-ergonomic nature of the instrument's handle. Existing hand-held instruments have failed to address this problem so far; yet an effective solution to this problem is necessary.

4. Technology: the problem of realizing an intuitive, precise, dexterous and ergonomic instrument usable by a surgeon.

   Although serial comanipulation can help solve the problems mentioned above, attempts at making dexterous hand-held instruments for laparoscopy have been limited to research labs and except for a few manual instruments, none of them has been commercialized; For the simple reason that these instruments are not usable by the surgeons in the OR. They may be dexterous or intuitive, but they are also too heavy, too long or not sterilizable.

0.6 Thesis Outline

This research starts by conducting a global study of the above aspects of serial comanipulation in laparoscopy to compare and evaluate different solutions. This study led to the selection of an easy to use handle with an intuitive control mode, a dexterous kinematics and an ergonomic handle configuration. This was followed by the development of a robotic instrument, designed and realized considering the three different aspects—control, dexterity, ergonomics—of a suitable instrument for laparoscopy.

In the following chapters, different steps of this global study are explained and the results are presented. In Chapter 1, state of the art manipulator instruments for laparoscopy are reviewed. Some of these instruments are developed in research labs and some others have reached the commercial stage and have been used in several surgeries. None of them however provides an integrated solution to different problems of laparoscopy.

Chapter 2 presents the structure and development of a Virtual Reality Simulator that will be the major study tool throughout this research. Because most of our conclusions are based on the test results of this simulator, the literature on the Virtual Reality Simulator and their effectiveness in evaluating different solutions is first reviewed to establish the basis of this work.

Chapter 3 discusses the problem of control of a hand-held instrument. We did not aim to study the influence of handle design or the place and form of its

controlling elements on the user's performance, as this was beyond the scope of this work. Rather, we wanted to choose between two types of handle: an articulated one and a finger-operated one by comparing them on our Virtual Reality Simulator.

In Chapter 4, the problem of dexterity of the instrument is studied. It is accepted that adding a multi-DOF wrist to the end effector of the instrument helps surgeons do more complex gestures, but the suitable end effector kinematics is still debated. Using the Virtual Reality Simulator, 3 different kinematics were compared to choose the one with the best performance results in frontal and sagittal suturing.

Chapter 5 discusses the ergonomics of a hand-held instrument. The Virtual Reality Simulator was used to evaluate a new solution to the problem of ergonomics and compare it with conventional solutions. These solutions were not only evaluated from the ergonomics point of view, but also from the performance point of view. The results show that the new solution outperforms other existing solutions in terms of ergonomics.

Chapter 6 presents the mechatronic design of an instrument prototype for laparoscopy. This prototype integrates the solutions provided in the three previous chapters as a proof of concept. Besides, the concept of active trocar, a new approach to the development of a robotic hand-held instrument, is introduced and validated.

Chapter 1

State of the Art Instruments for MIS

The shortcomings of telesurgery systems, particularly the loss of real haptic feedback and the distance between the surgeon and the patient, have prevented widespread use of telesurgery for various minimal access surgical procedures and despite their inconveniences, conventional hand-held instruments are still widely used in laparoscopy.

Serial comanipulation can provide dexterity for the surgeon while maintaining the proximity with the patient and preserving the direct contact and haptic feedback. Conventional hand-held instruments for laparoscopy have four DOF and a limited workspace. Adding a wrist to the instrument's end effector adds to its number of DOF, thus making it more dexterous. Dexterous hand-held instruments have been a subject of research for the past decade. A few manual articulated instruments have found their way to the markets in the recent years. But mechatronic hand-held instruments with additional DOF are still in the research stage.

The hand-held surgical tools that we consider are enhanced tools endowed with a certain degree of embedded intelligence and autonomy. They are generally driven by the surgeon's hand but they can support the surgeon during his/her procedures by correcting his/her actions, by amplifying or attenuating his/her interaction within the intervention area, and by bringing the surgeon dexterity and ability to take decisions *on the tip* of the device [Dario 2003].

In this chapter the state of the art hand-held dexterous instruments for laparoscopy and their advantages and shortcomings are presented. In particular, the following points are discussed for different instruments:

- human machine interface (HMI) and its ergonomics
- control models
- actuation systems
- force transmission system

- intracorporeal kinematics and their realization
- end effector design
- controller unit implementation
- usability

1.1 Manual Instruments

Manual instruments are manipulator instruments with passive mechanisms, i.e. all the DOF are actuated and controlled by hand, without using any electrical/pneumatic actuator.

An instrument of this type has an articulated handle, rotating knobs, triggers or similar mechanical controlling elements mounted on the handle or the shaft of the instrument, and a mechanical transmission system that transmits the motions of those controlling elements to the intracorporeal DOF of the instrument through cables or rods that pass through the shaft.

In general, the instrument conserves its four original DOF and with the additional DOF of a wrist added to the end effector, becomes more dexterous (Fig. 1.1).

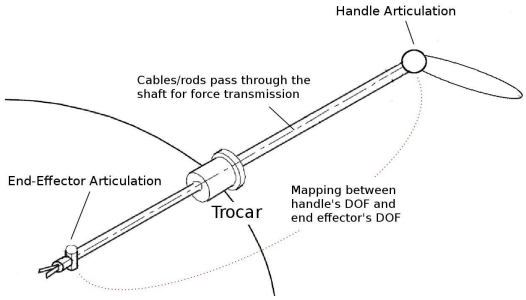

Figure 1.1: Sketch of a manual instrument with active articulated handle

These instruments are characterized by a clever mechanical design that transmits the motions of the instrument's handle to actuate the end effector (Fig. 1.2) and there is usually a 1:1 relation between the handle's articulation and the end effector's articulation. The force transmission has to have zero backlash or it would be difficult to perform precise manipulation. This is difficult to acheive in a cable transmission system due to the cables' flexibility.

Ease of use in these instruments is compromised, because the handle as the controlling part is constrained by the force transmission system. The user's hand has to provide enough force/torque for the actuation of the end effector, which makes the instrument's interface non-ergonomic.

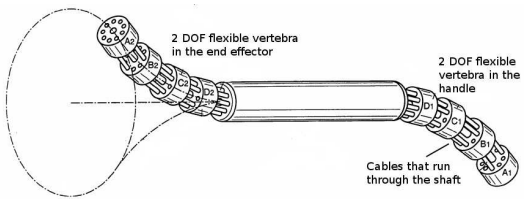

Figure 1.2: The manual transmission system in RealHand®lets a 2 DOF end effector be actuated by a 2 DOF articulated handle [Hinman 2007]

On the other hand, these instruments are easier to develop, not bulky and easy to put in place and have reached the commercial stage much quicker than their mechatronic counterparts. Most of them however, follow the general design rules used in conventional instruments, and while enhancing the dexterity of the surgeon, contribute little to the ergonomics of the instrument. The essential differences between them lie in their choice of kinematics for their intracorporeal wrist, and the form of controlling elements on the handle.

The development of manual instruments with articulated end effectors has contributed to the rapid development of Single Port Laparoscopy (SPL)[1] and Natural Orifice Transluminal Endoscopic Surgery (NOTES). Single-port surgery is surgery that is literally performed through a single incision in navel (Fig. 1.3). NOTES is an experimental surgical technique whereby *scarless* abdominal operations can be performed with an endoscope and instrument(s) passed through a natural orifice (mouth, urethra, anus, etc.) then through an internal incision in the stomach, vagina, bladder or colon, thus avoiding any external incisions or scars [Baron 2007]. The goal is to reduce post operative pain and recovery time as much as possible, and improve cosmetic results for the patient.

NOTES and SPL use similar techniques for tissue dissection and retraction with multiple instruments entering via the same port, and both must overcome problems such as in-line vision and loss of triangulation [Rao 2004]. The loss of triangulation is particularly problematic, and effectively prevents use of conventional instruments in this type of surgery. Instruments with additional DOF make it possible to operate through a single access port by crossing the two instruments and bending the end effectors inside the body.

[1] Also called Single Incision Laparoscopic Surgery (SILS)

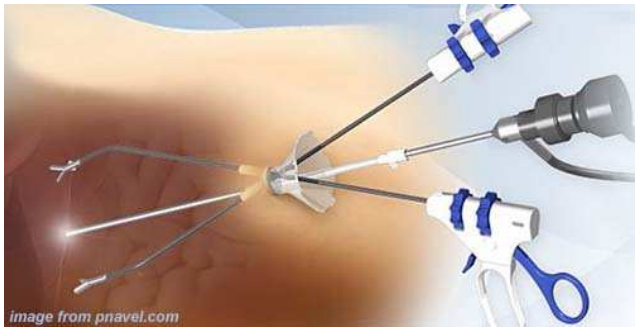

Figure 1.3: Single port laparoscopic surgery with prebent conventional instruments [Website 2007]

Fig. 1.4a shows the Deflectable Endoscopic Instruments System (DENIS) [Melzer 1997], one of the first six DOF manual instruments used in vivo. It provides variable deflection of end effector between 0° and 120° and 360° axial rotation of its jaws, controlled via two wheels in the axial handle. This instrument was used in laparoscopic cholecystectomy, appendectomy, hernia repair, and thoracic procedures. It is sterilizable to meet the required hygienic standards.

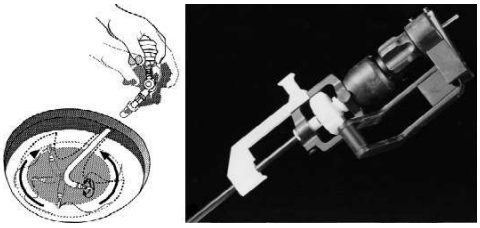

(a) Deflectable Endoscopic Instruments System (DENIS) [Melzer 1997]

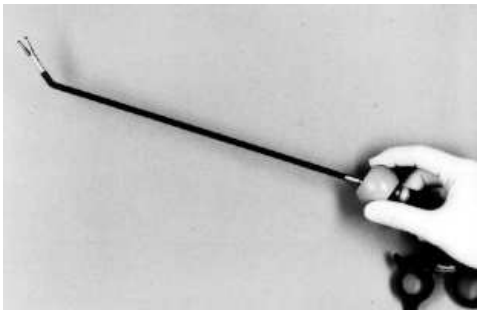

(b) 6 DOF instrument of Gossot et al. [Gossot 2001]

Figure 1.4:

In [Gossot 2001] an instrument is presented in which the knob that controls the roll angle in conventional tools is replaced by a hinged ring that can be used to steer two DOF of tip deflection (see Fig. 1.4b). However, precise manipulation of the ring needs two or three fingers and it is not possible for the surgeon to simultaneously open/close the grasper.

In [Tuijthof 2003] an arthroscopic cutter with an ergonomic handle is presented in which the end effactor can be steered sideways by a lever under the

thumb/index finger. The same lever is used for opening/closing the cutter (see Fig. 1.5a). The instrument is used in arthroscopic procedures were only sideway punches are needed.

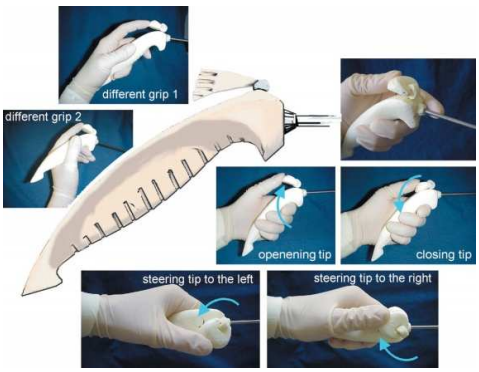

(a) 6 DOF cutter of Tuijthof et al. [Tuijthof 2003]

(b) Intuitool compared to a conventional instrument

Figure 1.5:

Fig. 1.5b shows Intuitool [Hallbeck 2005], a manual instrument with an articulated grasper designed for enhanced ergonomics and intuitiveness. the end effector can pitch/yaw, and is controlled by a sphere located on the handle. The control sphere can be moved by one or more of the surgeon's fingers to indicate direction. A preliminary study was done to determine the way the movements of the sphere should be coupled to those of the end effector [Doné 2003]. Another comparative study is done for ergonomic design of the handle [DiMartino 2004]. It is not clear however, if the end effector controlled in this way, will provide enough forces for laparoscopic manipulation.

One of the first manual instruments with additional DOF to hit the markets was RealHand^{TM}HD (High Dexterity) [Hinman 2007] from Novare Surgical (Fig. 1.6a). The wrist in RealHand instruments can yaw and pitch, thus offering complete six degrees of freedom of movement.

Its handle is articulated as well to control the end effector's additional DOF, and it has been designed to mirror the surgeon's hand direction, i.e. bending the handle makes the end effector bend in the same direction. The articulation between the handle and the shaft is a universal joint, so that rotating the handle makes the instrument's shaft rotate. It is possible to lock the end effector in the desired angle for increased precision.

Its intracorporeal bending structure called EndoLink®, is a stack of several circular disks and spheres on top of each other driven by a set of cables cables and making a vertebra.

Fig. 1.6b shows the typical configuration in SPL with 2 RealHand instruments. In May of 2007, Novare announced the first-ever Single Incision Laparoscopic cholecystectomy [Reuters 2007]. A total of 34 different types of single port procedures were performed later that year[Website 2007].

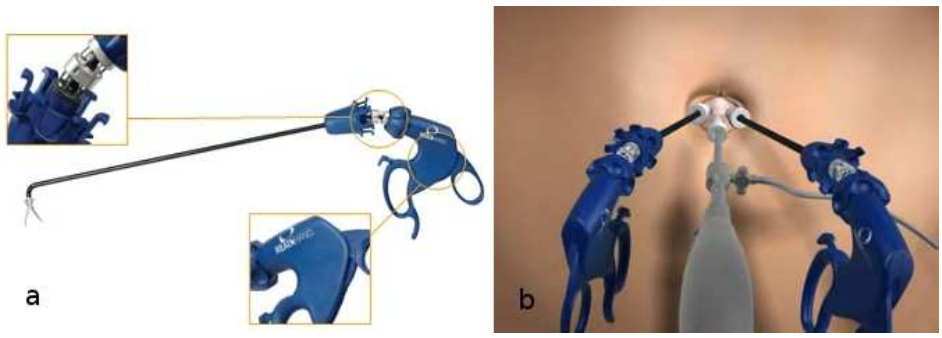

Figure 1.6: (a) RealHand HD instrument (b) 2 RealHand instruments in a single port surgery [Website 2007]

RealHand instruments have also been used in a number of transvaginal NOTES procedures. [Horgan 2009] for example, reports 9 transvaginal cholecystectomies, 1 transgastric appendectomy, and 1 transvaginal appendectomy.

Hand-held Autonomy Laparo-Angle^{TM}instruments from Cambridge Endo [Lee 2009] have been deigned similar to RealHand to map, in 1:1 proportion, the motion of the surgeon's hand holding the instrument. Autonomy Laparo-Angle (1.7a) has an articulated wrist and an articulated handle. But its end effector has one more DOF compared to RealHand: the distal tip can turn 360° at any angle using an axial rotation knob in the handle. The handle has a new, more ergonomic design. The force transmission mechanism for deflecting the end effector is similar to the vertebra structure used in RealHand. The distal rotation of the end effector is also cable driven and the problem of rigidity persists despite its angle locking mechanism.

[Wong 2010] reported the first SPL nephrectomy in a child in 2010 and [Raybourn 2010] reported a series of SPL nephrectomy in 11 patients all using Autonomy Laparo-Angle instruments.

Radius^{TM}[Schwarz 2005] is a needle holder/grasper made by Tuebingen Scientific, Tuebingen, Germany (1.7b). Its end effector has a two DOF wrist that can yaw and rotate. The handle is designed like a lever and its up/down movements correspond to the distal tip's up/down movements. A knob at the end of this lever is turned between the index and the thumb to rotate the distal tip, thus allowing for flexibility of movement sequences. Radius uses a

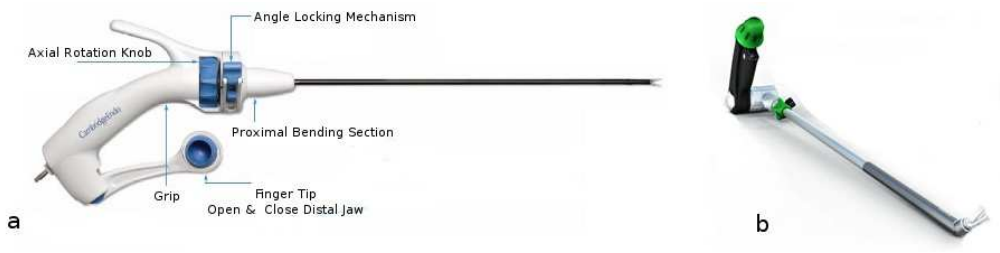

Figure 1.7: (a) Anatomy Laparo-Angle instrument®(b) Radius®surgical instrument

combination of rigid links and gears in its transmission mechanism (Fig. 1.2) and effectively solves the problem of rigidity. A new generation of this device, has a 5 mm shaft.

[Torres Bermudez 2009] demonstrated the feasibility of laparoscopic colorectal anastomosis using Radius in phantom model. Anastomosis with Radius was shown to be safer than with conventional instruments and the quality of the suture was superior with it, with a larger anastomosis diameter, higher bursting pressure, and fewer suturing failures being found. The Radius suture withstood a higher traction force and the participants showed more discomfort with conventional instruments.

Roticulator^{TM}[Marczyk 2008] from Covidien, Dublin, Ireland is a 5 mm instrument with a deflectable and turning distal tip capable of 0° to 80° deflection at the distal end and position lock that allows the articulating tip to lock in a specific position and function as a rigid instrument. The distal tip is bent by turning an axial knob on the shaft where there is usually a knob for turning the shaft in other instruments. As a result, it is not possible to change the distal tip's deflection during a gesture. This makes this instrument mostly suitable for use like a prebent instrument in SPL (Fig. 1.8).

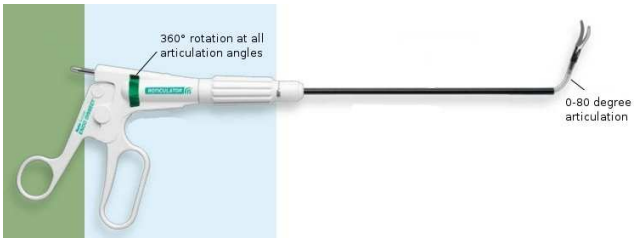

Figure 1.8: Roticulator®from Covidien Inc.

1.1.1 Reflections on Manual Instruments

Dexterous manual instruments are essentially used in single port laparoscopy where conventional instruments are unusable. The fact that two instruments passing through one port are crossed to make space for them, makes the additional DOF of the instrument crucial, without which manipulation would be impossible. However, the number of single port laparoscopies is a small fraction of the number of conventional triport laparoscopies.

Besides, the benefits of SPL are debated and and many surgeons are still skeptical about the trade off between its benefits (only one hidden scar in the umbilical) and its harms (bigger incision increases postoperative hernia and pain). Although initial studies suggest that SPL is a feasible surgical alternative to conventional laparoscopy with an equivalent level of safety and that SPL results in better cosmetic outcomes than conventional laparoscopy, data from larger research studies are necessary to confirm these findings and confirm the benefits of SPL over conventional laparoscopy [Cho 2010]. Even the existing promising results are challenged by another study that suggests the technical complexity of SPL naturally results in a steep learning curve and increased operating room time [Shussman 2010].

On the other hand, Stolzenburg et al. [Stolzenburg 2010] questions the advantages of using dexterous manual instruments, even in SPL. In theire study, they compared RealHand instruments with prebent and conventional instruments in a series of predetermined tasks in dry laboratory and also in twenty four nephrectomies and concludes that prebent instruments had a significant advantage over dexterous manual instruments in terms of time requirement to accomplish tasks and procedures as well as maneuverability.

Finally, manual instruments demand large forces and uncomfortable hand poses for driving the wires/links of the force transmission system to generate similar forces on the tip of the forceps (bending and grasping forces). This causes extra muscular pain for users even after short periods of time.

1.2 Robotic Instruments

Although hand-held tools with robotic functions are not yet clinically used, several teams have developed instrument prototypes aimed at improving different aspects of laparoscopy for surgeons. The work on these instruments is limited to research labs for the time being, but their appearance on the market is imminent.

Aside from the usual handle-shaft-end effector configuration, which is the characteristic configuration of a serial comanipulator for laparoscopy, a robotic hand-held instrument has also electrical/pneumatic actuators and an electronic controller to translate surgeon's commands to end effector motion. The surgeon manipulates the handle to send electronic control signals to the electronic controller which also receives the feedback from the actuators. Based on these inputs and the chosen control scheme which maps the inputs to the end effector's DOF, the electronic controller sends control signals to the actuators to make the end effector move. Fig. 1.9 shows a general schema of how a robotic hand-held instrument works.

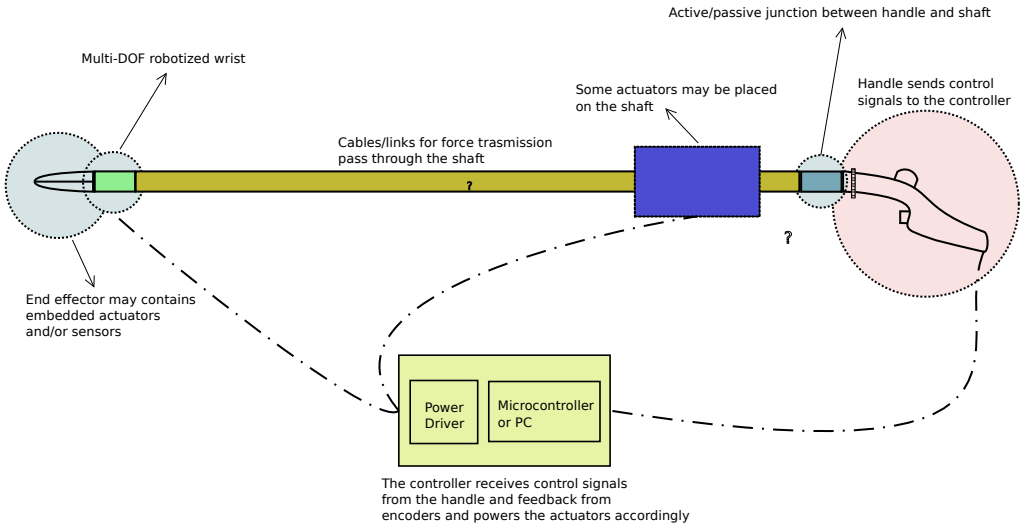

Figure 1.9: General schema of a robotic instrument's operation

Robotic/mechatronic instruments have several advantages compared to manual instruments:

1. The electric force generation system frees the surgeon's hand from actuating the instrument's additional DOF and generation of necessary forces for tissue manipulation, thus allowing precise and comfortable gestures. It is even possible to decouple the position/orientation of the hand from that of the end effector to improve the ergonomics of the instrument. This will be discusse in Chapter 5.

2. Preserving the orientation of the end effector is automatic assuming the transmission is irreversible because of a great reduction ratio between the electric motors and the joints.

3. Feedback control makes precise control of the end effector possible.

4. The end effector can be controlled in the Cartesian space making semiautomatic gestures possible, provided that enough robotic DOF are available.

The first mechatronic hand-held manipulators for MIS were endoscopic cameras and catheters that allow the surgeon to inspect restricted areas inside the body. An application where this feature is of particular interest is the field of arthroscopy, because it reduces the risk that delicate structures, such as cartilage and ligaments, are damaged during intervention.

Dario et al. [Dario 2000] present a prototype of a new mechatronic endoscope, integrated in a system for computer-assisted arthroscopy. Fig. 1.10a shows an enhanced version of the endoscope described in [D'Attanasio 2002]. The tool has a cable-actuated steerable tip and incorporates sensors for the detection of the tip position and of tip contact with the surrounding tissues. Moreover, the tool gives the surgeon the option of servo controlling the steering mechanism. The main feature of the mechatronic endoscope consists of a semiautomatic collision avoidance mechanism aimed at preventing contact between the tip and some anatomical regions that have been selected preoperative [Dario 2003].

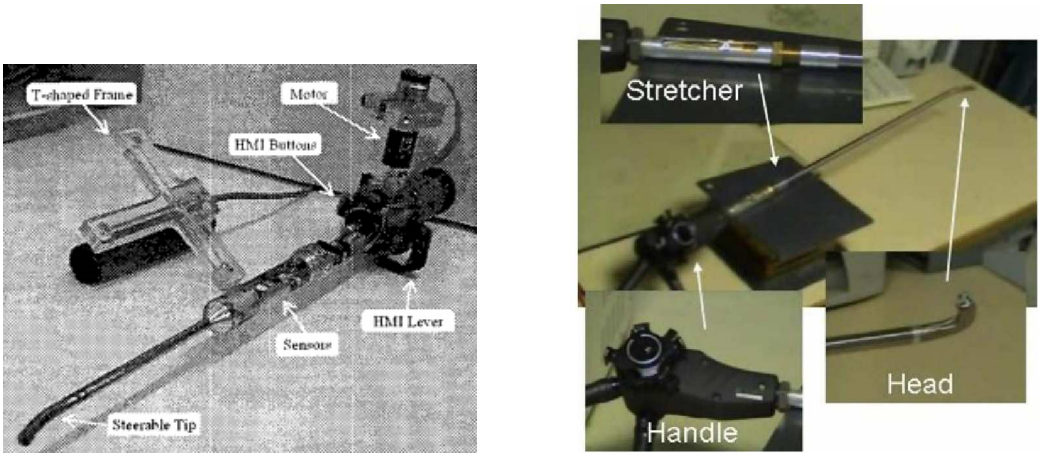

(a) The Mechatronic endoscope of D'Attanasio et al. [D'Attanasio 2002]

(b) De Sars' Active Catheter [De Sars 2010]

Figure 1.10:

[De Sars 2010] describes the structural design and dimensioning of a 2 DOF active endoscope actuated by four antagonist shape memory alloy (SMA) wires (Fig. 1.10b). This device is composed of an articulated head (made by Fort Imaging Systems Company), a 32 cm long tubular body containing the SMA wires, a stretcher for the preloading of the SMA wires and a handle.

The maximal bending angle is about 80° in all directions and the minimal curvature radius is less than 20 mm.

[Nakamura 2000] presents a multi DOF forceps manipulator with two additional DOF of bending on the tip of forceps developed at the University of Tokyo (Fig. 1.11a). The handle has a joy-stick for bending DOF and two buttons for grasping DOF. The bending mechanism is composed of four coupled stainless steel rings (Fig. 1.11b). This mechanism is driven by four stainless steel wires, connected to an actuation system and control unit placed in the non-sterilized area. The ranges of bending motion are 0° to ±90° degrees for each DOF.

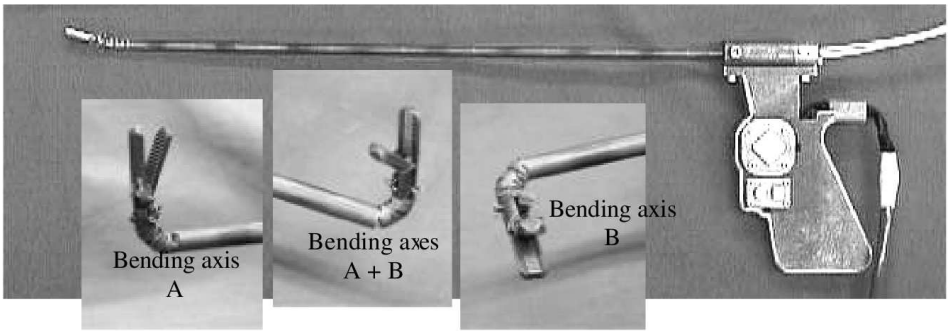

(a) General view and intracorporeal DOF

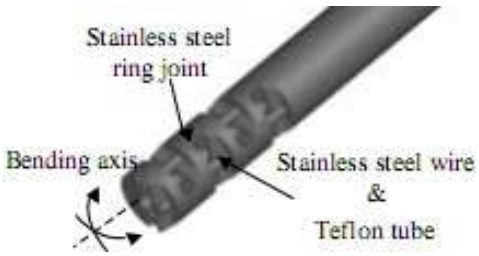

(b) Its bending mechanism

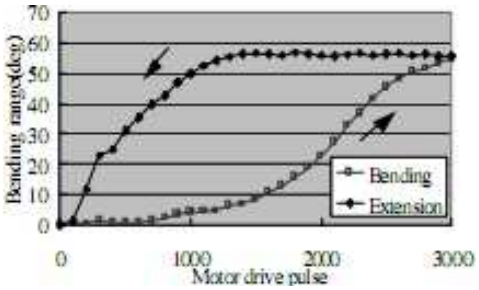

(c) Hysteresis loop in end effector movements

Figure 1.11: The mechatronic instrument of the University of Tokyo [Nakamura 2000]

The motors, which cannot be sterilized, are placed sufficiently far from the surgical field for maintenance of sterility, and stainless steel wires transmit the forces produced by the motors. Since there are no electronic components (motors, sensors, etc.) on the tip of the forceps manipulator, the manipulator is perfectly sterilizable. The prototype is 455 mm long and has a 6 mm diameter. Analysis of bending movements shows a hysteresis loop, with large backlash due to the stretching and friction of the wires (Fig. 1.11c).

This instrument is one of the most complete existing prototypes. But its problems, notabely its small unbending and grasping forces (0.5 and 8.5 N respectively), nonlinear response of movement and unacceptable bulk, and non-ergonomic handle make it an undesirable choice for surgeons.

[Nakamura 2001] presents a newer version of this instrument with a miniaturized mechanism and a new HMI (Fig. 1.12). The instrument's dimensions are reduced compared to the previous version: 5 mm diameter instead of 6 with a total length of 345 mm and a weight of 350 gr. In the new interface the index finger is put in a 2 DOF ring while holding the instrument to control the two bending DOF of the end effector.

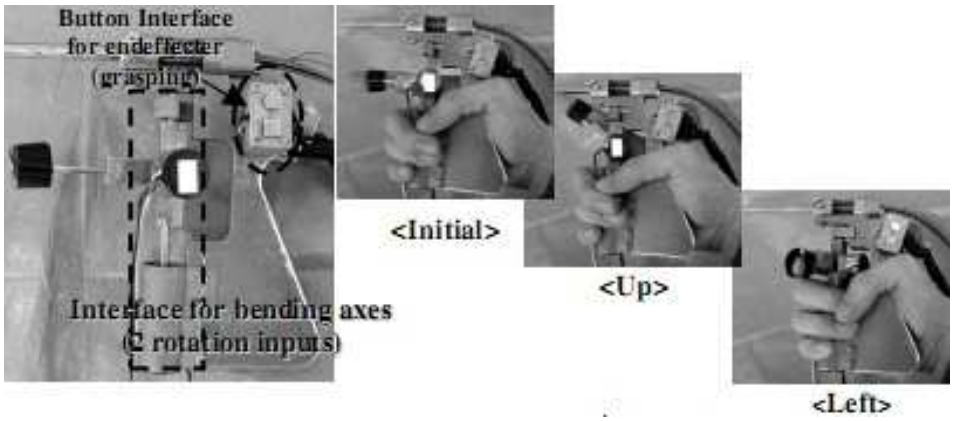

Figure 1.12: The HMI of Nakamura et al. [Nakamura 2001]

Fig. 1.13 shows a new multi-slider mechanism for the 2 DOF bending wrist [Yamashita 2003] and a new instrument prototype using this mechanism developed by the same group. [Yamashita 2004, Suzuki 2005]. Each of the bending axes generates at least 0.40 KgF and the grasper provides up to 0.83 KgF. But the two bending axes are not concurrent and the radius of curvature of bending has increased.

The instrument was successfully used to perform a complete cholecystectomy on a porcine model. But the authors confirm that additional DOF such as rotation and deflection are necessary for more effective, and precise operation.

Another instrument has been under development at Toshiba Medical Systems in collaboration with Keio University, School of Medicine. The first instrument prototype is presented in [Jinno 2002]. The instrument has a grasper with a 2 DOF wrist with roll ($\pm 90°$) and yaw axes ($\pm 90°$). These axes are cable-driven by DC servomotors mounted near the handle (Fig. 1.14). The

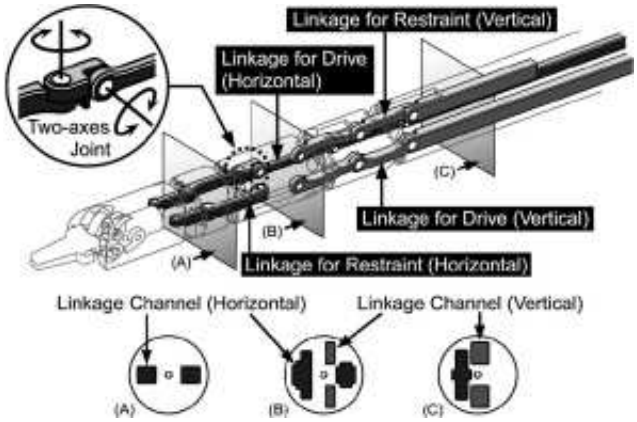

(a) The multi-slider bending mechanism of the instrument of Yamashita et al.

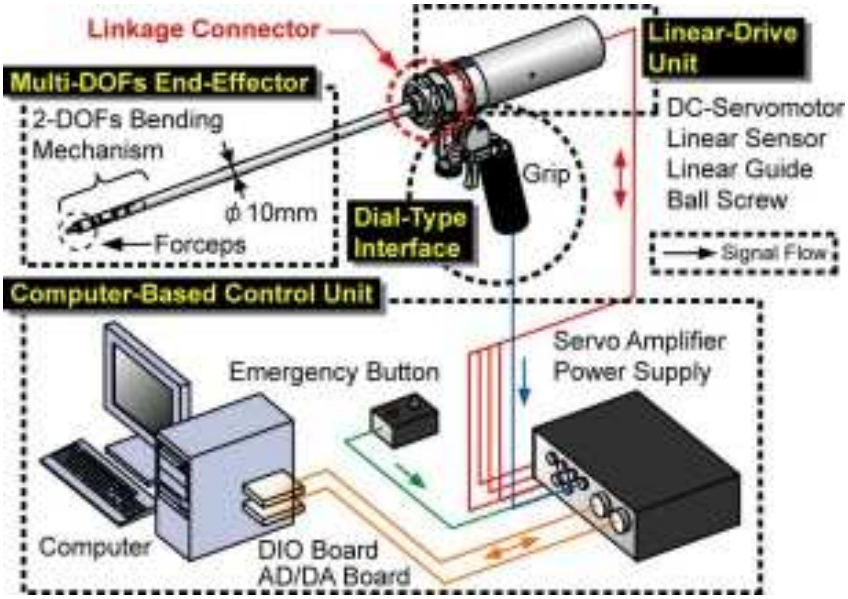

(b) A mechatronic instrument prototype using this mechanism

Figure 1.13: The mechatronic instrument of Yamashita et al. [Yamashita 2003]

grasper's open/close motion is controlled by a pinching mechanism between two fingers. The handle has yaw and roll axes and a gripper in the same order as the end effector. The three axes of the handle which are roll (the instrument's shaft), yaw and roll axes intersect at one point. The handle and the motor unit are to be separated from the body for sterilization.

Figure 1.14: The instrument made by Toshiba Medical Systems [Jinno 2002]

Each joint angle of the handle is detected using a potentiometer and the end effector is controlled to follow the joint angles by the encoders mounted on the servomotors. A notebook computer with an interface unit is used for the controller. However, the manipulator is 700 mm long, weighs 0.6 Kg and has a diameter of 12 mm making in difficult to use it laparoscopic surgery.

Basic evaluation tests were performed for the instrument using a phantom model (a sponge). Suturing and ligaturing tasks, notably 360° suturing was successfully performed by operators with no experience in surgery (Fig. 1.15).

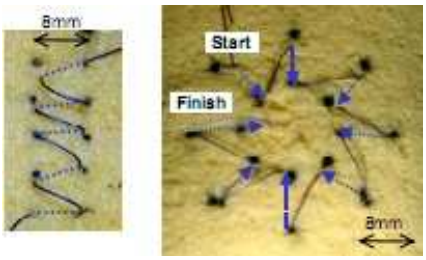

Figure 1.15: Suturing results with the instrument of Toshiba [Jinno 2002]

Another instrument of this type was developed at the University of Darmstadt and was first introduced in [Röse 2006] under the name of INKOMAN. A new, enhanced version with haptic interface, piezoelectric actuators and 4 intracorporeal robotic DOF is presented in [Röse 2009a] (Fig. 1.16). This

instrument has a laser cutting tip instead of a grasper, but the approach used in the development of its multi DOF mechanism is interesting nonetheless.

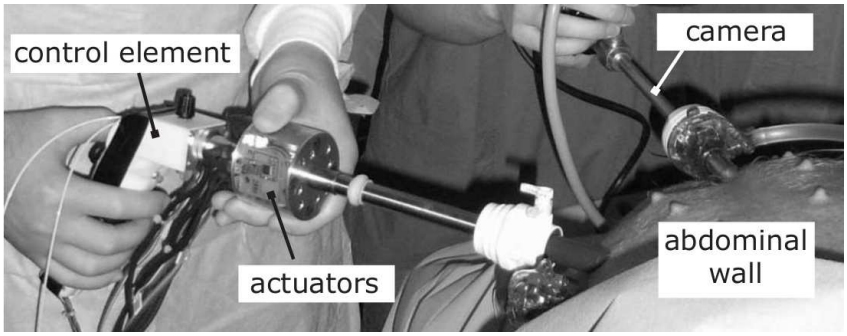

Figure 1.16: The instrument of the University of Darmstadt [Röse 2006]

The intracorporeal parallel kinematic structure has 4 DOF: one prismatic for moving the end effector forward and backward along the axis of the instrument's shaft and 3 revolute yaw-pitch-yaw axes [Röse 2009b]. The prismatic joint can move ± 20 mm and each revolute joint can rotate at least $\pm 40°$. The combination of a prismatic and revolute joints increases the instrument's workspace considerably.

The end effector is controlled by a 3 DOF haptic joystick on the handle. 3 DOF force sensors are integrated in the parallel mechanism. Piezoelectric motors that drive the parallel mechanism are integrated inside the shaft and provide 14 N at the end of each driving rod.

This instrument was tested in vivo to do some cutting tasks. Although the new parallel mechanism and the Cartesian control scheme present some interesting features, its use remains restricted to applications where large forces at the end effector are not needed.

The last mecatronic instrument presented in this chapter was developed at the University of Pisa [Piccigallo 2008] (Fig. 1.17).

In this instrument, the wrist is cable-driven, and the motors and the controller are all away from the instrument. A Bowden cable actuation system with eight pretensioned cables transmits forces of the motors to a pulley box on the instrument's shaft. The actuation has been designed considering the order of magnitude of the forces exerted on a laparoscopic instrument during operation, as estimated in [Richards 2000, Brown 2004], and it is composed of four DC motors coupled with a $43:1$ gearbox and connected to a cable-tensioning system. The end effector has a Roll-Pitch-Roll kinematics. Joint ranges are $\pm 180°$ for both roll articulations and $120°$ for the deflection.

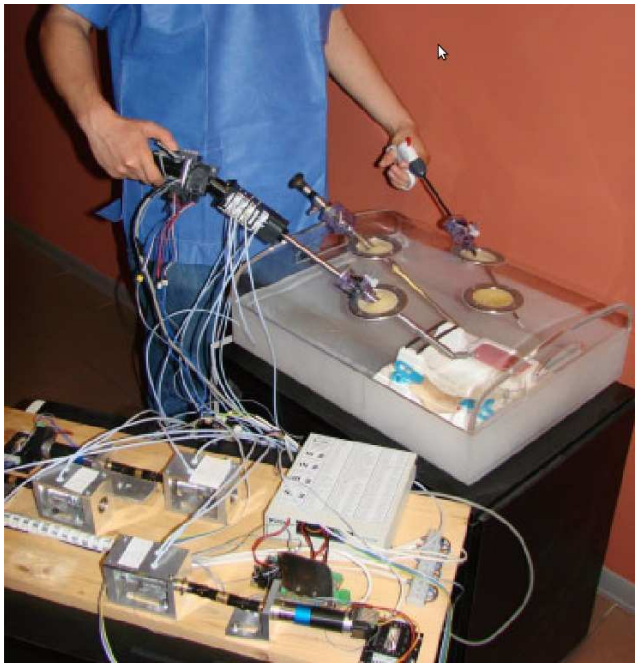

Figure 1.17: The instrument of the University of Pisa [Piccigallo 2008]

The handle is of cylindrical shape and has a lever to control opening and closing of the forceps by thumb movement. The handle can yaw or pitch and 2 encoders measure the yaw/pitch angles. The position of the end effector is controlled by these DOF while a switch allows for rolling the end effector around its own axis.

The purpose of the cited research studies was to have the advantages of a teleoperated robotic system in terms of dexterity and ergonomics in a hand-held instrument. The research has shown that this is a promising approach.

1.3 Conclusion

Mechatronic serial comanipulators offer solutions to the shortcomings of telesurgery as well as those of manual instruments. Unlike a telesurgery system, these instruments can be used in direct interaction with patient and the procedure can be converted rapidly to open surgery in case it is necessary. The hand-held character of the instrument gives the surgeon the haptic feedback he had using conventional instruments. Unlike manual instruments, they provide the necessary dexterity for complex conventional gestures, and are intuitively controlled.

In summary, mechatronic/robotic hand-held instruments can offer an integrated solution for the problems of laparoscopy considering different aspects of these problems: intuitiveness, dexterity, ergonomics and usability.

However, existing mechatronic instruments have several shortcomings that have prevented them from reaching the operating rooms:

1. Their human machine interface (HMI) and control mode is not intuitive enough.
2. They are not sterilizable; thus not usable in surgery.
3. Their considerable weight causes excessive fatigue.
4. Their inconvenient dimensions make them useless for surgeons.
5. Relatively bulky end effectors prevent their use in confined spaces.
6. Their poor ergonomics cause fatigue and muscular pain.
7. Their robotic DOF generate insufficient forces for performing certain surgical tasks.
8. The liaison between the instrument and the electronic controller, and/or the electrical actuators limit the manual movements of the instrument.

The aim of this thesis is to study dexterous mechatronic instruments globally, taking into account all the major aspects of serial comanipulation for MIS, i.e. HMI, kinematics, ergonomics and mechatronic design and their influence on the instrument's performance and usability in the operating room. Based on this study, new solutions to different difficulties that face laparoscopists are proposed.

This work starts by developing a simulation platform to study human-instrument interactions in laparoscopy. The next chapter presents this simulator.

Chapter 2

Simulator for Evaluation of Instruments

2.1 Introduction

Evaluating and comparing different laparoscopic instruments and their interfaces, control modes, ergonomics, kinematics and performance when these instruments are not realized yet suggests a simulation platform is needed. This platform should allow an easy integration and modification of different parameters that compose these instruments.

It is shown that Virtual Reality (VR) Simulators can provide metrics for performance evaluation of different subjects or instruments in the context of MIS.

VR Simulators are increasingly used to train and evaluate surgical skill. Existing commercial simulators have the following similar characteristics:

- Virtual surgical scene and absence of haptic feedback
- Closed source. It is not possible to modify the source code, for example to add new scenes, components etc..
- Closed hardware. It is not possible to use these simulators with instruments other than those provided by the maker.

The validity of these simulators is shown through comparative evaluation studies. Mathis et al. [Mathis 2007] studied the SurgicalSIM laparoscopic simulator (Fig. 2.1a) to see if it can discriminate between novices and experts and to assess learning curves among novices. Twenty novices and five experts performed five repetitions on the following modules: place arrow, retract, dissect, and traverse tube. For each module, median baseline performance was calculated.

The results showed that experts outperformed novices at baseline for time to completion on the dissect, place arrow, and traverse tube modules, as well

(a) SurgicalSim®from METI

(b) LAP Mentor®from Simbionix

Figure 2.1: 2 VR surgical simulators available on the market

as for error frequency on the traverse tube and retract modules. Novices' performance improved significantly with practice, approaching the experts' baseline in all modules. These results show that the SurgicalSIM laparoscopic simulator exhibits construct validity[1] on three of four basic-skills modules when considering completion time and on two modules when considering error frequency.

Another study [Yamaguchi 2007] was carried out to investigate whether eye-hand coordination skill on a virtual reality laparoscopic surgical simulator ,LAP Mentor (Fig. 2.1b), was able to differentiate among subjects with different laparoscopic experience. A total of 31 surgeons were divided into two groups: experienced surgeons (more than 50 laparoscopic procedures) and novice surgeons (fewer than 10 laparoscopic procedures). The subjects were tested using the eye-hand coordination task of the LAP Mentor (pointing at balls with the instrument), and performance was compared between the two groups. Assessment of the laparoscopic skills was based on parameters measured by the simulator.

The experienced surgeons completed the task significantly faster than the novice surgeons. The experienced surgeons also achieved a lower number of movements, better economy of movement and faster average speed of the left instrument than the novice surgeons, whereas there were no significant differences between the two groups for the average speed of the right instrument. This study shows that eye-hand coordination skill measured using the LAP Mentor was able to differentiate between subjects with different laparoscopic

[1]Validity of a test or a measurement tool that is established by demonstrating its ability to identify or measure the variables or constructs that it proposes to identify or measure. The judgment is based on the accumulation of correlations from numerous studies using the instrument being evaluated [Med 2009].

experience. This study also provides evidence of construct validity for eye-hand coordination skill on the LAP Mentor.

A new version of the Lap Mentor surgical simulator, the Lap Mentor II can provide haptic feedback to the user. Salkini et al. [Salkini 2010] compared medical students' performance on Lap Mentor with and without haptic feedback.

Twenty laparoscopically novice medical students were enrolled in the study. Each student was asked to perform three different tasks on the Lap Mentor II and repeat each one five times. The chosen tasks demanded significant amount of traction and counter traction. The first task was to pull leaking tubes enough and clip them. The second task was stretching a jelly plate enough to see its attachments to the floor and cut these attachments. In the third task, the trainee had to separate the gallbladder from its bed on the liver. The students were randomized into two groups, comparable in age, sex, and videogame playing, to perform the tasks with and without haptic feedback. The authors used accuracy, speed, and motion economy as metrics to compare the performance between the two groups.

No differences in accuracy, motion economy, and speed of hand movement were noticed. In fact, adding haptic feedback to the Lap Mentor II simulator did not contribute to any improvement in the performance of the trainees. The authors conclude that the presence of haptic feedback has less effect than it thought to have, on the performance of the novice trainees. This may suggest that better haptic feedback is still needed. However, there may be visual compensation for the lack of haptics. Further research is needed to clarify the value of haptics to the expert surgeon and compare it to the new trainees.

Other simulators such as Xitact LS500, MIST-VR, Endotower, CELTS and LapSim have also been used by surgeons with various levels of experience following similar test protocols, and have demonstrated significant construct validity [Schijven 2003, Maithel 2006, Van Dongen 2007]. These studies show that metrics such as time to completion, movement economy or number of errors used in VR Simulators can distinguish between different levels of performance by the subjects.

In [Kundhal 2009] the authors aimed to investigate whether performance in the operating room, assessed using a modified Objective Structured Assessment of Technical Skill (OSATS) [Martin 1997], correlated with the performance parameters registered by a virtual reality laparoscopic trainer (LapSim).

The study enrolled 10 surgical residents with similar limited experience in

laparoscopic surgery (median, 5; range, 1-16 laparoscopic cholecystectomies). All the participants performed three repetitions of seven basic skills tasks on the LapSim laparoscopic trainer and one laparoscopic cholecystectomy in the operating room. The operating room procedure was video recorded and blindly assessed by two independent observers using a modified OSATS rating scale. Assessment in the operating room was based on three parameters: time to completion of task, error score, and economy of movement score. During the tasks on the LapSim, time, error, and economy of movement parameters were registered. The correlation between time, economy, and error parameters during the simulated tasks and the operating room procedure was statistically assessed using Spearman's test. The results show a significant correlation between the time to completion and motion economy in the operating room procedure and on LapSim.

These studies prove that a subject's performance on a VR Simulator is strongly correlated to his performance in laparoscopy. Consequently, a VR simulator can be used to evaluate and compare the performance of different subjects with different instruments.

In the next section, the VR Simulator developed for our evaluation tests will be presented and the metrics used in the simulator to measure a subject's performance using different instruments are introduced.

2.2 Virtual Reality Simulator for Evaluation of Instruments

The simulator is developed for evaluation of novel hand-held instruments for laparoscopy:

- Supposing a wrist is added to the end effector to add intracorporeal DOF to the instrument, different kinematics of these DOF can be evaluated and compared. The series of intracorporeal DOF may have any arbitrary morphologie.

- The instrument's handle can be chosen between a conventional laparoscopic instrument handle, an articulated handle like that of manual hand-held instruments and a finger-operated handle with joystick/buttons controlled by fingers. These 2 types of handle can also be compared. The finger-operated handle may have any arbitrary number of control elements (Fig. 2.2).

(a) A conventional laparoscopic instrument handle

(b) The articulated handle of the RealHand®instrument

(c) Nunchuck®, a finger-operated handle for video games from Nintendo

Figure 2.2: 3 different types of instrument handle compatible with the simulator

- Different control modes, i.e. different mappings between the handle's DOF and the end effector's DOF can be compared. Each mapping may be position to position or position to speed.
- The ergonomics of the handle, in particular, the influence of the connection between the handle and the instrument's shaft on the instrument's ergonomics can be studied. The handle can be connected to the shaft with a rigid connection, a universal joint or a knee joint.

Other parameters in the simulator can also be modified, in order to study their influence on the performance or to simply change the scenario or test conditions for a given test. These parameters are:

- Position of instrument ports
- Instrument length
- Position of endoscope port
- Endoscope's line of sight
- Endoscope's angle of view
- Amplification or attenuation coefficient of user commands
- Parameters related to the virtual scene such as the working plane orientation and position of targets

The simulator automatically saves the positions of all the objects in the scene and different states or flags (type of task, data entry, opening and closing grasper, etc.). It is then possible to reconstruct a test session for later subjective examination of the gestures.

Figure 2.3: Our VR simulator

2.2.1 The Components of the Simulator

The VR Simulator (Fig. 2.3) has the following components:

- A Polaris®Hybrid tracking system (Northern Digital Inc., Fig. 2.4)that can keep track of the position and the orientation of several targets, using infrared cameras, infrared emitters and reflective markers on each target.
- A laparoscopic training box or pelvitrainer[2], with a Polaris target on it that defines the relative position and the orientation of the virtual endoscope to the incision points (see Fig. 2.5).
- Two surgical instruments with Polaris targets on their shafts (and on their handles for articulated handles).
- A PC that receives the position and orientation of each target from Polaris and the control signals from the handles, calculates the position and orientation of the instruments and their end effectors, and renders the virtual scene on the screen.
- A 19" computer screen with adjustable height.

[2]From Hillway Surgical

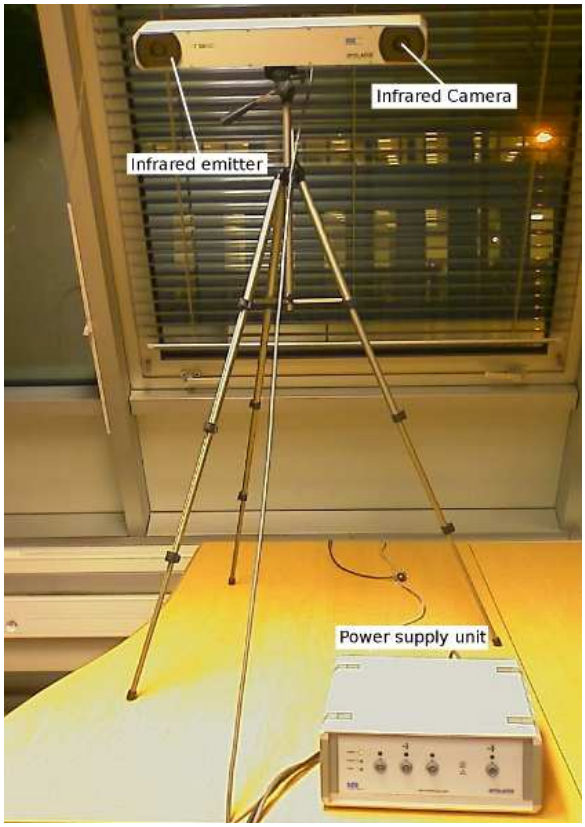

(a) Infrared camera and power supply unit

(b) A Polaris target with 3 markers

Figure 2.4: NDI's Hybrid Polaris®tracking system

- An Arduino Nano board with an ATMega168 microcontroller that relays the signals comming from a conventional or finger-operated handle to the PC (Fig. 2.6).

For Polaris targets, a calibration procedure using proprietary software (NDI 3D Architect), allows associating a local coordinate system to each target. Polaris sends the position and orientation of visible targets in its field of view according to its own local coordinate system, through a serial connection (RS232) to a PC. The maximum transmission baud rate is 115200 bps. The hybrid Polaris system has a resolution of 0.3 mm. It can track up to 9 wireless targets simultaneously.

For communicating with a finger-operated handle, the commands can be detected via microswitches or potentiometers on the handle and sent to the PC via the Arduino board. In case of a proportional signal coming from a potentiometer, the analog value of the voltage is read by the internal Analog

Figure 2.5: Pelvitrainer, 2 instruments and their Polaris targets

to Digital converter (6 channel, 10 bit) of the microcontroller. The analog pins have internal pullup resistors.

For digital signals coming from microswitches, a pull-down resistor is needed on each input pin. The board has 14 digital input pins.

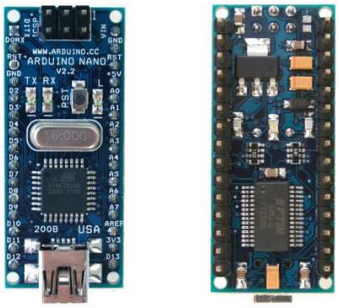

Figure 2.6: The electronic circuit for relaying finger-operated handle signals to the PC

2.2.2 Simulated Tasks

In order to quantify the performance of laparoscopists and their instruments, many studies over the last decade have suggested various protocols for learning laparoscopic gestures and evaluating laparoscopists' skills and performance, during and after training [Derossis 1998, Schijven 2002, Feldman 2004, Hance 2005]. These exercises are generally performed by surgical interns on pelvitrainer, virtual reality simulator or animal model.

Derossis et al. [Derossis 1998] have proposed a series of 7 exercises summarizing all gestures made by surgeons in any laparoscopic operation: (1) grasping an object and passing it from one instrument to another, (2) dissecting and cutting along a prescribed path, (3) placing clips and severing a vessel, (4) tieing a vessel with a ligature, (5) place and fix a retention net on an organ, (6) intracorporeal suturing and knot tieing, and finally (7) suturing with an extracorporeal knot.

Cao et al. [Cao 1996] have gone further in decomposing laparoscopic tasks by identifying five basic kinematic gestures performed by the surgeon with his/her instruments for every task: (1) reach a target and orient the end effector, (2) close the end effector to catch, hold or cut, (3) push with the instrument, (4) pull, and (5) open the end effector.

The low level decomposition of Cao et al. is the underlying level of the tasks in the methodology of Derossis et al. Our objective was to simulate tasks that are representative of real surgical tasks, but can distinguish between different users and instruments based on their dexterity and hand-eye coordination capabilities. Besides, we also wanted to evaluate different instruments from an ergonomics point of view, and tasks that greatly solicit the arm are prefered for this evaluation.

Based on these facts, 3 different tasks were simulated on the VR Simulator:

1. Pointing (Fig. 2.7): consists of

   (a) back and forth movements along a defined axis (instead of push and pull, in the absence of haptic feedback),

   (b) move to different targets in successive free path,

   (c) hit a target with a specific orientation of the end effector.

   This tasks does not need high dexterity, but challenges the user's ability of hand-eye coordination.

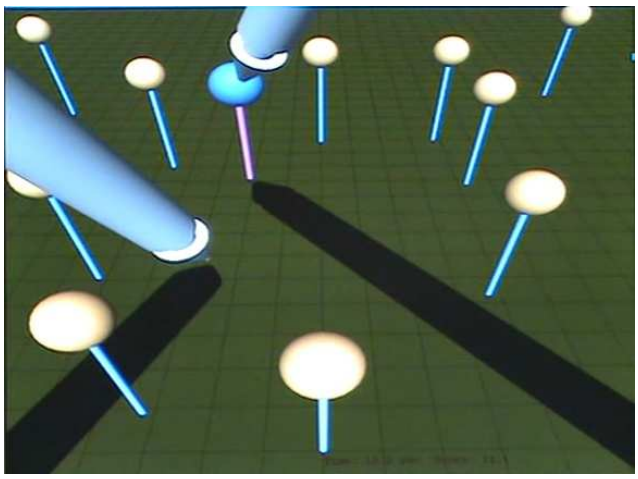

Figure 2.7: Pointing task on the VR Simulator

2. Stitching (Fig. 2.8): the stitching task is meant to test the dexterity of a user by making a stitching gesture. The simulated stitching consists of putting the needle in the right orientation so as to insert it in the working plane with the right angle, then reaching the start point and finally turning the needle to bring it out of the end point.

   On the simulator, a stitch is considered precise enough when the needle is inserted and brought out in a predefined vicinity of the desired insertion point and end point (indicated on the image with circles around the points).

   Knot tieing is not simulated as it requires modeling of the thread and demands heavy mathematical modeling with minimal added value.

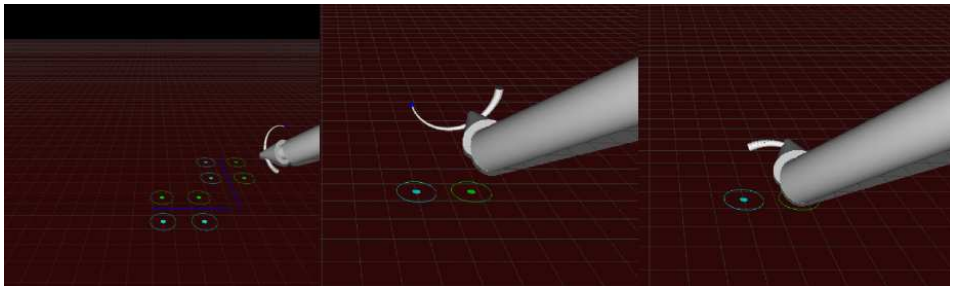

Figure 2.8: Stitching task on the VR Simulator

3. Pick & Place (Fig. 2.9): the user has to pick a ring and place it on a column in another position. This is a more complex task than pointing

and an exercise closer to basic surgical actions. This exercise needs using all the articulations of the arm and allows for a good evaluation of the instrument ergonomics.

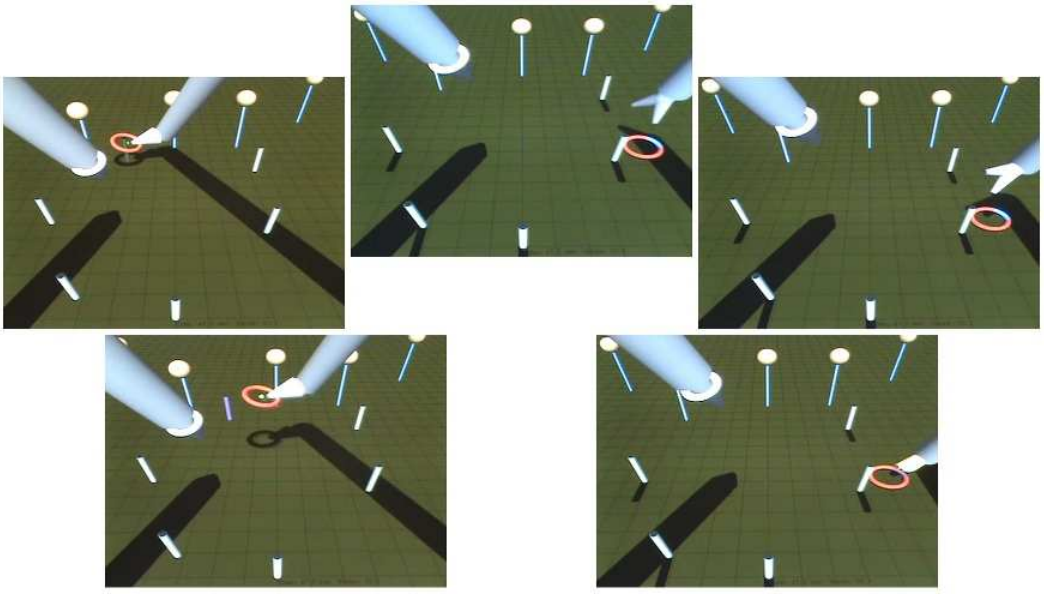

Figure 2.9: Pick & Place task on the VR Simulator

Different levels of difficulty may be considered in successive repetitions of this task. At the easiest level, the ring can be picked, by simply touching it; In a more difficult level it can be picked, by opening and closing the grasper. Imposing a specific grip area to force the user to properly position the instrument, or imposing a specific orientation of the end effector while picking, for example allowing to pick the ring only from top side, would make the task even more difficult. Similarly, the constraints on placing (size of column, imposition of a particular orientation) can be varied to change the difficulty level.

The loss of haptic feedback and the simple 2 dimensional image make working on the VR Simulator difficult for an unexperienced user. Indications such as change of color and audio feedback have been added to help working without the sense of touch. The perspective in the image gives an indication of depth and dummy objects put in various depths emphasize this perception of depth.

An important helping factor is the implementations of objects' shadows for easier perception of depth. Kersten et al. [Kersten 1994] showed that cast

shadow information overrides a number of other strong perceptual constraints, including viewers' assumptions of constant object size and a general viewpoint. Moreover, their results support the hypothesis that the human visual system incorporates a stationary light source constraint in the perceptual processing of shadow motion.

For this reason, the virtual light source for casting shadows is supposed to be stationary. Contrary to the real light source in laparoscopy that comes from the endoscope and generates little visible shadows, the light source here is placed at the top of the pelvitrainer. As a result, cast shadows are completely visible to the viewer of the scene and can help him/her perceive object position and size better.

2.2.3 Simulator's Software Implementation

The software implementation of the simulator includes a graphical user interface (GUI), a graphic engine, and the virtual scene window.

The graphic engine receives the tracking data from the Polaris and simulates a real-time image of the inside of the training box from the virtual endoscope's point of view. The graphic engine is implemented on top of the OpenGL 2.0 library. It creates a 900×900 pixel virtual scene window to cover the whole width of the screen (1440×900 pixel resolution).

Fig. 2.10 shows the flow of the program rendering the virtual image. The data coming from the Polaris is filtered before being used by the program to calculate the position and orientation of each instrument in the endoscopic camera's coordinates. The orientation of the end effectors relative to the shafts and their opening and closing is calculated based on the commands coming from the handle. The position of the end effector is calculated according to its orientation for use in the collision detection phase later. After calculating the position and orientation of all the objects in the scene, this information is saved in a text file for later analysis or reconstruction of the test session.

This process is repeated for each frame in a loop, at the update frequency of Polaris which is 60 Hz. As a result, the simulated image will have 60 FPS.

2.2.3.1 Filtering data from Polaris

The tracking data is first filtered by an exponentially weighted moving average filter to remove the measurement noise. The output of such a filter for an input sequence x_k (n is length of the window) is:

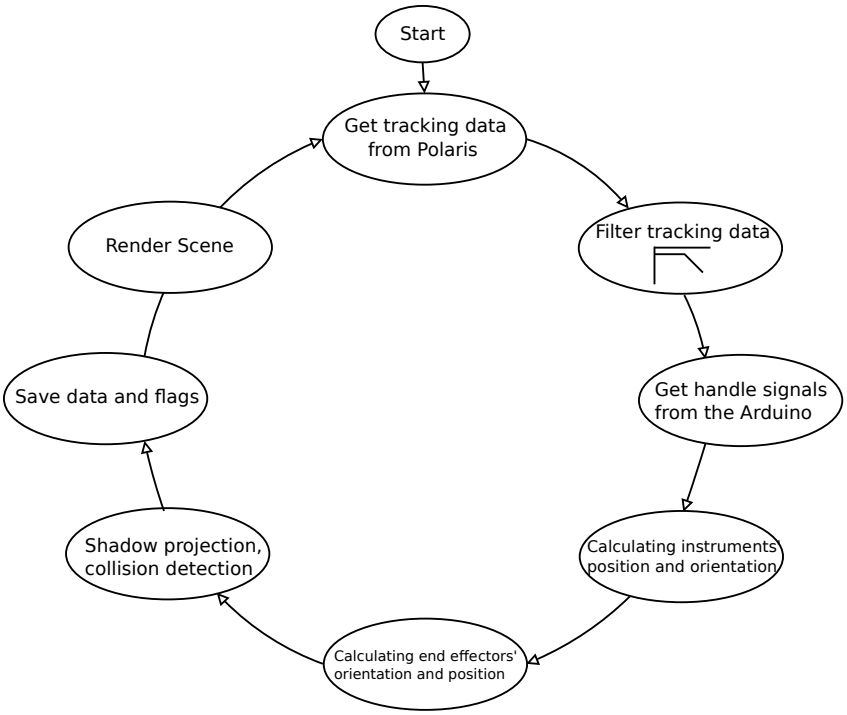

Figure 2.10: Simulator software flowchart

$$\bar{x}_k = \alpha \bar{x}_{k-1} + (1 - \alpha) x_k \tag{2.1}$$

$$\alpha = \frac{n}{n+1} \tag{2.2}$$

The filter introduces a lag in the simulation. There's a trade-off between the noise still left on the output and the lag. We tested different degrees of filtering (α) from 0.5 to 0.91 ($1 < n < 10$). $\alpha = 0.75$ ($n = 3$) seemed to give the strongest filter that didn't introduce a perceivable lag, while filtering enough noise to give a steady pose for a stationary target.

2.2.3.2 Calculating each instrument's shaft position and orientation

To render the virtual image, the graphic engine needs the position and the orientation of each instrument and its end effector in the virtual endoscope's coordinate system C. The point of view of the camera, as well as its line of sight are defined arbitrarily in C. This line of sight will be the user's line of sight when looking in a perpendicular direction at the center of the screen.

Local coordinate systems are associated to the Polaris targets on the training box, and each instrument's shaft and handle. These coordinate systems are denoted Si (for instrument i's shaft), Hi (for instrument i's handle), B (for the fixed target on the pelvitrainer). The coordinate systems associated with the virtual objects are C (for endoscopic camera) and Ei (for instrument i's end effector). The position and the orientation of each target is given by Polaris in its own coordinate system (denoted A) which is fixed between its 2 infrared cameras (Fig. 2.11).

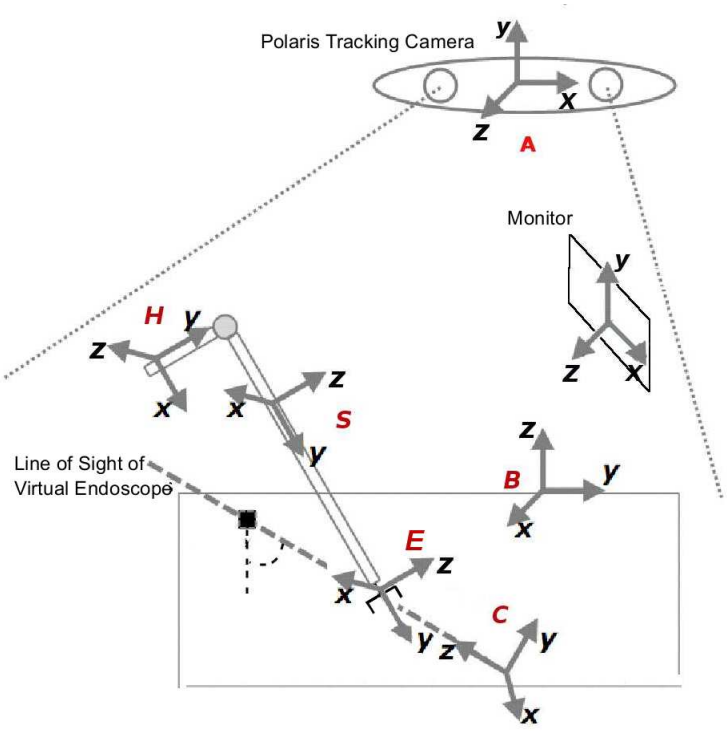

Figure 2.11: Local coordinates of the objects in the scene

The tracking data for any target i with the associated local coordinates I is composed of two components:

- a 3×1 vector ${}^{A}P_I = \begin{pmatrix} p_x \\ p_y \\ p_z \end{pmatrix}$ containing the position of the target.

- a 4×1 vector ${}^{A}_{I}Q = \begin{pmatrix} q_x \\ q_y \\ q_z \\ q_0 \end{pmatrix}$ containing the quaternions for a rotation of θ around the axis ${}^{A}\vec{K} = \begin{pmatrix} k_x \\ k_y \\ k_z \end{pmatrix}$ with

$$q_x = k_x Sin(\frac{\theta}{2}) \tag{2.3}$$

$$q_y = k_y Sin(\frac{\theta}{2}) \tag{2.4}$$

$$q_z = k_z Sin(\frac{\theta}{2}) \tag{2.5}$$

$$q_0 = Cos(\frac{\theta}{2}) \tag{2.6}$$

At first, the ${}^{A}_{I}Q$ vector for each target is transformed to a rotation matrix.

$${}^{A}_{I}R = \begin{pmatrix} 1-(2q_y^2+2q_z^2) & 2q_xq_y+2q_zq_0 & 2q_xq_z-2q_yq_0 \\ 2q_xq_y-2q_zq_0 & 1-(2q_x^2+2q_z^2) & 2q_yq_z+2q_xq_0 \\ 2q_xq_z+2q_yq_0 & 2q_yq_z-2q_xq_0 & 1-(2q_x^2+2q_y^2) \end{pmatrix} \tag{2.7}$$

This rotation matrix, combined with the position vector ${}^{A}P_I$ give a 4×4 homogeneous transformation matrix:

$${}^{A}_{I}T = \left(\begin{array}{ccc|c} & {}^{A}_{i}R & & \begin{matrix} p_x \\ p_y \\ p_z \end{matrix} \\ \hline 0 & 0 & 0 & 1 \end{array}\right) \tag{2.8}$$

The transformation matrices for the shaft and handle targets of the i^{th} instrument, and the base (pelvitrainer) target will be ${}^{A}_{S_i}T$, ${}^{A}_{H_i}T$ and ${}^{A}_{B}T$ respectively.

In order to reconstruct the geometry of the simulator, we need to find the position and the orientation of each instrument's shaft in the virtual endoscope's coordinate system C, i.e. we need to find the transformation matrix ${}^{C}_{S_i}T$.

The endoscopic camera's coordinate system C, is placed arbitrarily according to B. The relation between B and C is defined by the user as

$$ {}^{B}_{C}T = \left(\begin{array}{ccc|c} & {}^{B}_{C}R & & {}^{B}P_{C} \\ \hline 0 & 0 & 0 & 1 \end{array} \right) \tag{2.9} $$

where ${}^{B}P_{C}$ is the position of the origin of C in B coordinates. Thus,

$$ \begin{aligned} {}^{C}_{S_i}T &= {}^{C}_{A}T.{}^{A}_{S_i}T \\ &= ({}^{B}_{C}T)^{-1}.({}^{A}_{B}T)^{-1}.{}^{A}_{S_i}T \end{aligned} \tag{2.10} $$

The dimensions of the instruments' shafts are known. Each shaft is a 5 mm thick cylinder with an arbitrary length of l. The target on the shaft is installed in a way that the shaft is along its coordinates' Y axis. The position of its tip (L) in these coordinates is thus given by:

$$ {}^{S_i}P_{L} = \left(\begin{array}{c} 0 \\ l \\ 0 \\ 1 \end{array} \right) \tag{2.11} $$

The position of the instrument's tip in the endoscopic camera's coordinates ${}^{C}P_{L}$, is given by:

$$ {}^{C}P_{L} = {}^{C}_{S_i}T.{}^{S_i}P_{L} \tag{2.12} $$

2.2.3.3 Calculating each end effector's position and orientation

The end effector's orientation relative to the shaft can be controlled either by an articulated handle, based on the handle's orientation relative to the shaft, or by a finger-operated handle.

For the articulated handle of instrument i, a target with the local coordinate system H_i is installed on the handle. For the initial handle orientation:

$$ {}^{S_i}_{H_i}R = \mathbf{I} \tag{2.13} $$

For any other handle to shaft orientation, the equivalent angle-axis rotation of the handle relative to shaft is calculated, so that the rotation angle θ can be amplified by an arbitrary gain of g ($\Theta = g\theta$), if this is needed:

For a given rotation matrix:

$$ {}^{S_i}_{H_i}R_{(\vec{K})}(\theta) = \begin{pmatrix} r_{11} & r_{12} & r_{13} \\ r_{21} & r_{22} & r_{23} \\ r_{31} & r_{32} & r_{33} \end{pmatrix} \tag{2.14} $$

The equivalent angle-axis representation is given by:

$$ \theta = \arccos\left(\frac{r_{11} + r_{22} + r_{33} - 1}{2}\right) \tag{2.15} $$

$$ \vec{K} = \frac{1}{2\sin(\theta)} \begin{pmatrix} r_{32} - r_{23} \\ r_{13} - r_{31} \\ r_{21} - r_{12} \end{pmatrix} \tag{2.16} $$

After amplifying the handle motion, the angle-axis representation is converted back to the rotation matrix form. For a given rotation of Θ around the axis ${}^{S}_{i}\vec{K}$, the equivalent rotation matrix is given by:

$$ {}^{S_i}_{H_i}R_{\vec{K}}(\Theta) = \begin{pmatrix} k_x k_x v\Theta + c\Theta & k_x k_y v\Theta - k_z s\Theta & k_x k_z v\Theta + k_y s\Theta \\ k_x k_y v\Theta + k_z s\Theta & k_y k_y v\Theta + c\Theta & k_y k_z v\Theta - k_x s\Theta \\ k_x k_z v\Theta - k_y s\Theta & k_y k_z v\Theta + k_x s\Theta & k_z k_z v\Theta + c\Theta \end{pmatrix} \tag{2.17} $$

where $c\Theta = \cos\Theta$, $s\Theta = \sin\Theta$, $v\Theta = 1 - \cos\Theta$ and ${}^{S_i}\vec{K} = \begin{pmatrix} k_x \\ k_y \\ k_z \end{pmatrix}$

The sign of Θ is determined by the right hand rule with the thumb pointing along positive sense of ${}^{S_i}\vec{K}$.

Finally, the rotation matrix describing the relative orientation between the endoscopic camera's coordinate system C and the instrument's end effector with its local coordinate system E attached to the articulation point (see Fig. 2.11) is:

$$ {}^{C}_{E_i}R = {}^{C}_{S_i}R . {}^{S_i}_{H_i}R \tag{2.18} $$

In case of a finger-operated handle a speed control mode is often used. Signals coming from the handle define the rotation speed of each intracorporeal

articulation. For a binary signal, the rotation speed will be 0 or constant non-zero according to the control mode matrix M:

$$\begin{pmatrix} \dot{\mu} \\ \dot{\nu} \\ \dot{\xi} \end{pmatrix} = M. \begin{pmatrix} c_1 \\ c_2 \\ c_3 \end{pmatrix} \tag{2.19}$$

Where c_1, c_2, c_3 are binary commands from the handle.

This rotation speed vector is then used to calculate XYZ rotation angles, μ, ν and ξ and the rotation matrix describing the orientation of E_i relative to S_i:

$$\begin{aligned} {}^{S_i}_{E_i}R_{XYZ}(\mu,\nu,\xi) &= R_Z(\xi)R_Y(\nu)R_X(\mu) \qquad (2.20) \\ &= \begin{pmatrix} c\xi & -s\xi & 0 \\ s\xi & c\xi & 0 \\ 0 & 0 & 1 \end{pmatrix} \begin{pmatrix} c\nu & 0 & s\nu \\ 0 & 1 & 0 \\ -s\nu & 0 & c\nu \end{pmatrix} \begin{pmatrix} 1 & 0 & 0 \\ 0 & c\mu & -s\mu \\ 0 & s\mu & c\mu \end{pmatrix} \end{aligned}$$

where $c\alpha$ is shorthand for $\cos\alpha$ and $s\alpha$ for $\sin\alpha$, etc. Finally, the end-effector orientation in the C coordinate system is given by:

$${}^{C}_{E_i}R = {}^{C}_{S_i}R.{}^{S_i}_{E_i}R \tag{2.21}$$

For both articulated and finger-operated handles, the instrument and its end effector will be then translated to the position ${}^{C}P_L$.

To see the mathematic details behind shadow projection and collision detection in the VR Simulator, please refer to App. A.

2.3 Conclusion

The VR Simulator is a valid tool for comparing the performance of different groups of subjects, using different instruments in laparoscopy. The simulator let's us compare and evaluate different possible solutions to each of the problems of laparoscopy that we intent to solve by using serial comanipulation.

The simulator allows the subjects try different exercises that correspond to real exercises in laparoscopy. These exercise include moving the instrument in the operational space, pointing to targets, picking objects, transferring objects between instruments, placing objects, and stitching.

In the following 3 chapters, the simulator will be used to compare different handles, control modes, kinematics and ergonomics of a serial comanipulator for laparoscopy.

Chapter 3

Handle Type and Control Mode

3.1 Introduction

In a hand-held dexterous instrument for laparoscopy, with a wrist added to the grasper, the instrument's DOF need to be controlled in an intuitive and effective manner. The indirect vision and the mechanical constraints on the instrument and the fulcrum effect, make the control of the instrument's manual DOF non-intuitive. Adding additional intracorporeal DOF to the instrument, makes the hand-eye coordination task even more complicated because the number of DOF to control by one hand is increased, and they have to be controlled separately.

The control mode[1] for the 4 manual DOF of the instrument is imposed by the mechanical constraints on the instrument. But for the additional DOF, it is determined by the designer of the instrument. Choosing a non-intuitive control for the additional DOF leads to long learning curves, longer operation times and more importantly, additional burden on the surgeon. Because the surgeon has to do a cognitive remapping to resolve the incompatibility of the viewpoint presented by the endoscope and his spatio-motor expectations [Lai 2000], and a non-intuitive control mode makes this remapping more complicated. Therefore, choosing the optimal control mode is a major issue in the design of a hand-held dexterous instrument devoted to laparoscopyi.

For controlling the additional DOF of the end effector by hand, one approach is to make an articulated handle by adding a joint between the handle and the shaft (Fig. 3.1a). Tonet et al. [Tonet 2006] have concluded that an articulated handle is intuitively controlled by surgeons. The articulations of the handle can then be mapped to those of the end effector.

Another approach is to control the end effector using control elements integrated in the handle and manipulated by fingers i.e. buttons, dials or joysticks (Fig. 3.1b). Jinno et al. [Jinno 2002] argue that a finger-operated handle allows for more precise gestures. This approach is privileged in mechatronic instruments, where electrical actuators relieve the surgeon's hand from

[1] Mapping between the DOF on the handle and the end effector's DOF

Table 3.1: Type of handle in state of the art hand-held instruments

Instrument		Handle	
Type	Name	Articulated	Finger Operated
Manual	RealHand	✓	-
	Laparo-Angle	✓	-
	Radius	✓	✓
	Intuitool	-	✓
	Roticulator	-	✓
Robotic	U of Tokyo	-	✓
	Toshiba	-	✓
	Inkoman	-	✓
	U of Pisa	✓	✓

the burden of generating movements, necessary to actuate the end effector's DOF.

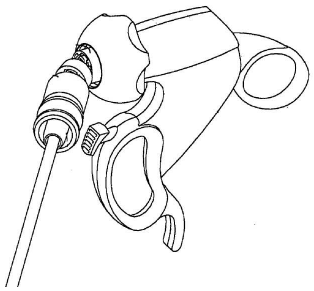

(a) Articulated handle of RealHand®[Hinman 2007]

(b) Finger-operated handle of Intuitool®[Hallbeck 2005]

Figure 3.1: An articulated handle vs. a finger-operated handle

The dexterous instruments with articulated effectors mentioned in Chapter 1 have used one of the two types of interfaces mentioned above or a mixture of the two. Table 3.1 shows the type of handle in each of them.

Our first step in the study of hand-held dexterous instruments is a series of primary evaluation tests on the VR simulator, to compare these two approaches, and choose the one with the best performance results. This study will be limited in nature as a great number of different handle-control mode configurations are imaginable. But it will let us choose a good solution between the best candidates to continue our study towards a suitable instrument for MIS.

3.2 Evaluation Tests

3.2.1 Objectives and Methodology

In this study an instrument with an articulated handle, is compared to an instrument with a finger-operated handle on the VR Simulator.

Here, we are going to consider an end effector with a wrist with 3 intracorporeal DOF, and a handle with 3 controlling elements. Such instrument has 6 DOF for arbitrarily positioning and orienting its end effector. 3 controlling elements on the handle will be enough to control the intracorporeal DOF.

The control matrix M, that maps the control signals from the handle to the intracorporeal wrist's DOF would be a 3×3 matrix, and

$$\begin{pmatrix} r_1 \\ r_2 \\ r_3 \end{pmatrix} = \begin{pmatrix} m_{11} & m_{12} & m_{13} \\ m_{21} & m_{22} & m_{23} \\ m_{31} & m_{32} & m_{33} \end{pmatrix} . \begin{pmatrix} c_1 \\ c_2 \\ c_3 \end{pmatrix} \tag{3.1}$$

Where c_1, c_2, c_3 are the commands from the handle and r_1, r_2, r_3 are the desired responses by the end effector. For an articulated handle

$$\begin{pmatrix} c_1 \\ c_2 \\ c_3 \end{pmatrix} = \begin{pmatrix} \gamma \\ \beta \\ \alpha \end{pmatrix} \tag{3.2}$$

where γ, β, α are the handle's rotations around X,Y,Z fixed axes of the instrument's shaft coordinates. For a finger-operated handle c_1, c_2, c_3 are either analog signals in a limited range or binary signals.

For a position control of the end effector

$$\begin{pmatrix} r_1 \\ r_2 \\ r_3 \end{pmatrix} = \begin{pmatrix} \mu \\ \nu \\ \xi \end{pmatrix} \tag{3.3}$$

where μ, ν, ξ are the end effector's rotations around X,Y,Z axes of the instrument's end effector.

For a speed control of the end effector:

$$\begin{pmatrix} r_1 \\ r_2 \\ r_3 \end{pmatrix} = \begin{pmatrix} \dot{\mu} \\ \dot{\nu} \\ \dot{\xi} \end{pmatrix} \tag{3.4}$$

So 4 different handle-controled variable confihurations are possible:

- position control with articulated handle
- speed control with articulated handle
- position control with finger-operated handle
- speed control with finger-operated handle

However, position control with a finger-operated handle does not seem to be a wise choice as motion range of controlling elements under the fingers are often limited and precise control of the end effector becomes difficult.

Speed control with an articulated handle does not seem to be intuitive, as the static deflection of the handle is mapped to the continuous motion of the end effector and the analogy between the controlling motion and its resulting effect is minimal.

So, the two other possibilities, i.e. an articulated handle with position control and a finger-operated handle with speed control will be compared during the tests.

Concerning the elements of the control matrix, there is an infinite number of possibilities. Considering only matrices with elements of 0, 1 or -1 for the element m_{ij} that maps the handle's control signal/DOF number j to the end effector's DOF number, i, $3^9 = 19683$ different control matrices exist. Comparing all these solutions in a study involving human participants is very difficult and demands an enormous amount of time.

We are going to consider only control modes where the mapping between the handle and the end effector is 1 to 1, i.e. each end effector DOF is mapped to one and only one control signal/DOF of the handle. As a result, all non-diagonal elements of the control matrix will be null.

$$\begin{pmatrix} r_1 \\ r_2 \\ r_3 \end{pmatrix} = \begin{pmatrix} k_1 & 0 & 0 \\ 0 & k_2 & 0 \\ 0 & 0 & k_3 \end{pmatrix} . \begin{pmatrix} c_1 \\ c_2 \\ c_3 \end{pmatrix} \tag{3.5}$$

Mapping more than 1 control signal to a DOF of the end effector has simply no advantage and only complicates the controlling task for the user. Mapping more than 1 DOF of the end effector to 1 control signal makes the task of coordinating end effector motions much more difficult.

In Equ. 3.5, $k_i = 0$ results in the suppresion of the end effector's DOF number i from the kinematics, and the total number of the instrument's DOF

is reduced by one. If $\forall i \in 1,2,3 : k_i \neq 0$, then the end effector has 3 controlled DOF.

Elements with 1 or -1 values for matrix elements mean that control signals are not amplified nor attenuated. Amplifying the control signals results in reduced precision. On the other hand, attenuating control signals limits the end effector's range of motion and solicits the user's hand more. In order to keep both precision and ergonomics, the control signals are nor amplified nor attenuated. Thus, the diagonal elements of the control matrix will all be 1 or -1:

$$\begin{pmatrix} r_1 \\ r_2 \\ r_3 \end{pmatrix} = \begin{pmatrix} \pm 1 & 0 & 0 \\ 0 & \pm 1 & 0 \\ 0 & 0 & \pm 1 \end{pmatrix} . \begin{pmatrix} c_1 \\ c_2 \\ c_3 \end{pmatrix} \tag{3.6}$$

As a result, the number of possible control modes for this 3 DOF intracorporeal wrist is reduced to 2^3.

The kinematics of the end effector will be yaw-pitch-roll. This end effector corresponds to 3 consecutive rotations around X, Z and Y axes of a coordinate system fixed to the end effector. This is the same kinematics used in the da Vinci Surgical System. It is proved to be fully dexterous and gives the surgeons an unprecedented precision in complex gestures, as the end effector can mimic the hand's motions (Fig. 3.2). Choosing a dexterous kinematics for the end effector helps compare only the influence of the handle and control mode on the performance.

Among the remaining choices of control mode, those that result in a homogenous functionality of the handle seem to be more intuitive. This leaves us with only the following choices of control mode:

- Inverse mode: where $M = \begin{pmatrix} -1 & 0 & 0 \\ 0 & -1 & 0 \\ 0 & 0 & -1 \end{pmatrix}$

  With an articulated handle, this means that the handle's yaw, pitch and roll are mapped to the end effector's yaw, pitch and roll in the inverse direction.

$$\begin{pmatrix} \mu \\ \nu \\ \xi \end{pmatrix} = \begin{pmatrix} -1 & 0 & 0 \\ 0 & -1 & 0 \\ 0 & 0 & -1 \end{pmatrix} . \begin{pmatrix} \gamma \\ \beta \\ \alpha \end{pmatrix} \tag{3.7}$$

  When the handle turns clockwise around an axis passing through the connection point between the handle and the shaft, the grasper turns

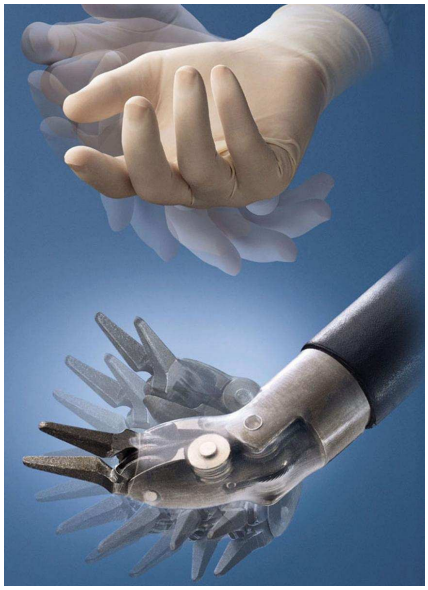

Figure 3.2: Da Vinci's EndoWrist®instrument [Guthart 2000]

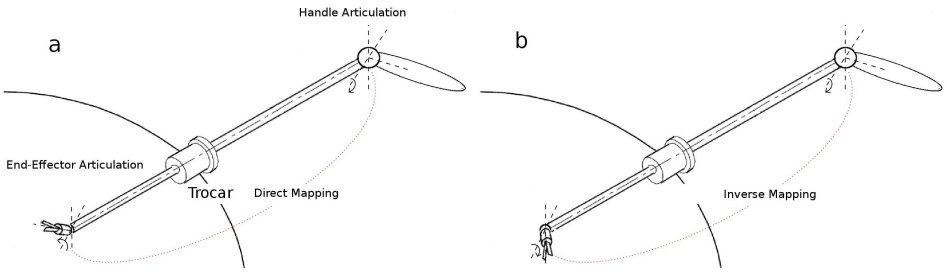

Figure 3.3: (a) Direct and (b) Inverse control modes in the instrument with an articulated handle

counter-clockwise around a parallel axis passing through the connection point between the shaft and the grasper.

From the user's point of view, bending the handle to right makes the grasper bend to right and vice versa (Fig. 3.3b).

For the finger-operated handle only this control mode was used. Because finger-operated handles with joysticks have been used in video games for a long time and this particular control mode that offers complete analogy between the 2 DOF joystick's movements and the end effector's movements on a 2 dimensional screen is established as the most intuitive one. It is the control mode that maps each movement of the joystick to a movement of the character on the screen in the same direction. From the

user's point of view, the joystick's up/down and left/right movements are mapped to the end effector's up/down (pitch) and left/right (yaw) movements. 2 buttons on the handle are mapped to the rotation of the end effector (roll) in clockwise and counter clockwise directions. As said before, the speed of the end effector is controlled with the finger-operated handle:

$$\begin{pmatrix} \dot{\mu} \\ \dot{\nu} \\ \dot{\xi} \end{pmatrix} = \begin{pmatrix} -1 & 0 & 0 \\ 0 & -1 & 0 \\ 0 & 0 & -1 \end{pmatrix} . \begin{pmatrix} c_1 \\ c_2 \\ c_3 \end{pmatrix} \tag{3.8}$$

- Inverse mode with lock: this mode is similar to the inverse mode, except that the effector's yaw and pitch DOF can be locked. When locked, the control matrix changes to

  $$M = \begin{pmatrix} 0 & 0 & 0 \\ 0 & -1 & 0 \\ 0 & 0 & 0 \end{pmatrix}$$

  and the effector can only roll.

  The lock allows the user to preserve the 2 dimensional deflection of the grasper while rotating it to make a stitch. In speed control mode, locking the end effector is not necessary as its position is static when no control signal is sent by the handle.

- Direct mode with lock: where $M = \begin{pmatrix} 1 & 0 & 0 \\ 0 & 1 & 0 \\ 0 & 0 & 1 \end{pmatrix}$

  In direct mode, the grasper turns about its rotation axis in the same clockwise or counter-clockwise direction as the handle. This makes the grasper follow the orientation of the handle from the user's point of view. This seems to be an intuitive mode, because if one holds such an instrument in hand out of the training box, the grasper seems to be exactly mimicking the hand's motions. As in the previous mode, the user can lock the effector's yaw and pitch (Fig. 3.3a).

The articulated handle is connected to the shaft using a knee-joint (Fig. 3.4a). The finger-operated handle is rigidly fixed on the shaft (Fig. 3.4b). The finger-operated handle is a Nunchuck^{TM}, a handle made by Nintendo for its video game console Wii. It has an ergonomic design and connects easily to a PC through Bluetooth. It has a 2 DOF joystick under the thumb and 2 buttons under the index and middle fingers.

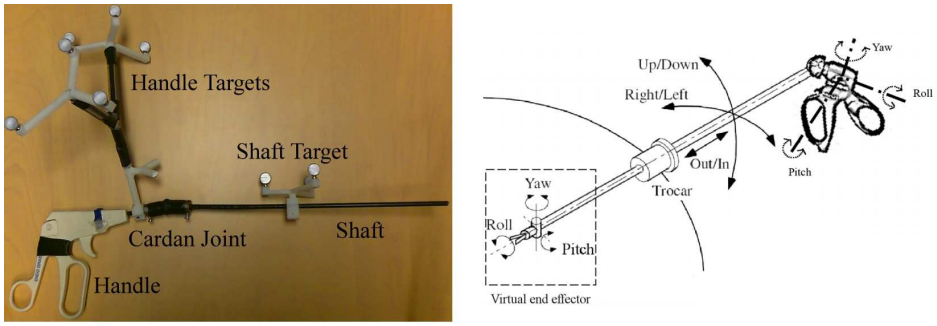

(a) With an articulated handle

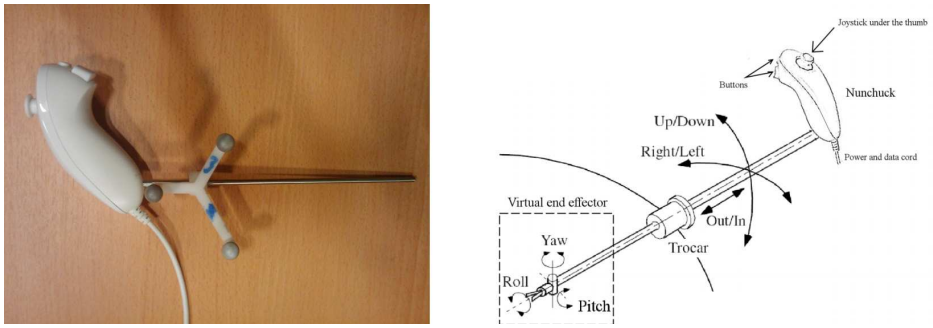

(b) With a Nunchuck handle

Figure 3.4: Instruments used with the simulator, at right the simulated instrument, at left the real instrument

3.2.2 Scenario

The tests are conducted under conditions as close as possible to current clinical practice as recommended by standard ergonomics guidelines [Berguer 2006, Cuschieri 1995]:

- The participants stand in front of the pelvitrainer, in accordance to common operating room practice.
- The display screen is placed in front of the participant's trunk, so that his/her line of sight is inclined about 25° downwards. The virtual endoscope's line of sight is 45° deviated from vertical.
- Trocars are placed on the vertices of an equilateral triangle with about 10 cm sides. Two instruments are handled by the participant: a conventional one in his/her minor hand and the instrument being evaluated in his/her major hand. The exercises require only one hand though.

3.2.3 Exercises

For each type of handle and control mode (3 control modes with the articulated handle and 1 control mode with the finger-operated handle), we asked test subjects to do frontal and sagittal stitches on a horizontal virtual working plane inside the training box (see Fig. 2.8 for the simulated scene). Each participant had 10 tries for frontal and 10 tries for sagittal stitches for each handle and control mode (40 frontal and 40 sagittal stitches in total for each participant. Before starting, each participant had the chance to familiarize with the simulator and the task i.e. each participant started doing the tests only after making 3 successful frontal and sagittal stitches.

Later, a referee observed saved trajectories of the instrument and the needle during a stitch to score it. A user's score with each control mode is the number of his successful stitches using that control mode.

In a perfect stitch, needle is inserted in the tissue on the start point of the stitch and comes out of the end point while it follows its curve, avoiding applying any side forces on the tissue (Fig. 3.5). Such a stitch is made by rolling the needle, around an axis of rotation that passes through the center of the the needle's curve (for a circular needle).

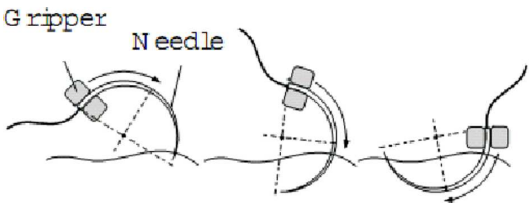

Figure 3.5: A perfect stitch [Jinno 2002]

This gesture is complex and difficult to make with a conventional instrument, and needs a combination of all the DOF, and even then the gesture is not perfect, because it puts 6 constraints on the instruments position and speed, while there are only 4 DOF available. If stitching is done only by rolling the end effector with the other DOF at rest, the needle deviates from the desired path and undesired side forces are applied on the tissue.

3.2.4 Metrics

The metric we use is the ability of the test subject to follow the needle's curve and stay in a certain vicinity of the insertion point to limit the side forces.

Some deviation from the perfect suturing path is however inevitable due to unintentional movements of hand and arm. The amount of acceptable side forces applied on the tissue, and thus the vicinity in which the needle has to stay for a successful stitch, depends on mechanical properties of the soft tissue on which the stitch is done. For example, muscle tissue is more elastic than liver, prostate or kidney can resist greater side forces without being damages.

After consulting laparoscopists and taking into account measurements of mechanical properties of soft tissues from [Chen 1996], [Bruyns 2002] and [De 2007], we established a simplified metric as follows: the needle has to stay in a 5 mm vicinity of the stitch's start point and come out in a 5 mm vicinity of the end point for the stitch to be successful. This is a rather easy criterion and corresponds to a hard tissue's tolerance to side forces. But the goal here is to compare the instruments and not the participants' ability to manipulate very precisely in the absence of haptic feedback.

The participants were 4 Ph.D. students with no experience in laparoscopy. Literature suggests that expert laparoscopists are significantly different from beginners in terms of applied forces and torques [Rosen 2002a], patterns of movement [Gallagher 2001], path length [Gallagher 2001], number of errors [Law 2004] and time to completion of tasks [Rosen 2006], [Oleynikov 2006].

However, it is not sure that expert surgeons do better than beginners with novel instruments as they do with conventional instruments. For example, there is some evidence that playing video games improves surgical skills in MIS [Rosser 2007], [Reilly 2008]. Younger participants though surgically beginner, have generally more experience with video games and the joysticks used to play them than middle age expert surgeons. Besides, they are not influenced by regular use of conventional instruments or the da Vinci system.

3.2.5 Results

Fig. 3.6 shows the scores of each participant in frontal and sagittal stitching using each of the 4 tested configurations. The results will be analized statistically (see Appendix B) to see if a significant performance difference exists between different handles and control modes.

3.2.5.1 Influence of control mode on performance

Fig. 3.7a and 3.7b show a higher average score for inverse mode with lock compared to direct mode with lock, both in frontal and sagittal suturing. An

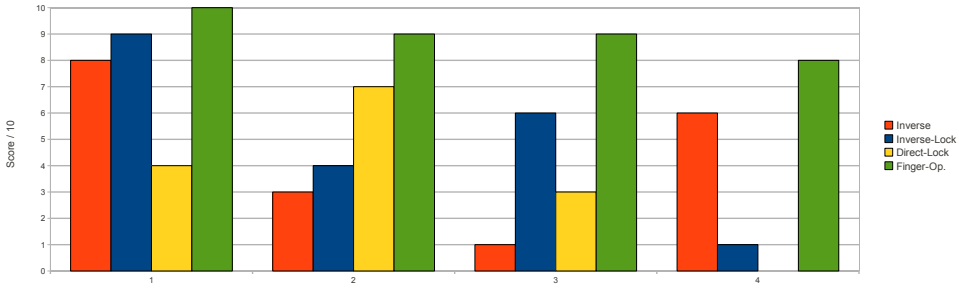

(a) Frontal

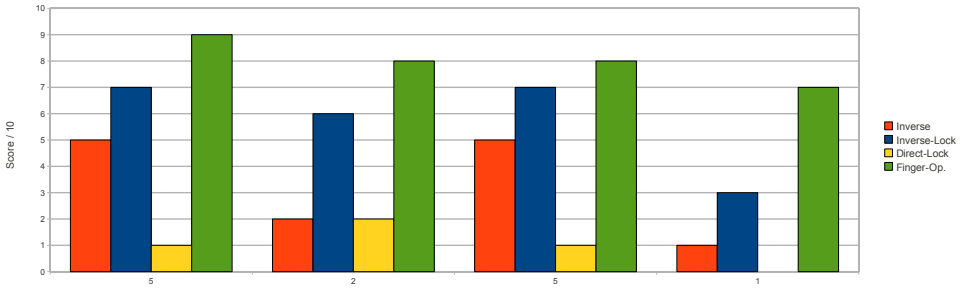

(b) Sagittal

Figure 3.6: Stitching scores with different configurations

ANOVA test of the 2 groups of data shows that the difference is not significant in frontal stitching (p=0.52), while in sagittal stitching, the difference is significant with a significance levelof 0.05 (p=0.003). This is also shown in the graphs based on the results of the ANOVA test (Fig. 3.7c and 3.7d). Notches in these graphs provide a test of group medians different from the F test for means in the ANOVA test. Two medians are significantly different at the 5% significance level if their intervals do not overlap. Interval endpoints are the extremes of the notches. There is an overlap between the intervals of the data groups in frontal stitching, while there is no such overlap in sagittal stitching, meaning that the medians of the 2 groups are significantly different.

The difference between the 2 control modes is more visible in sagittal stitching because the bending of the end effector is essential for making a stitch and the intracorporeal DOF are more solicted.

These results show that the inverse mode is easier to use when a combination of the DOF is needed to make a complex gesture.

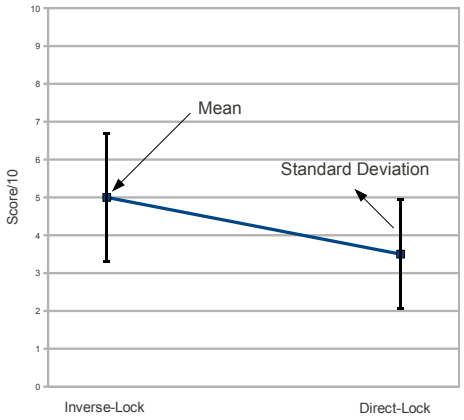

(a) Frontal-mean and standard deviation

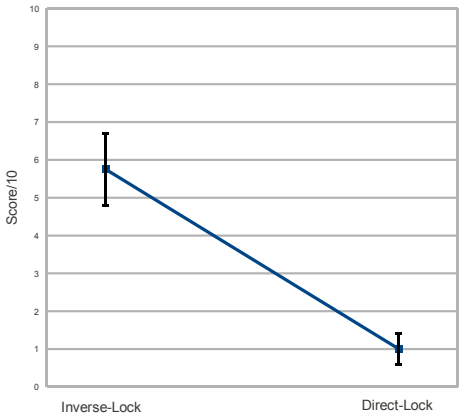

(b) Sagittal-mean and standard deviation

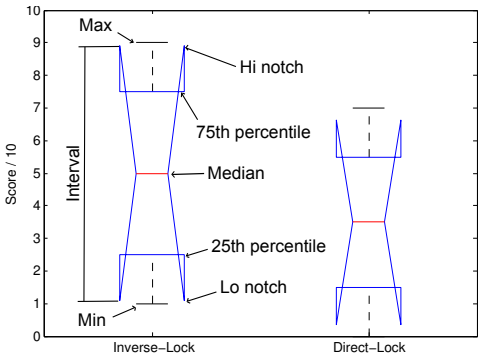

(c) Frontal-ANOVA test

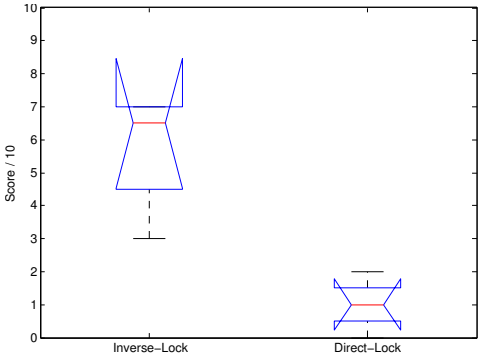

(d) Sagittal-ANOVA test

Figure 3.7: Stitching scores with inverse and direct modes with lock

3.2.5.2 Influence of end effector lock on performance

Fig. 3.8a and 3.8b show a higher average score for inverse mode with lock compared to inverse mode, both in frontal and sagittal suturing. However, an ANOVA test of the 2 groups of data does not show a significant difference in either case (p=0.83 for frontal and p=0.12 for sagittal stitching). The difference between the 2 medians is not difference either as the intervals overlap both in frontal (Fig. 3.7c) and sagittal (Fig. 3.7d) stitching.

Being able to lock the end effector improves performance results, especially in sagittal suturing, but not significantly.

One might say that this function is not essential and in a trade-off it can be given up on.

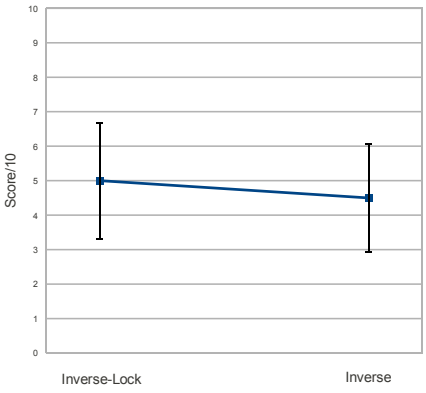

(a) Frontal-mean and standard deviation

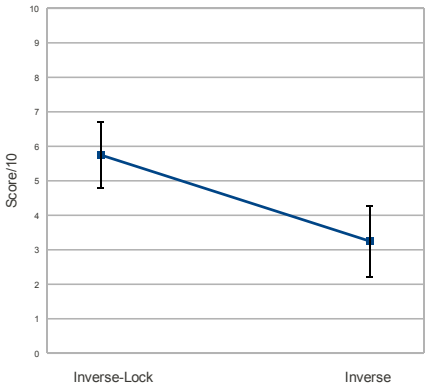

(b) Sagittal-mean and standard deviation

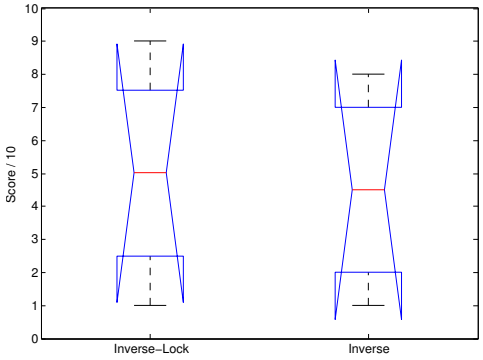

(c) Frontal-ANOVA test

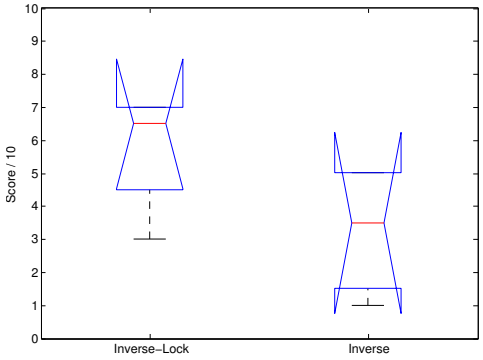

(d) Sagittal-ANOVA test

Figure 3.8: Stitching scores with inverse mode with and without lock

3.2.5.3 Articulated Handle Versus Finger-Operated Handle

Fig. 3.9a and 3.9b show a higher average score for the finger-operated handle with inverse control mode and speed control compared to the articulated handle, no matter what its control mode is, both in frontal and sagittal stitching. An ANOVA test of the 4 groups of data shows a significant difference in sagittal stitching (p=0.0002). But for frontal stitching the significance level is not reached (p=0.06), although it is not very far. The difference between the 2 medians is significnt between the finger-operated handle and 2 other configurations: articulated handle with inverse mode and direct-mode with lock. The only configuration that does not have a significantly lower median compared to the finger-operated handle is the articulated handle with inverse mode and lock (Fig. 3.9c and 3.9d).

The finger-operated handle is superior to the articulated handle, especially in sagittal stitching.

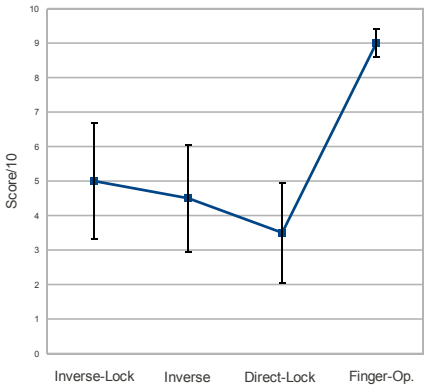

(a) Frontal-mean and standard deviation

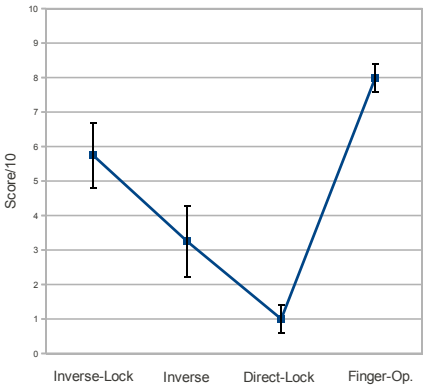

(b) Sagittal-mean and standard deviation

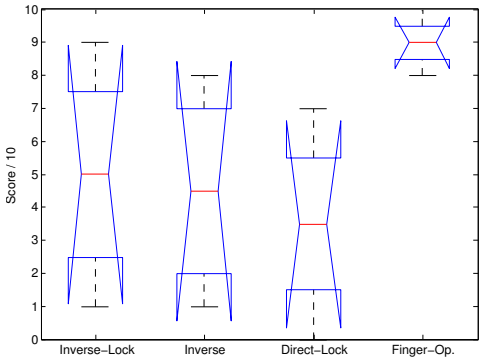

(c) Frontal-ANOVA test

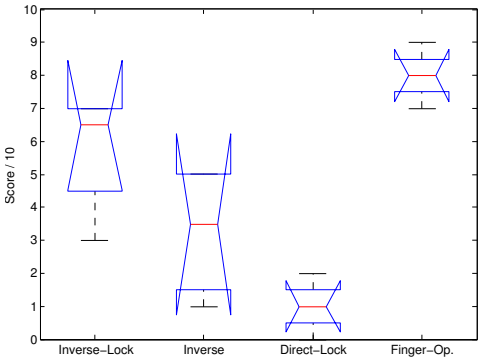

(d) Sagittal-ANOVA test

Figure 3.9: Stitching scores with articulated handle compared to the finger-operated handle

3.3 Conclusion

In an articulated handle with position control, the inverse control mode has a higher performance compared to the direct control mode. A locking mechanism, can improve precision even more. A finger-operated handle with speed conrtol and inverse control mode has even a higher performance.

Neuroscientific literature suggests that this is because moving the hand to articulate the handle causes a change in the upper arm's posture and unwanted

movements of the arm ensue that in turn influence the position of the end effector [Soechting 1995, Gielen 1997].

Our results suggest that a finger-operated handle is a better choice for a serial comanipulator. This study allows us to choose an efficient handle and control mode for the instrument and use this choice to compare different kinematics for the end effector. This comparison is the subject of the following chapter.

Finally, it should be noted that the study of control modes presented here has a somewhat limited character and it would be interesting to repeat this study with more subjects, including expert surgeons.

Furthermore, the influence of handle design and its control elements type, shape, placement, etc. on performance was not studied here. This is an important question in the design of surgical instruments and needs a seperate indepth study.

Chapter 4

Instrument Kinematics

4.1 Introduction

As said before, conventional hand-held instruments have only 4 DOF in laparoscopy and the surgeon can not make every desired gesture in space.

An example of such impossible gestures is stitching, where fully controllable 6 DOF movements are needed. To complete the stitch, the surgeon has to position the needle on the stitching point, reorient it in order to put it in a plane orthogonal to the stitching surface and rotate it around its central axis while maintaining the position and the orientation of the needle. This is practically impossible to do with a conventional instrument.

With conventional instruments, the surgeon has to use his second instrument to reorient the needle by holding and turning it in the first grasper. This is a difficult and time consuming task.

Adding a wrist to the instrument's end effector with 1 or more controllable DOF, increases the instrument's dexterity. First of all the grasper could be reoriented instead of the needle itself. Then, if the total number of instrument's DOF is equal to or greater than 6, making an exact stitching gesture would be possible by correctly coordinating the manual DOF of the instrument with the DOF of the wrist of the end effector (*cf.* 3.2.3).

But making a dexterous instrument with at least 6 DOF, in mesoscale dimensions[1] with a mechanical force transmission system that can satisfy the force/torque requirements of MIS is difficult and costly. Besides, each extra DOF added to the end effector can make the visuomotor coordination more difficult for the surgeon depending on the DOF type and location. So, choosing the suitable kinematics, i.e. the simplest kinematics that allows performing all needed movements, is critical.

The instruments mentioned in Chapter 1 have followed different paths when it comes to the end effector kinematics. Table 4.1 shows dexterous

[1] the instrument's diameter must not exceed 5 mm

instruments presented in Chapter 1 and major differences between them in terms of kinematics.

Table 4.1: Differences between 4 dexterous instruments

	RealHand	Laparo-Angle	Roticulator	Radius
Kinematics	Y-P	Y-P-R	Y-R	Y-P
Controllers	articulated handle	articulated handle,knob	knobs	articulated handle
End effector lock	No	Yes	Yes	No
Needs use of the other hand	No	For lock	For yaw	No
Shaft rotation	by a shaft screw	by rotating the handle	by rotating the handle	by a shaft screw

4.2 Evaluation Tests

4.2.1 Objectives and Methodology

In order to address the above issue, i.e. the choice of distal kinematics of a hand-held laparoscopic instrument, a series of comparative evaluation tests were conducted on the VR Simulator, presented in Chapter 2. In these tests, instruments with similar handle and control mode, and different end effector kinematics were used by to do the stitching task on the simulator. The instrument's handle and control mode were the finger-operated handle (Wii Nunchuck) and its intuitive control mode validated in Chapter 3.

This study is limited to instruments with 6 or 7 DOF kinematics in total. A manipulator with at least 6 DOF provides the surgeon with a completely dexterous instrument and allows him/her to perform any complex gesture in the instrument's workspace.

The manipulators that we consider here, consist of a 4 DOF holder external to the patient's body, and a 2 or 3 DOF wrist internal to the patient's body. The holder's DOF are imposed by the trocar kinematics at the insertion point and consist of limited frontal and sagittal inclinations of the shaft around insertion point, rotation about the insertion axis and translation in and out of

the body. The 3 rotational DOF have intersecting axes and can be represented by a knee joint. The kinematics of the holder is shown in Fig. 4.1.

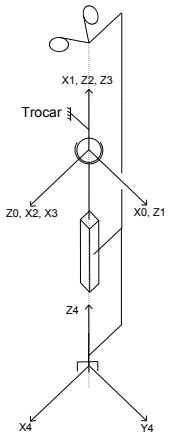

Figure 4.1: Kinematics of the instrument's holder

The local frames attached to the links are selected according to the Denavit-Hartenberg (D-H) convention. The D-H parameters for the holder and each of the wrist kinematics studied in this chapter can be found in App. C.

The kinematics of the wrist is the object of our study in this chapter. In order to simplify, only 2 or 3 DOF wrist kinematics with concurrent axes are considered. To count the number of possible kinematics, only 2 parameters are considered: the type of joints (revolute or prismatic) and the angle between 2 consecutive joint axes (0 or 90°). In fact, except in particular cases, consecutive axes are in general either parallel or perpendicular [Khalil 2002]. The number of possible kinematics based on the number of joints is calculated from the combination of these 4 values that the parameters can take [Delignieres 1987, Chedmail 1990].

In our wrist here, the joints are all revolute and the angles between 2 consecutive joints of the wrist are 90°. As a result, 3 different wrist kinematics are possible. Fig. 4.2 shows these wrist kinematics added to the holder.

Taking the end effector orientation where it is along the instrument's shaft as the equilibrium state, we would call the rotation of the end effector about the axis of the shaft, Roll, and the rotation of the end effector about the other 2 axes of a fixed coordinate system attached to the shaft, Yaw and Pitch. With this naming convention of our own, the 3 wrist kinematics studied in this chapter can be called Yaw-Pitch-Roll (YPR, Fig. 4.2a), Yaw-Roll (YR, Fig. 4.2b), and Yaw-Pitch (YP, Fig. 4.2c). Note that the kinematic diagrams

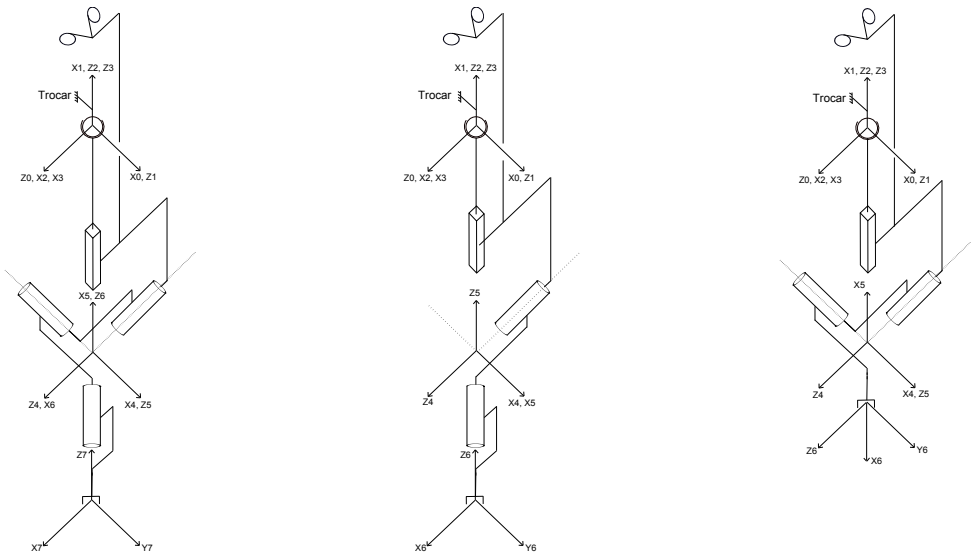

(a) YPR (b) YR (c) YP

Figure 4.2: Kinematic diagram of our 6 DOF instrument with 3 possible wrists

of Fig. 4.2 are drawn for non-zero joint displacements, according to the D-H convention. YR and YP kinematics are used in existing devices (LaparoAngle, RealHand, etc.) and YPR is a combination of the 2.

The handle used in the instrument for this study was the finger-operated Nunchuck handle that had the best performance in the study of the previous chapter. This handle was used with the same intuitive control mode as in the previous chapter, i.e. the joystick's up/down and left/right movements were mapped to the end effector's 2 first rotation speeds respectively. The buttons were mapped to the end effector's distal rotation speed, when this distal rotation exists.

4.2.2 Scenario

As in the previous study, the tests are conducted under conditions as close as possible to current clinical practice as recommended by standard ergonomics guidelines [Berguer 2006, Cuschieri 1995]:

- The participants stand in front of the pelvitrainer, in accordance to common operating room practice.
- The display screen is placed in front of the participant's trunk, so that his/her line of sight is inclined about 25° downwards. The virtual endoscope's line of sight is 45° deviated from vertical.

- Trocars are placed on the vertices of an equilateral triangle with about 10 cm sides. Two instruments are handled by the participant: a conventional one in his/her minor hand and the instrument being evaluated in his/her major hand. Stitching is done using the major hand only and the participant has to handle the conventional instrument in his minor hand only to keep close to the real conditions of laparoscopy.

4.2.3 Exercises

15 subjects were enrolled in this test. Each one made 5 frontal and 5 sagittal stitches using each of the 3 distal kinematics on the VR Simulator. The stitching task was similar to the one explained in the previous chapter with the same 5 mm acceptance criterion. Each user had the time to familiarize with the task and started doing the test only after he could make a stitch with each of the kinematics.

4.2.4 Metrics

The metrics used to evaluate the kinematics was the average time to completion of task (TCT) in frontal and sagittal stitching. [Mishra 2008] states that the TCT is a practical, easy and valid objective tool for assessing acquired technical skills of urology trainees in a laparoscopic simulated environment. It is also used for comparing different surgical instruments for laparoscopy [Dakin 2003].

4.2.5 Results

Fig. 4.3 shows the average TCT for each of the 15 subjects. Only 3 out of 15 subjects were able to make stitches with the YP kinematics in the 3 minute per stitch time limit.

The YP kinematics seems to be much less dexterous than YR or YPR and not suitable for complex gestures that need 6 DOF manipulation.

This shows the need for distal rotation in stitching.

In order to see if the difference in TCT between the YR and YPR kinematics is statistically significant or not, a one-way ANOVA test was done on the TCT data in frontal and sagittal stitching. The test shows that there is a significant difference ($p < 0.005$) between the YPR and YR kinematics.

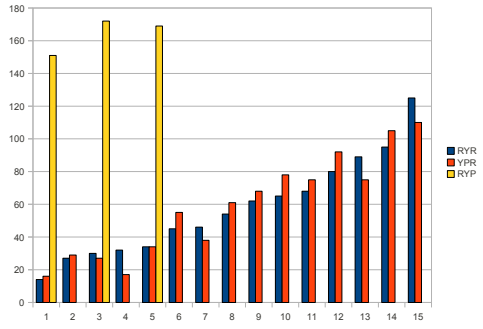

(a) Frontal stitching

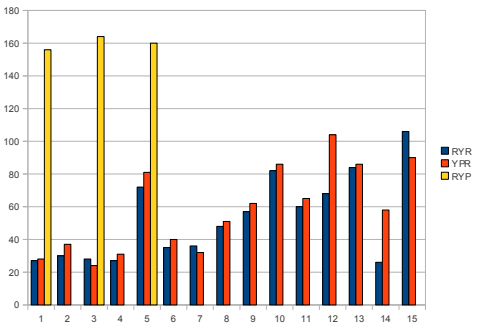

(b) Sagittal stitching

Figure 4.3: Average TCT in seconds for 15 subjects using 3 different end effector wrist kinematics

Fig. 4.4 shows the statistical representation of the results.

The YPR kinematics has a higher median TCT that the YR kinematics both for frontal (13% more) and sagittal (21% more) stitching.

For 9 subjects, the mean TCT with the YPR kinematics was higher than the YR kinematics in frontal stitching. In sagittal stitching this was true for 5 subjects out of 13.

4.3 Root-Cause Analysis of the Results

4.3.1 Hand Eye Coordination Difficulty Level with Each Wrist Kinematics

It is important to understand why one kinematics has better TCT than another one, when they all allow 6 DOF manipulation. In order to make a

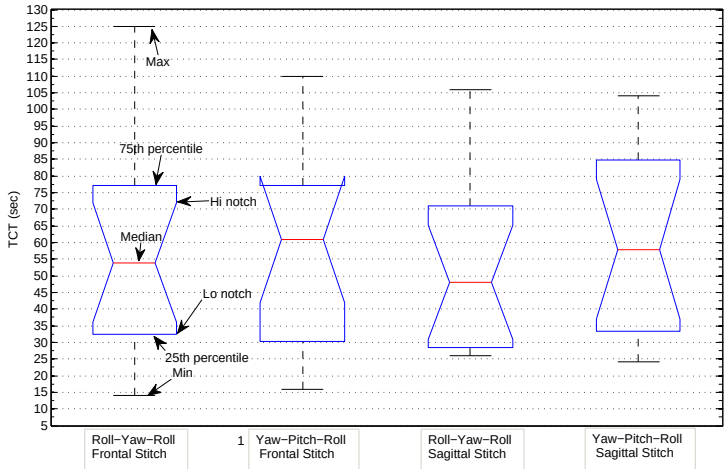

Figure 4.4: Statistical representation of the results

stitching gesture, i.e. rotating the needle about its central axis, the subject has to use all the DOF of the instrument. In a teleoperated robotic arm such as a da Vinci instrument, all the DOF are coordinated based on a precise algorithm to perform the desired motion of the end effector in the Cartesian space.

Using a hand-held instrument, the user has to control the DOF in the joint space. The manual motion of the instrument has to be coordinated with the distal mechatronic motion of the end effector. This is a difficult task and depending on the end effector kinematics, the trajectory that the user's hand has to follow to perform a stitching motion can be more or less complex.

A numerical analysis of the stitching motion with different kinematics was performed for a better understanding of the difficulty of the task. Using Matlab, the circular motion of the needle about its central axis with a constant pace was simulated. The inverse Jacobian of the instrument was calculated to trace the evolution of each DOF. The trajectory of the proximal end of the instrument (handle) is drawn to show the trajectory that the user's hand has to follow to make a perfect stitch (Fig. 4.5).

With all the 3 kinematics, the hand's trajectory has a half circle shape and the 3 first manual DOF i.e. inclinations around the incision point and translation along the shaft evolve similarly (Fig. 4.6). But it is the robotic wrists DOF that have different trajectories. With the YR and YPR kinematics that have a rotation at the end, the wrist's stitching gesture consists essentially of using this rotation, with minimal corrections using the other rotations to make the needle follow the trajectory of a perfect stitch. Fig. 4.6 shows the

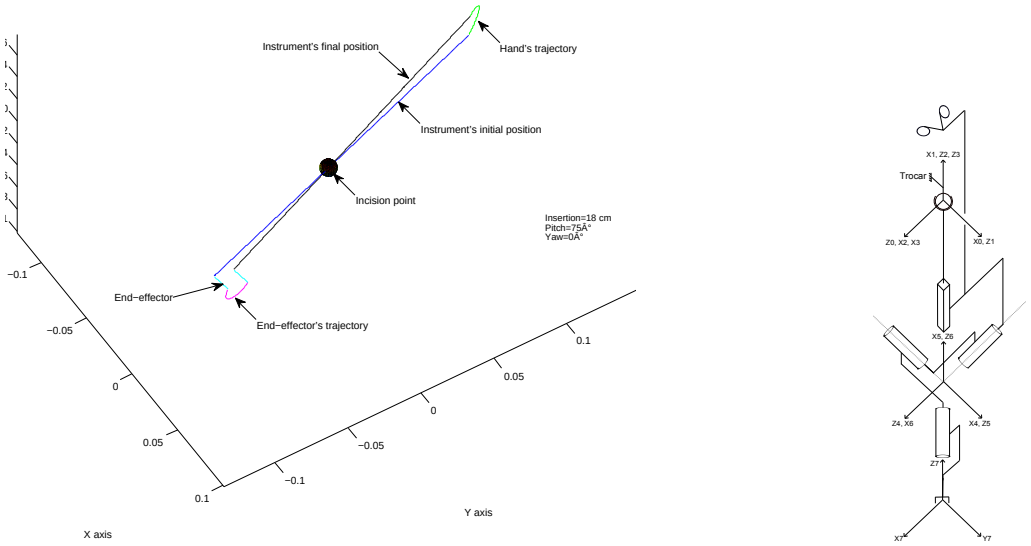

(a) YPR

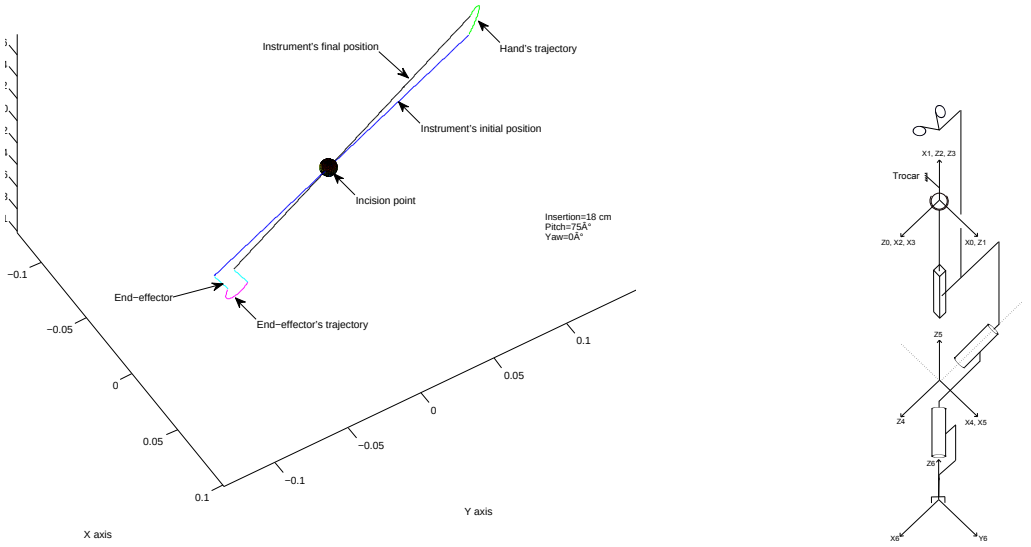

(c) YR

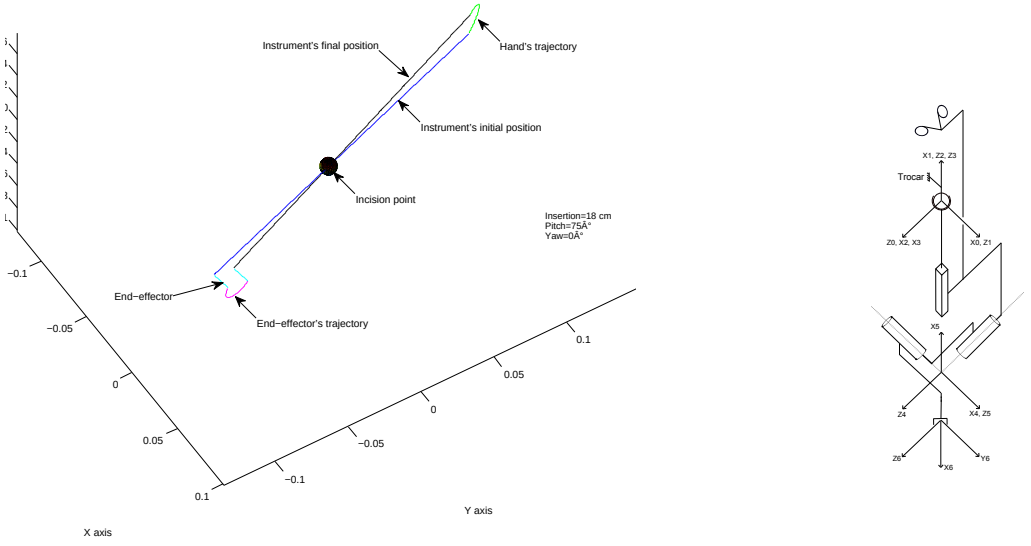

(e) YP

Figure 4.5: Hand's trajectory in a perfect stitch

evolution of the instrument's 6 DOF using each of the kinematics.

In contrary, the wrist's DOF and the shaft rotation with the YP kinematics evolve together in a complex manner and are very difficult to control in joint space, using the joystick and buttons on the handle. This is the main reason behind the poor results of the YP kinematics.

4.3.2 Singularity Analysis

A singular (velocity-degenerate) configuration is a configuration in which a robot manipulator has lost at least one DOF. In such a configuration, the manipulator is unable to execute an arbitrary motion. The determination of these special configurations is critical to understanding a robot manipulator's kinematics and can shed even more light on why one kinematics is more efficient than the others [Staniisic 2000].

Several methodologies exist for velocity degeneracy determination. The most common method is to evaluate expressions found by setting the determinant of the Jacobian matrix (J) to zero. This method works only for non-reduncant manipulators. For kinematically-redundant manipulators like the one with the YPR kinematics in our study, the Jacobian is not square and thus taking its determinant is not possible. Whitney [Whitney 1969] proposed using the Moore-Penrose pseudo-inverse of J (J^+) given by:

$$J^+ = J^T(JJ^T)^{-1}$$

Singular configurations occur when $|JJ^T| = 0$. Although the matrix formed by JJ^T is square, the expressions for its elements can be unwieldy. The resulting expressions for $|JJ^T|$ can be difficult to simplify, making it hard to identify degenerate configurations, as it is the case with the YPR kinematics studied here (the text file containing the expression for $|JJ^T|$ was 8 MB!).

Other methods for resolving singular configurations of redundant manipulators have been presented in the litterature. Using a modified-Gram-Schmidt-based decomposition of screws, Podhorodeski et al. [Podhorodeski 1989] identified a methode for calculating singular configurations of kinematically-redundant manipulators. An alternative methode would be to consider the conditions that would make all normally non-singular 6x6 sub-matrices of J concurrently singular [Podhorodeski 2000]. For a 6 DOF manipulator performing a 6 DOF task, a singularity occurs when the manipulator's joints become linearly dependant. A spatial joint-redundant manipulator will not be singular, if the screw coordinates of any six of its joints span the 6-system

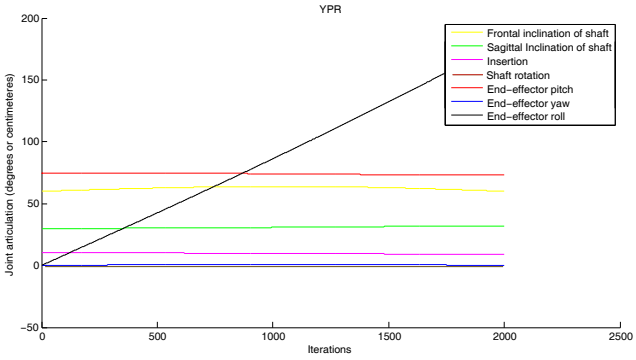

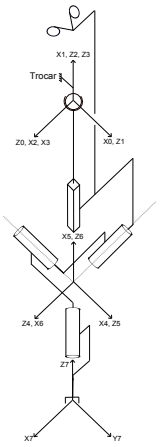

(a) YPR

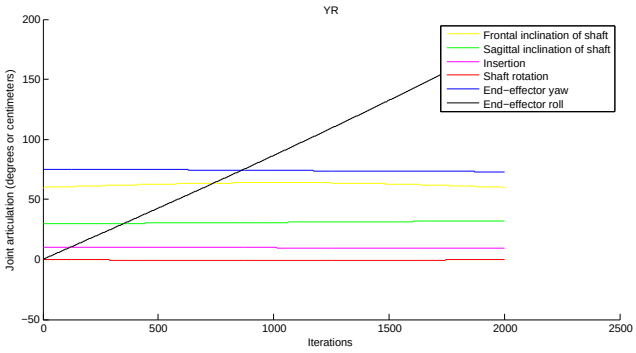

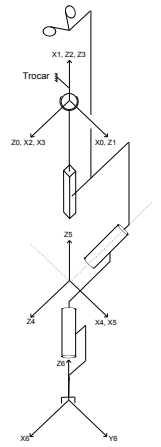

(c) YR

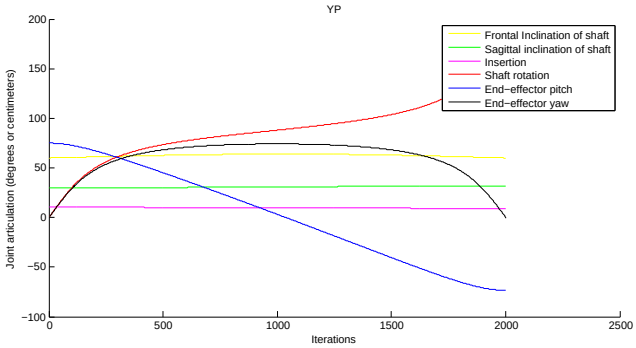

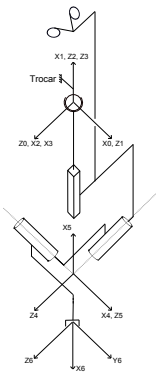

(e) YP

Figure 4.6: Evolution of joint angles during a half-circle perfect stitch

of general spatial velocity. Therefore, singularities can be determined by examining the determinants of 6-joint screw-coordinate matrices (SCMs). A 6-joint SCM is a 6×6 matrix comprised of the screw coordinates of a combination of 6 of the joints of the redundant manipulator. For example, for a 7 DOF manipulator, 7 unique 6-joint SCMs exist. A singularity in a 7-DOF manipulator occurs:

$iff\ |J_i| = 0,\ i = 1\ to\ 7$

where

$J_i = [...\$_j...],\ j \neq i$

with $\$_j$ indicating the screw coordinates of the j^{th} joint axis.

In order to make this section lighter, the mathematical calculations regarding singularaties for the 3 kinematics studied in this chapter are presented in App. C. Here, we are going to proceed with analyzing the results.

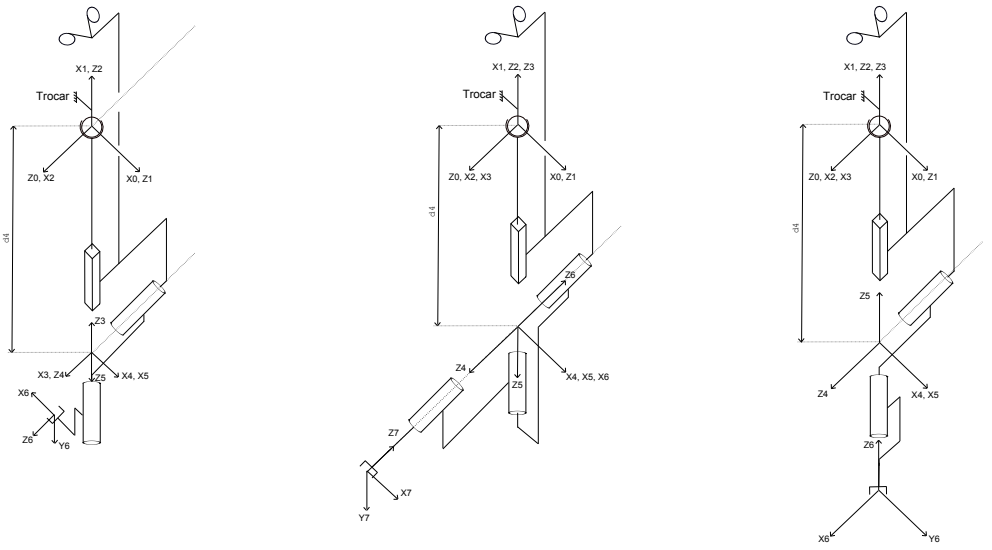

(a) YP wrist singularity

(b) YPR wrist singularity

(c) YR wrist singularity

Figure 4.7: Manipulator singularities for $d_4 \neq 0$

For all the 3 kinematics, a singularity occurs when:

$d_4 = 0$

This is when the shaft translation is zero, and the axes of inclination of the shaft and the intra corporeal wrist are merged (z_0 merged with z_4 and z_1 with z_5). But this configuration does not happen during any manipulation task, as intra corporeal manipulation is done with $d_4 \neq 0$

Apart from the holder's singularities, the intra corporeal wrists have also singularities of their own. For the YP kinematics, a singular configuration occurs when $\theta_5 = 0$ *or* π. Fig. 4.7a this configuration for $\theta_5 = 0$. The end effector is inclined for 90° and the wrist's second inclination axis (z_5) is merged with the shaft's rotation axis (z_2). This configuration can happen regularly during stitching, with the end effector inclined for 90° or near 90° to put the needle in right plane. With 1 less wrist DOF, the user will not be able to rotate the needle to finish the stitch.

The wrist singularity of the YP kinematics is another reason behind the poor results of stitching exercises with this kinematics.

For the YPR kinematics, a singular configuration occurs when $\theta_5 = 0$ *or* π *and* $\theta_6 = 0$ *or* π. Fig. 4.7b shows this configuration for $\theta_5 = 0$ *and* $\theta_6 = 0$. z_6 is merged with z_4 and the end effector has no more than 5 DOF (see Fig. 4.7b). This configuration may occur during stitching when the user tries to put the needle in the right plane. In this case, the user can still do the rotational stitching motion if the needle is in the right plane, but reorienting the needle to change the stitching plane is more difficult, and the end effector motions become easily confusing for the user as they do not correspond to his/her visuomotor expectations (e.g. the handle command that made the end effector incline, makes it rotate about the shaft axis in this configuration).

The wrist singularity of the YPR kinematics makes it more difficult to control.

For the YR kinematics, a singular configuration occurs when $\theta_5 = 0$ *or* π. Fig. 4.7c this configuration. The end effector is not inclined and the it is along the shaft axis. z_5 is merged with z_2 and the rotation along the instrument shaft produces the same motion as the rotation along the end effector axis. However, this singular configuration is not a problem. The instrument in this configuration is usually used for simple manipulation tasks that do not need 6 DOF motions. More complex tasks that need dexterous motions usually make the user bend the end effector to correctly orient the end effector. This will put the manipulator out of the singular configuration and it will maintain its 6 DOF.

The YR kinematics does not have any singularity when used in complex tasks that need dexterous manipulation of the end effector.

4.4 Conclusion

In this chapter, dexterous kinematics of a hand-held instrument were studied. 3 kinematics were compared in terms of TCT in stitching using our VR Simulator.

The results show that the YR and YPR kinematics are largely better than the YP kinematics, in terms of mean TCT. The performance difference between YR and YPR kinematics is statically significant. The YR kinematics has a lower mean TCT than YPR or YP kinematics.

The YR kinematics does not lose its DOF during dexterous manipulation due to singular configuration. Besides, it is more affordable technologically to make an YR mesoscale wrist than a YPR one.

The choice of handle and control mode for a hand-held laparoscopic instrument was made thanks to the study of Chapter 3. The results of this chapter determined that among the 3 tested kinematics, the YR kinematics is the best choice for a laparoscopic instrument. To complete our fundamental study of serial comanipulation for laparoscopy, an ergonomic solution for the human-robot interface is needed. This question will be addressed in the following chapter.

Chapter 5

Ergonomics of the Instrument

5.1 Introduction

Numerous studies in the operating room or on pelvitrainer or simulator, as well as wide surveys of surgeons performing laparoscopy, have demonstrated that they operate in non-ergonomic conditions [Cuschieri 1995, Person 2001, Vereczkei 2004, Wauben 2006]. Monoscopic vision on a screen, absence of direct view of the operating scene and the unnatural line of sight, inversion and scaling of movements, and reduced mobility due to the passage through the abdominal wall are all problems that contribute to the non-ergonomic nature of laparoscopic surgery.

There is evidence that the general lack of ergonomics in laparoscopy is also a source of pain and discomfort for surgeons [Berguer 2006, Berguer 2001]. This pain is particularly due to increased efforts in the upper limb. Stiffness of neck and back also appear because of the static position of trunk and head, a result of the surgeon's watching the screen most of the time [Berguer 1999]. Most instruments are operated with the thumb and application of too much force on the small contact surface compresses the nerves, causing numbness in thumb and consequently in hand.

The shape and mechanical structure of the handle in conventional laparoscopic instruments are also seriously questioned [Berguer 1997, Berguer 1998, Emam 2001, Ahmed 2004]. The configuration of the handle (pistol) with respect to the shaft and its considerable length (required to reach remote areas of the peritoneal cavity) increase the amplitude of upper limb movements and stress the shoulder (internal rotation), the elbow (flexion) and above all the wrist (flexion, ulnar deviation, supination) [Nguyen 2001]. Specific arm posture, coupled with the low mechanical efficiency of opening and closing the grasper, increase the muscular effort significantly.

Besides instructions for improvement of the ergonomic configuration of the operating room (trocar placement, positioning of the screens, adjusting the table) that surgeons can use to be in the best possible posture (Fig. 5.1), the development of new instruments can greatly improve comfort and

quality of laparoscopic surgery [Matern 1999, Tendick 1997]. In particular, two approaches are regularly put forward: increasing intracorporeal mobilities by placing various joints at the distal end of the instrument, and developing more ergonomic handles.

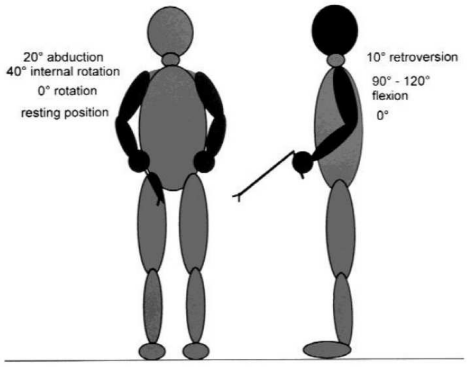

Figure 5.1: Ideal posture for laparoscopy [Matern 1999]

The first approach was exlored in the previous chapters. The second approach, i.e. the study of ergonomic handles, adapted to hand's shape and enabling the surgeons to control the additional mobilities of the instrument comfortably is the subject of this chapter. The Nunchuck handle used in previous evaluation tests has an ergonomic design and allows the user to have a firm, yet comfortable grip on it. However, it does not solve the problem of difficult postures, in which the surgeon has to raise his/her elbow, turn his/her arm outward/inward or bend his/her wrist when using conventional instruments.

In this chapter, a novel solution to the problem of non-ergonomic postures in laparoscopy is proposed. It consists of putting a free (passive) knee-joint between the instrument's handle and its shaft. Using this passive articulated handle, the surgeon would avoid non-ergonomic postures by holding his/her arm in a natural posture close to his/her body when inclining the instrument around the incision point (Fig. 5.2). The use of a passive joint also implies motorized actuation of the rotation of the shaft by means of an electrical actuator. This would further help the ergonomics of the instrument, although it would complicate its mechatronic design.

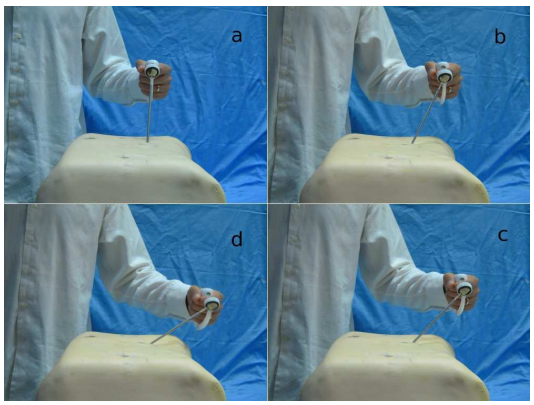

Figure 5.2: Using the passive articulated handle to avoid non-ergonomic postures

5.2 Evaluation Tests

5.2.1 Objectives & Methodology

The performance of the proposed solution should be evaluated through experiments. The first goal is to quantify the ergonomics of the new handle in comparison with other types of handle (the performance of internal mobilities was previously validated in Chapter 4). It is necessary to prove an ergonomic improvement in terms of enhanced posture of the surgeon, decreased range of arm and hand motion, and minimized intramuscular workload. As before, the VR Simulator is used to perform simple, but representative tasks using different instruments.

The next step is to globally assess and validate the proposed solution by measuring the gesture quality and the surgeon's performance with this instrument and comparing it to that obtained with the other instruments.

5.2.2 Scenario

The tests are conducted under conditions as close as possible to current clinical practice as recommended by standard ergonomics guidelines [Berguer 2006, Cuschieri 1995]:

- A pelvitrainer is placed on an adjustable table according to the surgeon's height, so that he/she is in a posture close to the ideal posture of Fig. 5.1.

- The participants stand in front of the pelvitrainer, in accordance to common operating room practice.
- The display screen is placed in front of the participant's trunk, so that his/her line of sight is inclined about 25° downwards. The virtual endoscope's line of sight is 45° deviated from vertical.
- Trocars are placed on the vertices of an equilateral triangle with about 10 cm sides. Two instruments are handled by the participant: a conventional one in his/her minor hand and the instrument being evaluated in his/her major hand. Some exercises require only one hand and in this case, the participant should just make sure he/she does not commit any errors with the minor hand (moving the instrument out of sight of the camera, unintentional contact with an object).

5.2.3 Exercises

For our purpose of evaluating both performance and ergonomics, we needed a series of task that are at the same time limited in number and time, and representative of laparoscopic tasks. Exercise groups that were chosen for the tests of this chapter are therefore as follows:

- The first exercise group, a series of kinematic manipulations derived from the classification of Cao et al. [Cao 1996], designed primarily to analyze the movements of the surgeon's arm. The Pointing task on the VR Simulator is used for this purpose (see Fig. 5.3a). It comprises 3 of the 5 basic laparoscopic tasks mentioned by [Cao 1996]: push, pull and reach. The tasks of opening and closing the end effector should not cause significant movements of the arm and thus present no interest in this study. Moreover, there is no need to use the distal mobilities of the instrument for the pointing task. The exercise is still feasible with a conventional instrument that serves as reference.
- The next exercise group, a series of Pick & Place exercises, to assess the gesture quality with each instrument. This task is inspired from the first task in the protocol of [Derossis 1998]: catch an object by the minor instrument and transfer it to the major one, then place it in a receptacle (see Fig. 5.3b). The cutting task proposed in the protocol of [Derossis 1998] is not simulated as cutting along a prescribed path without force feedback appears to be very difficult and not representative of the reality.

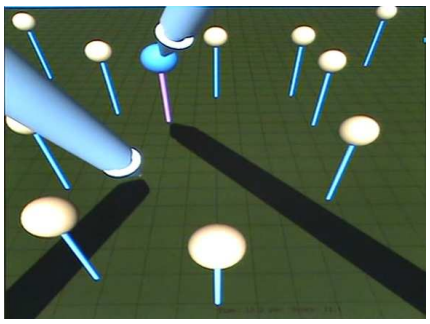

(a) Pointing

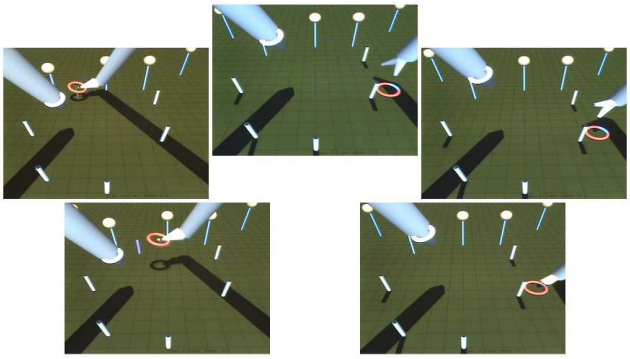

(b) Pick & Place

Figure 5.3: The scene on the simulator's screen for the 2 exercises used in the ergonomics evaluation

These tasks are different from the stitching task used in our previous studies of Chapters 3 and 4. Indeed, the stitching task used in previous chapters does not seem to suit the purpose of ergonomic evaluation tests. The stitching task requires high dexterity, but does not demand the arm's DOF greatly. It is suitable to compare instruments from a dexterity point of view, but it would not be able to differentiate precisely the instruments from an ergonomics point of view.

Each of the 2 exercises is repeated with 3 different instruments:

- a conventional laparoscopic instrument (Fig. 5.4a)
- a dexterous instrument with a fixed finger-operated handle (Fig. 5.4b)
- a dexterous instrument with a finger-operated handle and a free knee-joint between the handle and the shaft (Fig. 5.4c)

The dexterous instruments have the same handle and control mode that was validated in Chapter 3 and the optimal Y-R kinematics, validated in

Chapter 4. The difference between the 2 dexterous kinematics is the rotation of the shaft, which is motorized and controlled by the joystick in the instrument with knee-joint (Fig. 5.4). The order in which each participant uses the 3 instruments varies randomly and is discussed later. A conventional instrument is held in the minor hand, as explained previously.

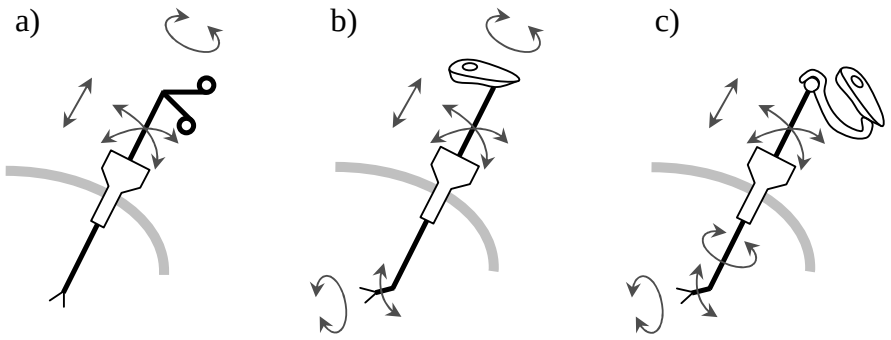

Figure 5.4: Principles of working of the 3 compared instruments a) conventional instrument with 4 manual DOF, b) instrument with fixed handle, 4 manual DOF and 2 robotic DOF c) instrument with a free knee-joint, 3 manual DOF and 3 robotic DOF

5.2.4 Ergonomics Metrics

The Rapid Upper Limb Assessment (RULA [McAtamney 1993]) is a method of quantifying the ergonomics of work environment on a scale of 1 to 7. The RULA score is calculated from the upper limb members angles, general posture of trunk and neck, muscular load and temporal evolution of posture[1]. It is based on a table (see Appendix E), where a series of angles between different segments of the arms and the trunk are given in detail to calculate the RULA score. A low score indicates an acceptable posture, while a score of 7 means urgent stop of the work.

Person et al. [Person 2001] established a real-time ergonomics index based on RULA, adapted to laparoscopic surgery. This index takes into account the movements of both arms, the trunk and the neck and is calculated Using position sensors placed on the torso.

For our study that concentrates on the arm to evaluate the ergonomic performance of each instrument's handle, a modified RULA index adapted

[1] A static posture is not desired.

to this purpose was used: the general posture of trunk and neck and the muscular load vary little during laparoscopic surgery, and this part of score is calculated only once, while the arm is constantly moving and the part of the score related to the arm has to be calculated in real time.

The movements of the different segments of the upper limb are recorded during the tests, using the Codamotion®system — that consists of a set of infrared cameras and infrared active markers placed on those segments —, at a frequency of 10 Hz. The spatial positions of 7 points on the participant's major arm are recorded: left and right acromioclavicular joints (shoulder), lateral and radial epicondyle (elbow), ulnar and radial styloid (Wrist) and end of the metacarpal of the hand (see[2] Fig. 5.5). The shoulder elevation angle, the elbow flexion angle, the wrist flexion and deviation angles and the forearm rotation angle are calculated from the marker positions.

In order to calculate these angles, a series of planes and axes need to be reconstructed. The detailed calculations of the angles used in RULA are explained in Appendix D. The minor arm's ergonomics is not included as most of the manipulation is undertaken by the major arm. In post-treatment, the angles of interest for the RULA score are calculated using the positions of the markers. There is a chance that a marker is hidden from the Codamotion cameras for brief periods of time. The visibility state of each marker is saved along with its position, and can be used later to interpolate missing positions. The maximum and average values of the index during a test is used as an ergonomics metrics for an instrument [3].

5.2.5 Gesture Quality Metrics

Satava et al. [Satava 2003] presented a complete state of the art of laparoscopic skill assessment devices and metrics. The gesture quality is usually measured through different simple metrics, such as the duration or the number of movements to accomplish a task, the total distance traveled by the end of the instrument and the velocities and accelerations spectrum (slower movements and fluid being considered better than sudden jerky movements).

In this study, 3 metrics are used to measure the performance or the gesture quality of an instrument:

[2]In Fig. 5.5b, the stars indicate arm joints and the circles indicate points followed by CodaMotion (markers).

[3]The RULA score is calculated in real time during a test. The average RULA score is the average of instantaneous RULA scores over the period of the test. The maximum (Max.) and minimum (Min.) RULA scores are the Max. and Min. values of the instantaneous RULA scores.

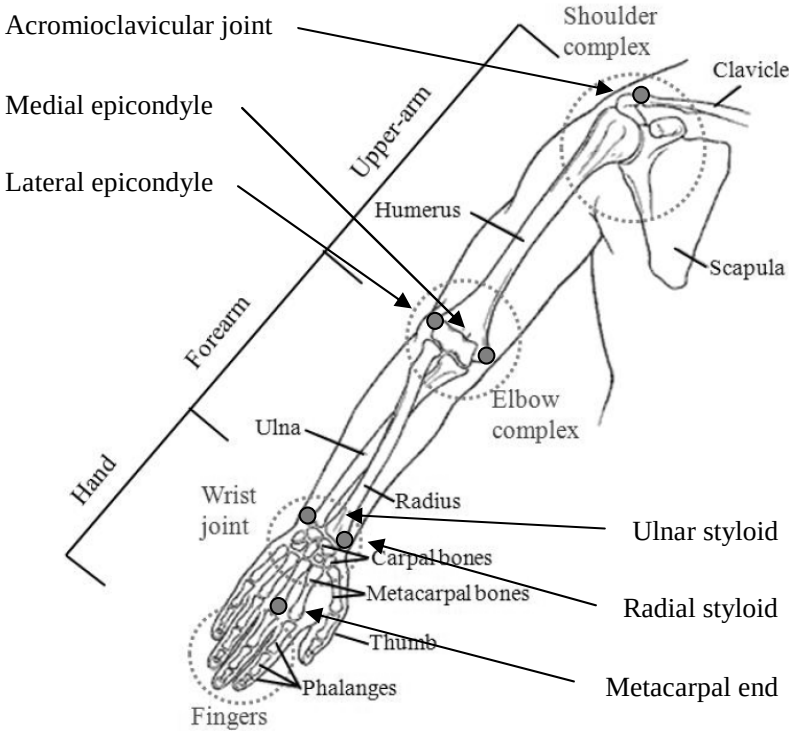

(a) Position of markers on the arm[Gopura 2009]

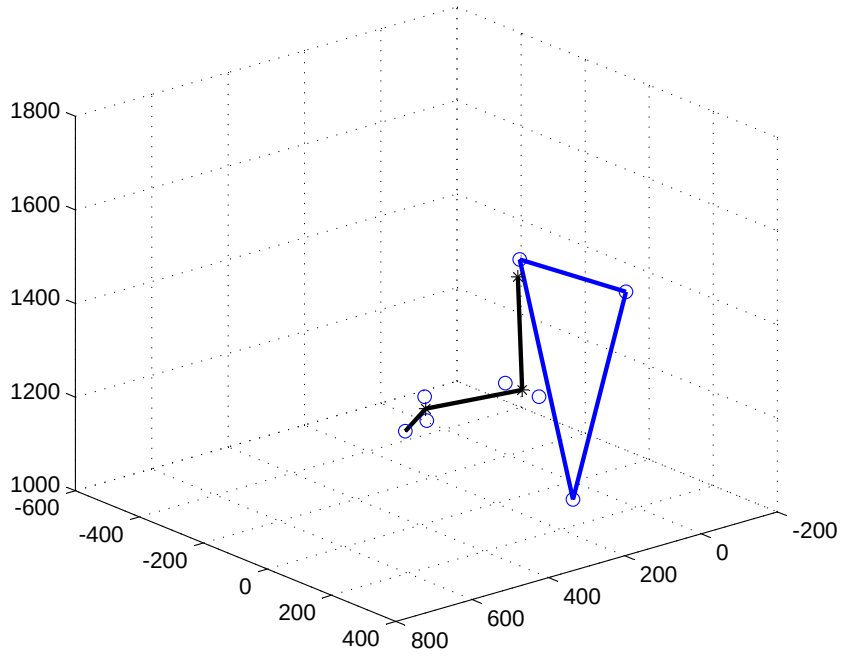

(b) Arm segments and joint angles reconstructed in Matlab

Figure 5.5: CodaMotion markers placed on the arm for calculating joint angles and RULA score

- time to completion of task (TTC)
- motion economy[4] (Eco)
- number of errors (Err), i.e. the number of times an instrument goes out of the visual field or passes through a solid object during a test

5.2.5.1 Learning Curve

To ensure that test results are representative, it is essential to compare the gestures at the same level of proficiency of each instrument. To achieve this purpose, a learning phase precedes each test with each instrument.

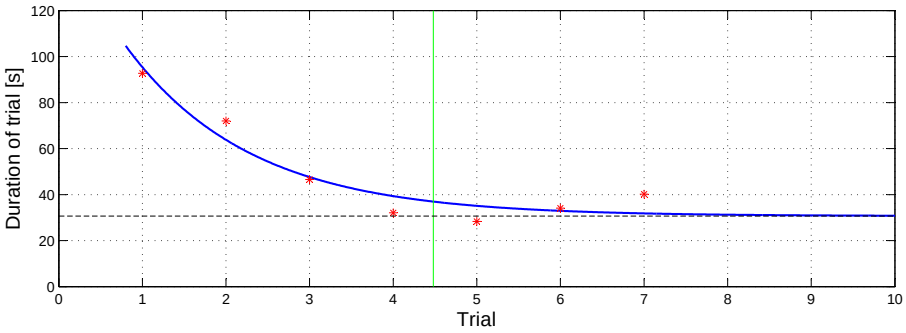

Figure 5.6: A typical learning curve

During a learning phase, a short exercise of the test is repeated several times and the duration (TTC) of each trial is saved. After each trial, an approximation of the exponential learning curve is calculated: $y = Ae^{-\frac{x}{\tau}} + B$ where y is the duration of the x^{th} trial. The constant τ gives an indication of the time required to reach characteristic plateau of the curves (where the exercise duration does not vary anymore). It is believed that this plateau is reached after 3τ tests. The constant B is the asymptotic height of the plateau (duration of test after the learning phase) and the report between B and A gives an idea of the progress made in learning (Fig. 5.6).

5.2.6 Protocol

The tests were conducted with 2 different groups of participants:

[4]Motion economy is defined in [Feng 2008] as the ratio between the total length traveled and minimum possible length to complete the task.

1. 6 Ph.D. engineering students with no experience in laparoscopy, but used to playing video games.

2. 10 surgeons with different specialties in urological, gastric or gynecologic surgery and various levels of expertise in laparoscopy and surgical robotics (see App. F for more detailed information on the surgeon participants).

Each participant does the 2 tasks of Pointing and Pick & Place with each instrument. Each of these tasks is done in 2 phases: the learning phase and the recording phase. During the learning phase, the learning curve is reconstructed until it reaches its plateau. Then the recording phase is done where the kinematics of the arm is recorded by CodaMotion and the gesture quality metrics are recorded by the VR Simulator. The complete protocol for each participant consists of the following steps:

1. Explications for the participant regarding the tests and their objectives. It is insisted upon the point that the instruments are compared and not the subjects, and that the participant has to try and do the tasks as fast as possible, following the shortest path possible, while avoiding errors. The CodaMotion markers are fixed on the major arm and shoulders and the calibration phase to find the shoulder's center of rotation is done.

2. Learning phase with a short Pointing exercise with the conventional instrument.

3. Pointing exercise with the conventional instrument.

4. After a short pause, Learning phase with a short Pick & Place exercise with the conventional instrument.

5. Pick & Place exercise with the conventional instrument.

6. Steps 2 to 5 are repeated with the first dexterous instrument, then with the second dexterous instrument.

The order in which the 2 dexterous instruments are used varies among participants in order to minimize the effect of learning the exercises with an instrument on the results of the other instrument (performance results with the last instrument could be better without this being directly linked to that particular instrument).

5.3 Results

The results of these tests can be analyzed in 2 groups: the RULA score of participants can be used to compare the 3 tested instruments from the ergonomics point of view, the gesture quality metrics can be used to compare the 3 tested instruments from the dexterity point of view. In this way, the instruments will be ranked both based on their dexterity and their ergonomics.

5.3.1 Ergonomics

During the Pointing task, each participant had the possibility to use only the manual DOF of the instrument to go from the current position to a desired position. The additional DOF of the dexterous instruments were not needed and thus, the difference in the results reflects only the influence of the instrument's handle.

5.3.1.1 Pointing

Fig. 5.7 shows the average RULA score for each participant using the 3 instruments for the Pointing task.

In order to see if there's a statistically significant difference between the instruments, an ANOVA test was done on the 3 sets of data in each of the 2 groups of participants. The test does not show a significant difference between the 3 instruments for the inexperienced participants. Nor does it show a significant difference between the instruments for surgeons (p=0.06). This is not very surprising, as the pointing task does not require a dexterous instrument and does not strain the participant's arm over long periods of time.

Fig. 5.8 is a statistical representation of all RULA scores for the Pointing task[5].

The average RULA score does not show, however, if there has been moments where the participant had momentary very high RULA score. We are going to look at the maximum RULA (Max. RULA) scores for each instrument to see if one of them forces the arm into non-ergonomic poses at certain

[5]Each group of data is centered on the mean value of all average RULA scores for that group. The rectangular box's upper and lower limits are $\pm\sigma$ of this mean value, where σ is the mean value of standard deviation of RULA scores for the group. The high and low points of each group are the mean values of maximum and minimum RULA scores for the group.

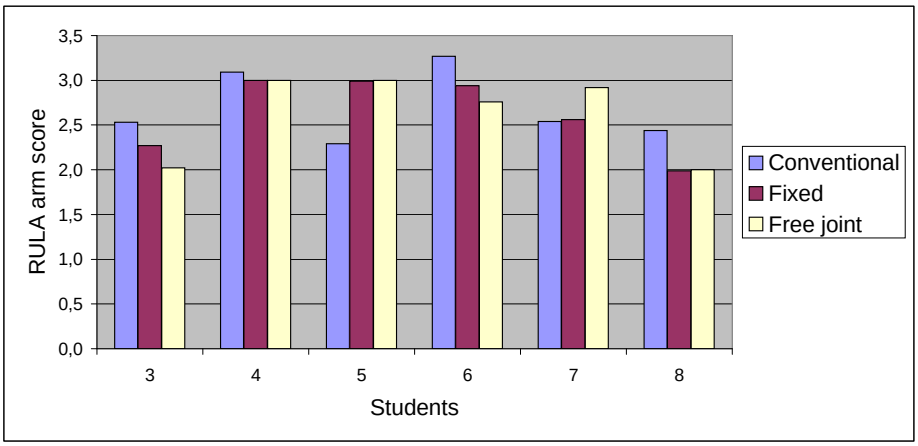

(a) Students

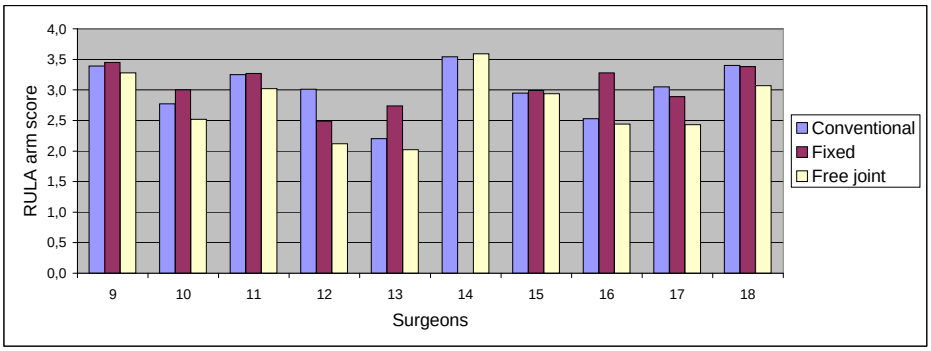

(b) Surgeons

Figure 5.7: Average RULA score of Pointing task for different participants

moments. The ANOVA test of the average Max. RULA scores for each instrument, shows a significant difference between the 3 instruments due to the influence of the handle ($p<0.003$) for both groups. The passive articulated handle has in average a lower Max. score, compared to the other 2 instruments, both for experts and inexperienced participants.

This means that the free joint can at least remove the momentary strains on the arm during the pointing task.

5.3.1.2 Pick & Place

Fig. 5.9 show the average RULA score for each participant using the 3 instruments for the Pick & Place task.

The ANOVA test of the results shows a significant difference between the

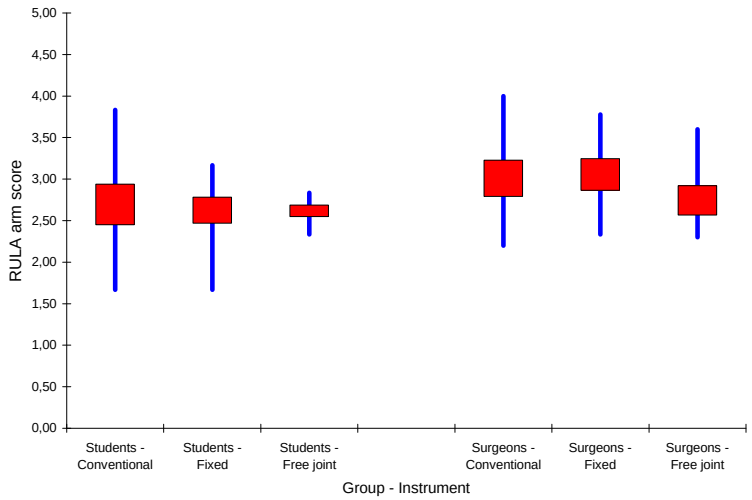

Figure 5.8: Statistical representation of RULA scores of Pointing task for different participants

instruments for the inexperienced participants ($p<0.001$). The 2 dexterous instruments are more ergonomic than the conventional instrument (Fig. 5.10). The tendency is more visible according to Max. RULA scores ($p<0.001$).

The difference between instruments is not significant among the surgeons, which can be related to the surgeons expertise with the conventional instrument, and the fact that they reproduce the same gestures out of habit, even with the dexterous instruments.

Comparing the two levels of expertise, there is a significant difference in average RULA scores between the surgeons and the inexperienced participants ($p<0.001$). The inexperienced participants have a higher average RULA score with the conventional instrument. This can be related to the fact that the surgeons have learned to use the conventional instrument as ergonomically as possible without straining their arm extensively and non-ergonomically. On the other hand, the inexperienced participants have a lower average RULA score, compared to the surgeons, with the dexterous instruments, especially the one with a free joint. This is because they do not have any habitual movements and they intuitively use the free joint to their ergonomic profit. The same tendency is visible according to Max. RULA scores ($p<0.05$).

This shows that the free joint has the potential of being ergonomically very effective and the surgeons can learn to use it, too.

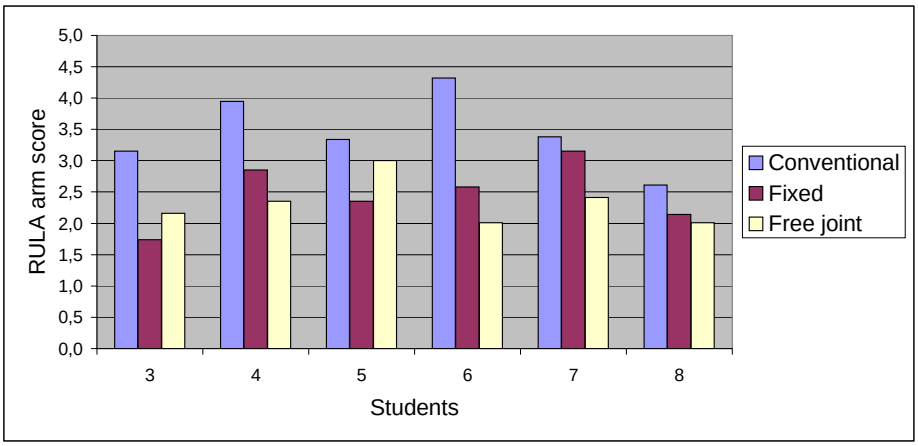

(a) Students

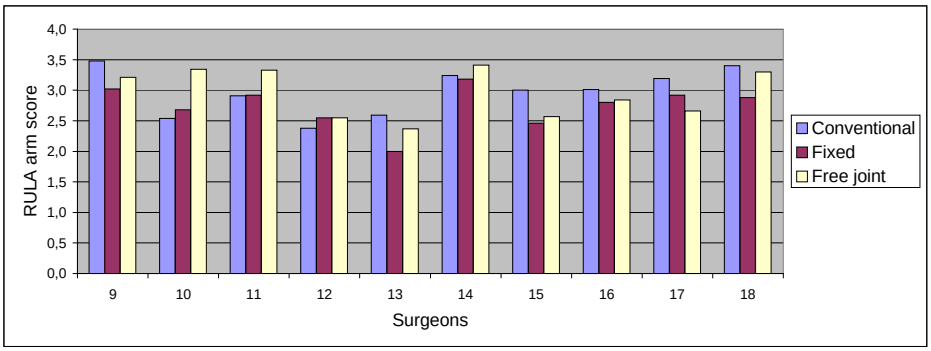

(b) Surgeons

Figure 5.9: Average RULA score of Pick & Place task for different participants

5.3.2 Gesture Quality

5.3.2.1 Pointing

The TTC results (Fig. 5.11) show that the instrument with a passive articulated handle — which was more ergonomic — has the highest TTC both for surgeons and inexperienced participants ($p<0.001$).

Besides, this instrument has the worst motion economy ($p<0.001$) (Fig. 5.12).

Another interesting outcome is the superiority of surgeons to inexperienced participants. Surgeons use shorter paths and have a better motion economy with all instruments compared to inexperienced participants.

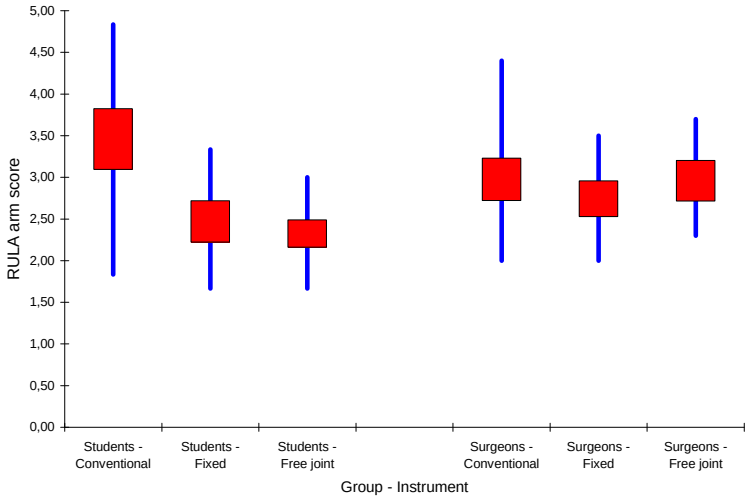

Figure 5.10: Statistical representation of average RULA scores of Pick & Place task for different participants

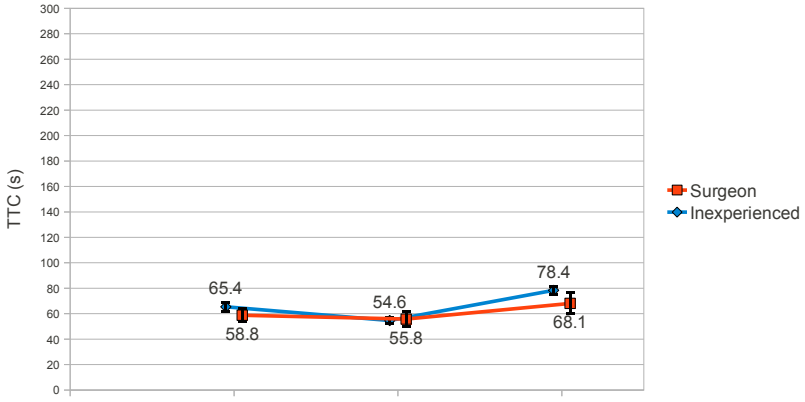

Figure 5.11: Statistical representation of TTC results for different participants

5.3.2.2 Pick & Place

Looking at the TTC measurements of the Pick & Place task (Fig. 5.13), a significant difference between the dexterous instruments and the conventional instrument is visible ($p<0.05$). As said before, this is related to the need for reorienting the objects in the Pick & Place task.

A similar tendency can be seen in the motion economy, where the dexterous instrument with a fixed handle has the lowest path length and thus the best motion economy (Fig. 5.14).

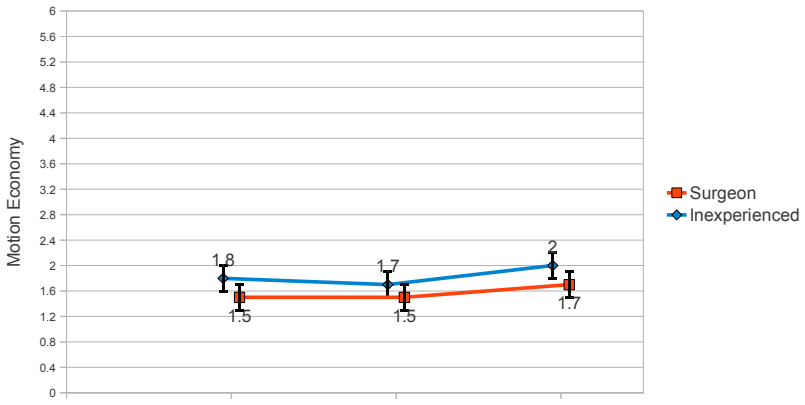

Figure 5.12: Statistical representation of motion economy results for different participants

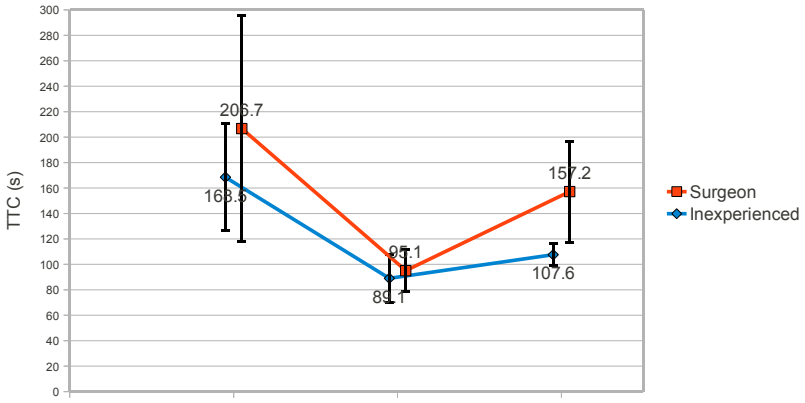

Figure 5.13: Statistical representation of TTC results for different participants

These results show that the instrument with an articulated handle is the least efficient while the dexterous instrument with a fixed handle is the most efficient.

5.4 Conclusion

In this study 16 participants in 2 groups with different levels of expertise evaluated 3 different instruments in 2 types of tasks, representative of most gestures in laparoscopy. Although the number of experiences is limited and, as a result, the significance limit ($p<0.01$ or $p<0.05$) is not always reached, certain tendencies are visible in the results.

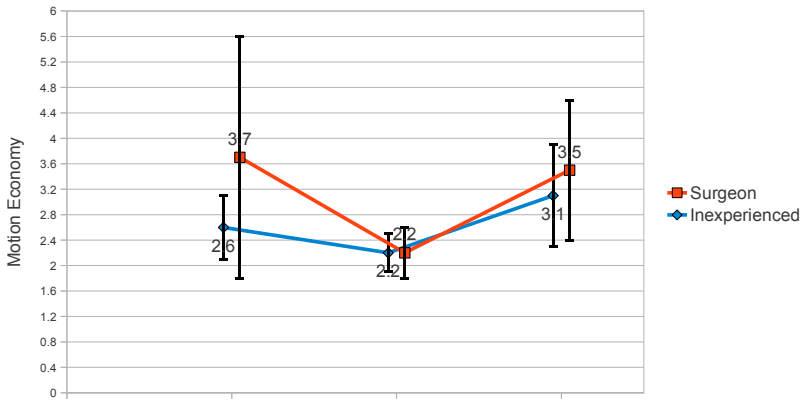

Figure 5.14: Statistical representation of motion economy results for different participants

The results of the Pointing task showed the difference between the instrument with a passive articulated handle and the other 2 instruments in terms of ergonomics and performance. But they did not differentiate clearly between those 2 instruments, i.e. the conventional laparoscopic instrument and the 6 DOF dexterous instrument with a fixed handle, because the task did not need the additional DOF and the control mode of the 2 instruments stays the same.

In the Pick & Place task, one needs to use the additional intracorporeal DOF for correct reorientation of the end effector during both phases of picking and placing. With a conventional instrument, one has to use the instrument in his/her minor hand to transfer the object between the 2 instruments and reorient. This increases the time and path length needed to complete the manipulation task, and shows the advantage of the 2 dexterous instruments over the conventional instrument.

From an ergonomics point of view, the novel solution of adding a free (passive) 3 DOF knee-joint to the handle seems to be effective. The instrument with the passive articulation has the lowest average RULA score in the Pick & Place task. Besides, a significant progress margin is visible for the surgeons to improve their posture during laparoscopy using a handle with a free joint. This is an interesting and encouraging result as none of the existing instruments in the context of serial comanipulation has a solution to the problem of ergonomics.

From an efficiency point of view, the free joint handle is not the best solution among the 3 instruments. The dexterous instrument with a fixed

handle is either the most efficient or as efficient as the conventional instrument. This is because controlling the position of the end effector is more difficult with the passive articulation. The reason behind this may be that with a passive knee joint at the handle, the user has to control the movements of the handle in a decoupled manner. While the position of the handle is directly related to the position of the end effector and has to be controled for best performance, the user controls the orientation of the handle aiming for an improvement in his ergonomics.

It would be interesting to work on this solution to improve it for more efficiency. A possible solution is a lockable free joint that lets the surgeon put his arm in a comfortable position according to the task in hand, then lock the joint to regain a better control over the instrument position.

Chapter 6

Mechatronic Design of a Prototype

In this chapter, a novel hand-held mechatronic instrument is presented that is designed based on the simulation results of the previous 3 chapters. According to the results of Chapter 4 The instrument has a yaw-roll wrist added to its end effector.

Based on the results of Chapter 3 the instrument is controlled using an ergonomic handle with a inverse control mode, that makes the end effector movements identical to those of the handle. The handle used in this proof-of-concept prototype is a Nunchuck handle from Nintendo, the same finger-operated handle that was used in the simulator.

The passive articulation between the handle and the shaft that showed to be a good solution to the ergonomics problem of a hand-held instrument in Chapter 4 is used also in the prototype.

6.1 Prototype design

6.1.1 General Description

The prototype instrument is composed of these parts:

- an ergonomic handle
- a 39 cm long shaft with a 5 mm diameter
- a multi-DOF distal tip
- an active trocar
- a electronic controller board.

Fig. 6.1.1 shows the instrument prototype and its kinematics. The instrument has a total of six DOF of which three DOF are manual and the other three, i.e. rotating the shaft, bending and rotating the distal tip, are robotic. To use the instrument, the active trocar is plugged on top of a medical trocar and the shaft of the instrument passes through both trocars.

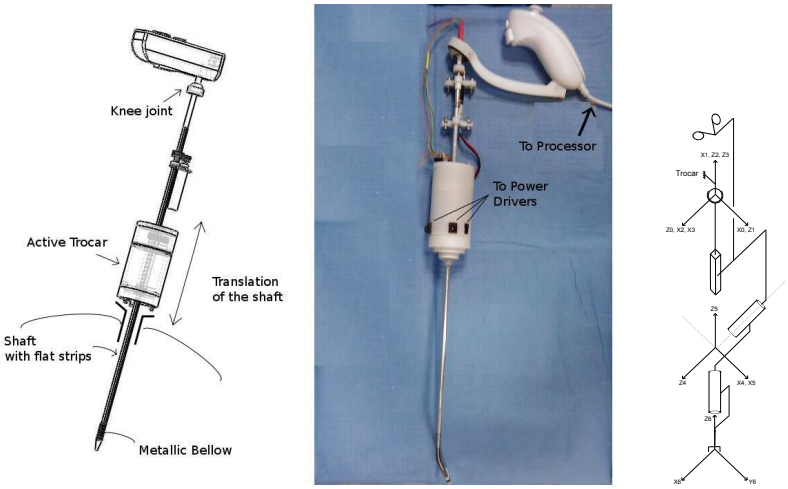

(a) The prototype instrument and its general schema (b) Instrument's 6 DOF kinematics

The handle is connected to the controller board through an I2C interface. The microcontroller on the board receives control signals from the handle and generates corresponding PWM signals for the power driver that in turn powers the actuators on the active trocar and the shaft (Fig. 6.1).

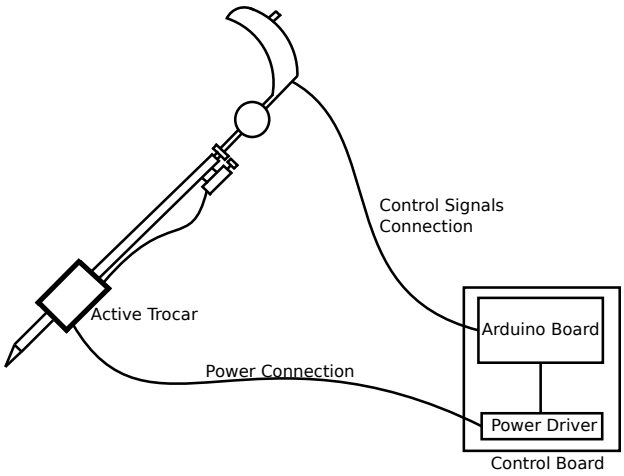

Figure 6.1: Synoptic principles of operation

The controller unit is composed of a microcontroller (an Atmel ATmega 328 on an Arduino Nano development board) and power drivers and is placed away from the instrument in the non-sterile zone and communicates with the handle through an electrical cable. The actuators are powered through the active trocar.

6.1.2 Ergonomic Handle

The handle we used for the prototype is a Wii Nunchuck controller. It has the advantage of being ergonomically designed, so the user has a good grip on it. It is available off the shelf and can be connected to a microcontroller through its I2C interface. On the handle, there are 2 buttons, and a joystick (Fig. 6.2).

Figure 6.2: The instrument's ergonomic handle

The mechanical connection between the handle and the shaft is made by a spheric joint (Igus EGLM-16 with a pivoting angle of approximately 70°) giving the surgeon complete three dimensional freedom and relieving his arm from the mechanical constraints imposed by the instrument's position. In this way, the surgeon's arm stays almost all the time near his body with his elbow lowered and his wrist straight (see Fig. 5.2). This greatly reduces the stress on the arm and the postoperative fatigue.

The shaft is connected to the spheric joint through a roll bearing, to compensate for the resistive momentum along the shaft axis due to friction.

6.1.3 Active Trocar

Our solution to make an ergonomic handle, the spheric joint between the handle and the shaft, makes it impossible to rotate the instrument's shaft manually. As a result, this rotation is motorized in our instrument by using an *active* trocar.

The active trocar holds a cylindric rotor concentric with the surgical trocar and an electric motor (Maxon DC motor with a 64:1 gearhead). The rotor is coupled to the motor inside with 2:1 gears. Inside the rotor is a cylindrical canal for the passage of the instrument's shaft. The shaft and the canal have two flat strips on opposite sides so that the shaft and the rotor make a 2-DOF revolute-prismatic joint together, i.e. the instrument can slide in the canal while the motorized rotation of the rotor makes the shaft rotate (see Fig. 6.3).

Except from the Nunchuck cable that goes directly to the instrument's controller unit and could easily be replaced by a wireless communication module, all the other electrical connections are on the active trocar.

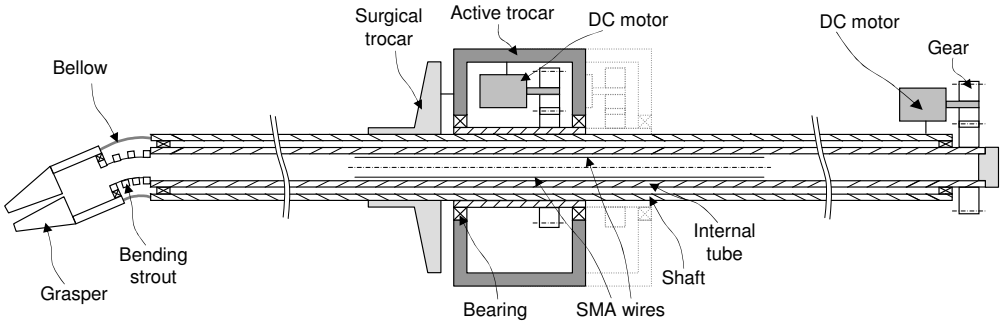

Figure 6.3: Active trocar with a double tube shaft

6.1.4 Actuation and transmission system

The shaft is composed of two centered tubes. The external tube is a 4-5 mm stainless steel tube with the two opposite flat strips on it for sliding inside the active trocar's rotor. The internal tube is a 3-4 mm aluminum tube through which all the wires pass. A motor (Maxon DC motor with 64:1 gearhead) is installed on top of the external tube and coupled to the internal tube through 2:1 gears. This motor makes relative rotation between the internal and external shafts possible.

The external tube is connected to the grasper through a bellow (see Fig. 6.3). The internal tube is connected to an articulated bending structure inside

the bellow. The articulated bending structure is borrowed from a bronchoscope (Olympus BF-P180). It is a multi-linkage sliding mechanism comprised of a cascade of pivots with parallel axes (see Fig. 6.4). The 3 distal mobilities are operated based on the following principles:

1. Shaft rotation: If the motor inside the active trocar rotates while the motor on the external tube does not, the two tubes rotate together, making the shaft turn around its axis.

2. Distal tip deflection: The bending structure is driven by two antagonist shape memory alloy (SMA) wires that continue all along the length of the instrument, inside the shaft. The SMA wires are pretensioned at the top of the shaft and powered through flexible wires connected on top of the active trocar.

3. Distal tip rotation: In order to make the distal tip turn around its own axis, the motor on the external tube turns synchronously, and in the opposite direction,with the one in the active trocar. The result is that the internal tube does not rotate with the external one, conserving the orientation of the bending structure, while the distal tip and the bellow turn around their own axis (see Fig. 6.3).

Figure 6.4: The bending structure used in the intracorporeal wrist

6.1.5 SMA Actuators Implementation and Control

The mechatronic prototypes mentioned in the state of the art section use electric motors with encoders to control the deflection of the distal tip. Using

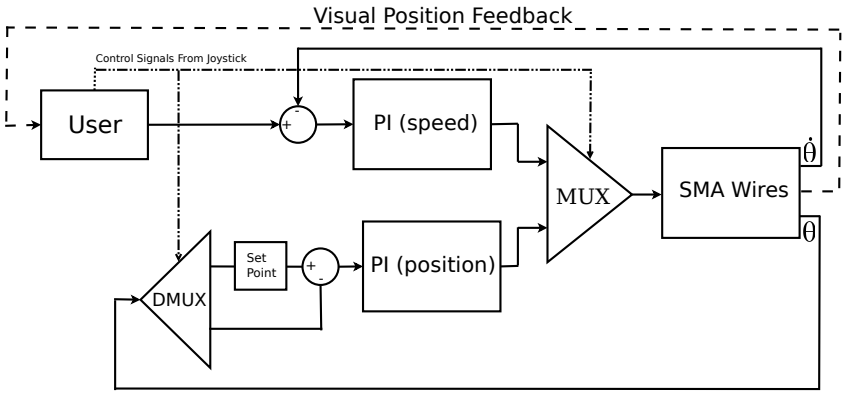

Figure 6.5: The speed-position control loop for antagonist SMA wires

SMA wires instead, we could remove the bulk of one motor from the instrument. An example of this type of actuator is the flexible distal tip with 2 DOF for endoscopic robot surgery presented in [Peirs 2002].

Control of SMA wires can be tricky considering their thermal issues, hysteresis loops and slow dynamics. México et. al [México 2004] present a miniature articulation with antagonist SMA wires and position and force control and confirms its usefulness through experiments as the first step of the development of a robot hand. The PWM technique is used to control the position through a proportional-integral (PI) controller and the force and stiffness through a proportional controller.

Ma et al. [Ma 2003] present the design and experimental results of controlling a SMA actuator using PWM to reduce the energy consumption by the SMA actuator. Experiments demonstrate that control of the SMA actuator using PWM effectively saves actuation energy while maintaining the same control accuracy as compared to continuous PD control.

The control algorithm of the SMA wires in our instrument switches between speed or position control depending on the control signals from the joystick (Fig. 6.5). When the user is commanding the deflection, the speed control loop is active. The moment he stops, the deflection of the distal tip is measured through a shape sensor placed inside the bending structure and registered as the position control loop's set point.

We used a PI controller to eliminate the steady state position error and the PWM technique to control the actuator.

In order to measure the deflection of the distal tip, a shape sensor is needed. There are fiber optics miniature shape sensors that could be used to measure the deflection of the distal tip (see Fig. 6.6b). But they can not be custom

modified for this application.

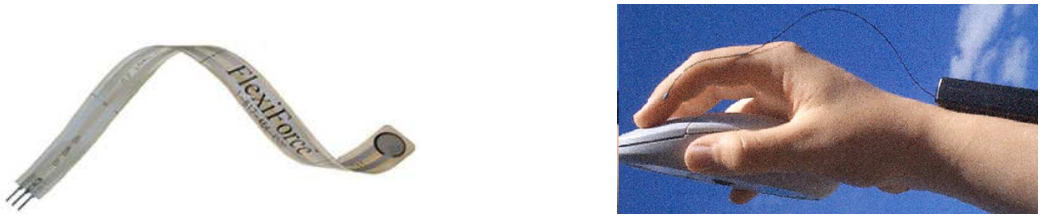

(a) resistive FlexiForce®

(b) fibre optic S720 ShapeSensor™ from Measurand

Figure 6.6: 2 types of shape sensor

The shape sensor we used is made of a carbon film on a plastic support and as a result is very low cost and can be cut to the desired form to satisfy the application's needs in terms of size and form (see Fig. 6.6a). But it is also prone to changes in its characteristics with temperature and deformations.

6.1.6 Distal Grasper

A miniature grasper for such an instrument needs to provide the grasping forces needed in surgery. These forces are estimated to be between 30 N and 50 N for holding a needle when suturing [Rosen 2002b]. In general, a manual grasper actuated through a cable or bar is used in laparoscopic instruments. But it needs great traction forces and is difficult to use. A robotic grasper would make openning/closing the grasper much easier.

In [Kode 2007] a grasper actuated by a miniature DC motor and SMA wires is presented. A major problem of this grasper is its length (4.5 cm) that causes extra forces on the bending structure of the distal tip. We made a simple hydraulic grasper that is closed by filling a balloon placed under the near end of its jaws with water. The balloon is filled through a canal that runs along the wires inside the shaft and is connected to a syringe. Fig. 6.7 shows the closed grasper. Note that the balloon does not increase the instrument's outside diameter when it is flat and the grasper is not actuated.

6.2 Performance Results

Table 6.1 presents approximate speed and torque limitations of the instrument's robotic DOF, based on the actuators' speed and torque limits.

In order to validate the proof of concept prototype, we did some in vitro and then in vivo experiments. In vitro tests were to see if a naive user could combine the manual and robotic movements of the distal tip to make a desired gesture such as picking a needle and turning it to make a stitch. This was done successfully.

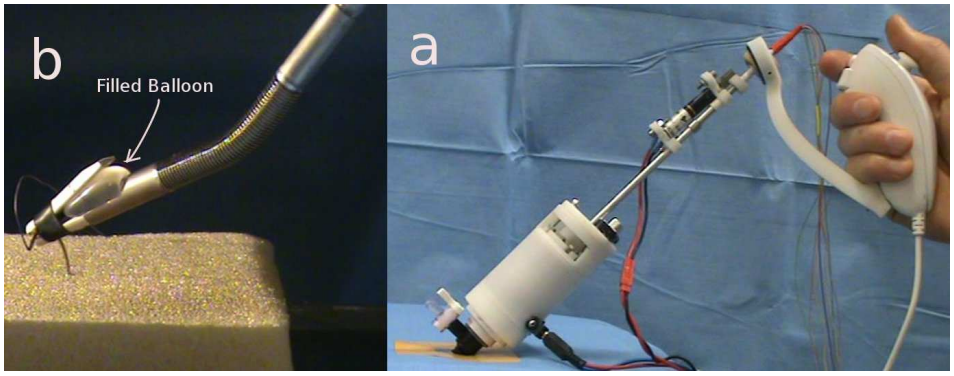

Figure 6.7: In vitro setup: (a) External view (b) Internal view with the grasper holding a needle

An in vivo test on a porcine model ensued to have the instrument tested by 2 expert surgeons (Fig. 6.8). The surgeons were able to coordinate easily the distal tip movements with the endoscopic vision to grasp a needle and reorient it. Besides, the surgeons were quite satisfied with the ergonomics of the instrument with the passive spheric joint.

6.3 Conclusion

A novel solution to the technological problem of mechatronic design of hand-held laparoscopic instrument was proposed in this chapter. The proof of concept prototype is developed based on the results of the global study of human-instrument interactions conducted in previous chapters. The instrument includes an active trocar that removes the bulk of electrical components

Table 6.1: Speed and force limits of the robotic DOF

	Max. Speed	Max. Torque
Roll	220 deg/sec	819$N.mm$
Yaw	18 deg/sec	NA
Roll	220 deg/sec	819$N.mm$

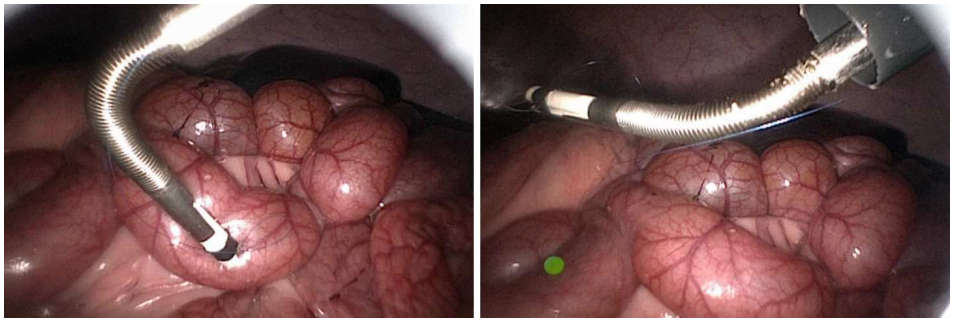

Figure 6.8: In vivo setup: (a) External view (b) Internal view with the grasper holding a needle

on the handle and allows using a free joint between the handle and the shaft to improve the instrument ergonomics.

The concept of SMA driven distal bending tip was implemented and tested successfully in such an instrument. The use of SMA wires in this prototype is promising and this concept can be used in future prototypes.

A bellow to transmit distal rotation was used for the first time in this prototype. This is an efficient method to add a distal rotation to an articulated end effector, which is indispensable according to the study of Chapter 4.

The prototype was used in vitro by inexperienced users in laparoscopy successfully to make 6 DOF movements in a training box. It was then tested in vivo by expert surgeons and they expressed great satisfaction as to the instrument's ergonomics and distal movements.

Conclusion

In this research, serial comanipulation systems, i.e. hand-held robotic instruments that have motorized and manual DOF were the subject of a global study in the context of MIS. These instruments can help surgeons gain greater dexterity and performance and operate in a more comfortable and ergonomic environment. But before introducing such instruments to the operating room, major obstacles have to be overcome.

Human-Machine Interface

Existing laparoscopic instruments have non-intuitive and under-performing human-machine interfaces or handles that limit the surgeon's performance. To improve this aspect, 2 types of handles are proposed in the litterature for a dexterous instrument with high precision and optimal performance:

1. articulated handle with an articulation between the handle and the shaft, adding extra-corporeal DOF to the handle;

2. finger-operated fixed handle where the handle remains fixe to the shaft and control elements on the handle and under the fingers command the intra-corporeal DOF of the instrument.

The first stage of this work consisted in comparing these 2 types of handle, and their different control modes. The results of a study with 4 participants on a VR Simulator, show that in an articulated handle, a direct control mode, like the control mode used in RealHand and Laparo-Angle instruments, gives better scores. A direct control mode generates end-effector movements that, seen on the screen, are in the same direction as handle movements. A locking mechanism, like what is used in the Laparo-Angle instrument can improve precision even more. But the results show that a finger-operated handle has an advantage over an articulated one in terms of precision and offers a superior quality of gesture.

Furthermore, the results suggest that a finger-operated handle results in higher precision compared to an articulated handle and is a better choice for a serial comanipulator.

Kinematics

The second phase of the study consisted of comparing different distal kinematics for the instrument. 2 possible 2 DOF wrists with YR and YP kinematics were compared with a 3 DOF wrist kinematics (YPR).

The results show that the YR and YPR kinematics are largely better than the YP kinematics, in terms of mean TCT. TCT results also show a statically significant difference between the YP and YPR kinematics. Singularity analysis of the 3 manipulator kinematics shows that YP and YPR wrist kinematics have singular configurations that may happen during dexterous manipulation in laparoscopy and degrade user performance.

Moreover, it is much more affordable technologically, to make a 2 DOF mesoscale wrist than a 3 DOF one. These results suggest that the YR wrist kinematics is the best choice out of the 3 tested kinematics for a dexterous laparoscopic manipulator. The YR kinematics provides 6 DOF manipulation of the end-effector and can be easily used to perform complex gestures such as stitching in different angles.

Ergonomics

The instrument's ergonomics was the third aspect of designing a serial co-manipulator for laparoscopy. The non-ergonomic nature of MIS along with the somewhat simplistic design of the existing instruments has caused serious problems for laparoscopists. A novel solution for this problem was proposed that consisted of adding a free (passive) 3 DOF articulation to the handle to allow the surgeon freedom of movement without influencing the performance.

Using the VR Simulator, 16 participants in 2 groups with different levels of expertise evaluated 3 different instruments in 2 types of tasks, representatives of most gestures in laparoscopy. The RULA method was used to evaluate the instruments from an ergonomics point of view.

The results of the Pointing task showed that from an ergonomics point of view, the novel solution of adding a free 3 DOF knee-joint to the handle seems to be very effective. The instrument with the passive articulation has the lowest average RULA score in the Pick & Place task. Besides, a large progress margin is visible for the surgeons to improve their posture during laparoscopy using a handle with a free joint. This is an interesting and encouraging result as none of the existing instruments in the context of serial comanipulation has a solution to the problem of ergonomics.

From an efficiency point of view, the free joint handle is not the best solution among the 3 instruments. The dexterous instrument with a fixed handle is either the most efficient or as efficient as the conventional instrument.

Mechatronic Implementation

A novel solution to the technological problem of mechatronic design of hand-held laparoscopic instrument was proposed based on the results of chapters 3 to 5. The instrument includes an active trocar that removes the bulk of electrical components on the handle and allows using a free joint between the handle and the shaft to improve the instrument ergonomics.

The proof of concept prototype's distal DOF are actuated, using DC motors and SMA wires. The distal rotation of the end-effector is transmitted, using a bellow. The prototype was successfully tested in vitro and in vivo for manipulation tasks.

Future Works

The concept of serial comanipulation for laparoscopy was regarded in this research as a problem that needs to be studied from scratch.

In future studies, the problem of handle design for dexterous instruments needs to be addressed. A comfortable and intuitive human-machine interface for a hand-held instrument is still missing. This aspect of the laparoscopic instrument is actively under research and new interfaces such as the one made for Intuitool [Hallbeck 2005] are proposed.

The free joint solution to the problem of ergonomics has to be improved for performance. One possible approach is to leave the rotation of the shaft free to be able to use an active trocar for its advantages (light-weight, easy to use handle) and make the other 2 DOF of the knee-joint (frontal and sagittal inclinations) lockable. The surgeon would be able to lock the joint when he/she considers his/her posture to be comfortable and to continue using the instrument with improved precision.

An improved mechatronic design is necessary for the instrument to be used in an operating room. The grasper and the distal DOF forces need to be in the ranges necessary for laparoscopy. For this purpose, a new bending structure needs to be specially developped for the laparoscopic instrument.

The structure needs to bend only in one direction, and an example of such an structure is proposed in [Hassan Zahraee 2010].

The active trocar has also to be redesigned for a more compact and robust module that can be easily plugged on and off medical trocar and can also be sterilized.

Appendix A

Shadow projection and Collision detection in the Simulator

Shadow projection

In the absence of haptic feedback in the VR simulator, casting shadows can help the user to perceive the depth of the image. The cast shadows of the instruments, and the ring (in the pick & place task) are projected on the working plane in the virtual scene.

Considering the light source to be at point A, the shadow of point B on the plane s is the point C where line d, passing through A and B, and s coincide (Fig. A.1).

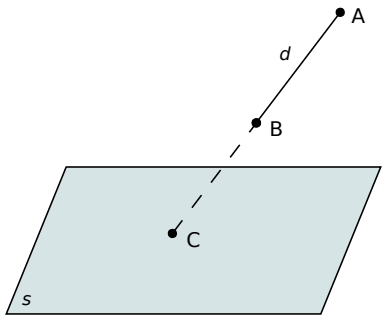

Figure A.1: Projection of a point's shadow on a plane

The parametric equation of the line which has the form of

$$d : \begin{cases} x &= n_x t + x_0 \\ y &= n_y t + y_0 \\ z &= n_z t + z_0 \end{cases} \tag{A.1}$$

is unknown. $\vec{n} = \begin{pmatrix} n_x \\ n_y \\ n_z \end{pmatrix}$ is a vector parallel to line and $P_0 = \begin{pmatrix} x_0 \\ y_0 \\ z_0 \end{pmatrix}$ is a point on the line.

The Cartesian equation of the plane is known:

$$s : N_x x + N_y y + N_z z + d = 0 \tag{A.2}$$

where $\vec{N} = \begin{pmatrix} N_x \\ N_y \\ N_z \end{pmatrix}$ is the normal vector to the plane.

One way of solving the problem and finding point C would be to put the coordinates of points A and B with arbitrary t parameters in the line equation and solve the resulting 6×6 linear equation system for $\vec{n}$ parallel to line and the point P_0 on the line. Then put the line equation in the plane equation and find the coincidence point. This approach is long and heavy in terms of calculations.

An easier way is to find $\vec{n}$ first, using A and B:

$$\vec{n} = \overrightarrow{AB} = \begin{pmatrix} x_b - x_a \\ y_b - x_a \\ z_b - x_a \end{pmatrix} \tag{A.3}$$

Now we attribute $t = 0$ to the point A (A is taken as the arbitrary point P_0 on the line). The equation of the line becomes instantly known as:

$$d : \begin{cases} x &= n_x t + x_A \\ y &= n_y t + y_B \\ z &= n_z t + z_C \end{cases} \tag{A.4}$$

This line is coincided with the plane s:

$$N_x(n_x t + x_A) + N_y(n_y t + y_B) + N_z(n_z t + z_C) + d = 0 \tag{A.5}$$

and the parameter t of the coincidence point is found as

$$t_C = -\frac{d + N_x x_A + N_y y_A + N_z z_A}{N_x n_x + N_y n_y + N_z n_z} \tag{A.6}$$

The shadow point coordinates are found using t_C and A.4.

To find the shadow of a line segment, it suffices to find the shadows of the line segment's 2 ending points.

To find the shadow of a cylinder (such as the shaft), or a torus (such as the ring), it is divided to a finite number of line segments.

A.1 Collision detection

In the absence of haptic feedback, collision detection for blocking instrument movements introduces a lag in the movements of the instrument and is not useful. But collision detection for controlling the flow of a task is necessary in the pointing and pick & place tasks. In the pointing task, it is necessary to detect the collision of the end effector and the balloon to score. In the pick & place task, it is necessary to detect the collision of the end effector and the ring to pick it, and the collision of the ring and the column to place it.

1. Collision detection between a point and a plane

The point $P = \begin{pmatrix} x \\ y \\ z \end{pmatrix}$ has collided with the plane s, if:

$$\left|N_x x^2 + N_y y^2 + N_z z^2 + d\right| < \varepsilon \tag{A.7}$$

In the stitching task, the collision between the needle and the working plane is used for a change of color that helps the user in depth perception.

2. Collision detection between a point and a sphere

The point $P = \begin{pmatrix} x \\ y \\ z \end{pmatrix}$ has collided with the sphere u, with a rayon of r and centered at $P_0 = \begin{pmatrix} x_0 \\ y_0 \\ z_0 \end{pmatrix}$ if:

$$\left|(x - x_0)^2 + (y - y_0)^2 + (z - z_0)^2 - r^2\right| < \varepsilon \tag{A.8}$$

In the pointing task, the value of ε is one factor in the difficulty level of the task.

3. Collision detection between a point and a torus

The ring in the pick & place task is a torus. The equation of the central circle q and the thickness of the torus, h are known (Fig. A.2).

$$q : (x - x_0)^2 + (y - y_0)^2 + (z - z_0)^2 = r^2 \tag{A.9}$$

Where $Q_0 = \begin{pmatrix} x_0 \\ y_0 \\ z_0 \end{pmatrix}$ is the center of the torus and r is its rayon. The point E, the center of the end effector, has collied with the torus if

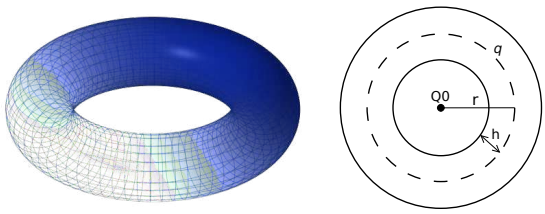

Figure A.2: The ring in the pick and place task is a torus

$$(r-h)^2 \leq (x_E - x_0)^2 + (y_E - y_0)^2 + (z_E - z_0)^2 \leq (r+h)^2 \tag{A.10}$$

The equation of the ring is however in its own coordinates, and the ring is placed in an arbitrary position and orientation during the task. It may have already been picked by an instrument, in which case its position and orientation depend on the position and orientation of the instrument and its end effector.

In any case, the transformation matrix between the ring's local coordinates R, and the camera coordinates C is known. In order to check the collision between the point ${}^{C}E$ and the ring, ${}^{C}E$ is transformed to

$${}^{R}E = ({}^{C}_{R}T)^{-1}.{}^{C}E \tag{A.11}$$

Now the collision between ${}^{R}E$ and the ring is checked using A.10.

4. Collision detection between a point and a cylinder

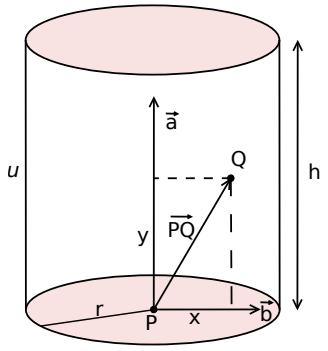

Figure A.3: Collision of a point and a cylinder

According to Fig. A.3, the point Q has collided with the cylinder u, placed at P and parallel to $\vec{a}$, if

$$x < r \qquad \&\& \qquad y < h \tag{A.12}$$

where

$$y = \frac{\vec{a}.\overrightarrow{PQ}}{|\vec{a}|} \tag{A.13}$$

$$x = \frac{\vec{b}.\overrightarrow{PQ}}{\left|\vec{b}\right|} \tag{A.14}$$

$$\vec{b} = \vec{a} \times (\overrightarrow{PQ} \times \vec{a}) \tag{A.15}$$

Appendix B

Analysis of Variance

The null hypothesis tested by one-way Analysis of Variance (ANOVA) is that two or more population means are equal. The question is whether (H_0) the population means are equal for all groups and that the observed differences in sample means are due to random sampling variation, or (H_a) the observed differences between sample means are due to actual differences in the population means.

The logic used in ANOVA to compare means of multiple groups is similar to that used with the t-test to compare means of two independent groups. When one-way ANOVA is applied to the special case of two groups, one-way ANOVA gives identical results as the t-test.

Not surprisingly, the assumptions needed for the t-test are also needed for ANOVA. We need to assume: 1) random, independent sampling from the k populations; 2) normal population distributions; 3) equal variances within the k populations.

Assumption 1 is crucial for any inferential statistic. As with the t-test, Assumptions 2 and 3 can be relaxed when large samples are used, and Assumption 3 can be relaxed when the sample sizes are roughly the same for each group even for small samples. (If there are extreme outliers or errors in the data, we need to deal with them first.) As a first step, we will review the t-test for two independent groups, to prepare for an extension to ANOVA.

Review of the t-test for independent groups

Let us start with a small example. Suppose we wish to compare two training programs in terms of performance scores for people who have completed the training course. The table below shows the scores for six randomly selected graduates from each of two training programs. These (artificially) small samples show somewhat lower scores from the first program than from the second program. But, can these fluctuations be attributed to chance in the sampling process or is this compelling evidence of a real difference in the populations?

The t-test for independent groups is designed to address just this question by testing the null hypothesis $H_0 : \mu_1 = \mu_2$. We will conduct a standard t-test for two independent groups, but will develop the logic in a way that can be extended easily to more than two groups.

$Program1$	$Program2$
102	100
90	108
97	104
94	111
98	105
101	102

Mean: $\bar{y_1} = 97$, $\bar{y_2} = 105$

Variance: $s_1^2 = 20$, $s_2^2 = 16$

The mean of all 12 scores = Grand mean = $\bar{y} = 101$

The first step is to check the data to make sure that the raw data are correctly assembled and that assumptions have not been violated in a way that makes the test inappropriate. In our example, a plot of the data shows that the sample distributions have roughly the same shape, and neither sample has extreme scores or extreme skew. The sample sizes are equal, so equality of population variances is of little concern. Note that in practice you would usually have much larger samples.

We assume that the variance is the same within the two populations (Assumption 3). An unbiased estimate of this common population variance can be calculated separately from each sample. The numerator of the variance formula is the sum of squared deviations around the sample mean, or simply the sum of squares for sample j (abbreviated as SS_j). The denominator is the degrees of freedom for the population variance estimate from sample j (abbreviated as df_j).

$$\text{Unbiased estimate of } \sigma_j^2 = \frac{\sum i(y_{ij} - \bar{y_i})^2}{(n_j - 1)} = \frac{SS_j}{df_j} = S_j^2 \qquad \text{(B.1)}$$

For the first sample, $SS_1 = (102 - 97)^2 + ... + (101 - 97)^2 = 100$, and for the second sample, $SS_2 = 80$. This leads to $S_1^2 = 100/5 = 20$, and $S_2^2 = 80/5 = 16$.

To pool two or more sample estimates of a single population variance, each sample variance is weighted by its degrees of freedom. This is equivalent to adding together the sums of squares for the separate estimates, and dividing by the sum of the degrees of freedom for the separate estimates.

$$\text{Pooled estimate of } \sigma_y^2 = \frac{(n_1-1)S_1^2 + (n_2-1)S_2^2}{n_1+n_2-2)} = \frac{SS_1+SS_2}{df_1+df_2} = S_y^2 \quad \text{(B.2)}$$

Thus, for our example

$S_y^2 = \frac{(6-1)(20)+(6-1)(16)}{(6+6-2)} = \frac{100+80}{5+5} = 18$

A t-test can be conducted to assess the statistical significance of the difference between the sample means. The null hypothesis is that the population means are equal ($H_0 : \mu_1 = \mu_2$).

$$t = \frac{\bar{y}_1 - \bar{y}_2}{\sqrt{s_y^2\left(1/n_1 + 1/n_2\right)}} = \frac{97-105}{\sqrt{18\left(1/6 + 1/6\right)}} = \frac{-8}{\sqrt{6}} = -3.266$$

df = (n_1 + n_2 - 2) = (6 + 6 - 2) = 10.

For a two-tailed t-test with alpha set at .01 and df=10, the tabled critical value is 3.169. Because the absolute value of the observed t just exceeds the critical value we can reject the null hypothesis $H_0 : \mu_1 = \mu_2$ at the .01 level of significance. The exact p=.0085. It is unlikely that the population means are equal, or that the population mean for Group 1 is larger than the population mean for Group 2.

An equivalent test of the null hypothesis can be calculated with the F distribution, because t^2 with df = ν is equal to F (df = 1,ν). For our example, t^2 = (-3.266)^2 = 10.67. From the F table, F(1,10; .01) = 10.04, so we find that the null hypothesis can just be rejected at the .01 level of significance (p = .0085). This test result is identical to the result of the t test.

ANOVA as a comparison of two estimates of the population variance

In this section we examine a second approach to testing two means for equality. The logic of this approach extends directly to one-way analysis of variance with **k** groups. We can use our data to calculate two independent estimates of the population variance: one is the pooled variance of scores within groups, and the other is based on the observed variance between group means. These two estimates are expected to be equal if the population means are equal for all **k** groups (H_0: $\mu_1 = \mu_2 = \ldots = \mu_k$), but the estimates are expected to differ if the population means are not all the same.

Within-groups estimate

Our single best estimate of the population variance is the pooled within groups variance, ${s_y}^2$ from B.1. In our example ${s_y}^2 = 18$, with df = 10. In ANOVA terminology, the numerator of B.1 is called the Sum of Squares Within Groups, or SS_{WG}, and the denominator is called the degrees of freedom Within Groups, or df_{WG}. The estimate of the population variance from B.1, SS_{WG}/df_{WG}, is called the Mean Square Within Groups, or MS_{WG}. B.3 is an equivalent way to express and compute MS_{WG}.

Within-groups estimate of

$$ {\sigma_y}^2 = \frac{\sum_{i,j} (y_{ij} - \bar{y}_j)^2}{\sum_j (n_j - 1)} = \frac{SS_{WG}}{df_{WG}} = MS_{WG} \tag{B.3} $$

$$ = \frac{100 + 80}{5 + 5} = \frac{180}{10} = 18.00 $$

Between-groups estimate

If the null hypothesis ($\mu_1 = \mu_2$) is true and the assumptions are valid (random, independent sampling from normally distributed populations with equal variances), then a second independent estimate of the population variance can be calculated. As is stated by the Central Limit Theorem, if independent samples of size **n** are drawn from some population with variance = ${\sigma_y}^2$, then the variance of all possible such sample means $\sigma^2_{\bar{y}}$ is ${\sigma_y}^2$/n. We can use our observed sample means to calculate an unbiased estimate of the variance for the distribution of all possible sample means (for samples of size **n**). Our estimate of the variance of means is not very stable because it is based on only two scores, $\bar{y}_1$=97 and $\bar{y}_2$=105, but nonetheless it is an unbiased estimate of $\sigma^2_{\bar{y}}$. With our data, $est\sigma^2_{\bar{y}} = s^2_{\bar{y}} = 32$ and df = 1, as calculated with B.4.

$$ est.\sigma^2_{\bar{y}} = s^2_{\bar{y}} = \frac{\sum_j (\bar{y}_j - \bar{y})^2}{k - 1} \tag{B.4} $$

$$ = (97 - 101)2 + (105 - 101)2 = (-4)2 + (4)2 = 16 + 16 = 32. $$

Because $\sigma^2_{\bar{y}} = {\sigma_y}^2$/n, it follows that ${\sigma_y}^2 = \mathrm{n}\sigma^2_{\bar{y}}$. Now we can estimate the variance of the population based on the observed variance of 32 for the sample means. With our data, where n=6 for each sample, we find ${s_y}^2$ =(n)($s^2_{\bar{y}}$) = 192.

This tells us that if we draw samples of size $n_j = 6$ from a population where ${\sigma_y}^2 = 192$, the expected variance of sample means is $\sigma_{\bar{y}}^2 = {\sigma_y}^2/n = 192/6 = 32$. Thus, if the groups in the population have equal means and variances, we can estimate this common population variance to be 192, because that would account for the observed variance of 32 between our sample means.

Calculation of this second estimate of the population variance using ANOVA notation is shown in B.5. The MS_{BG} is our best estimate of the population variance based only on knowledge of the variance among the sample means. B.5 allows for unequal sample sizes.

$$\text{Between-groups estimate of } {\sigma_y}^2 = \frac{\sum_j n_j \left(\bar{y}_j - \bar{y}\right)^2}{(k-1)} = \frac{SS_{BG}}{df_{BG}} = MS_{BG} \quad \text{(B.5)}$$

$$\frac{\sum_j n_j (\bar{y}_j - \bar{y}_{..})^2}{(k-1)} = \frac{6(97-101)^2+6(105-101)^2}{2-1} = 192. \frac{\sum_j n_j (\bar{y}_j - \bar{y}_{..})^2}{(k-1)} = \frac{6(97-101)^2+6(105-101)^2}{2-1} = 192$$

Comparing the two estimates of population variance

The estimate of the population variance based on the variability between sample means ($MS_{BG} = 192$) is considerably larger than the estimate based on variability within samples ($MS_{WG} = 18$). We should like to know how likely it is that two estimates of the same population variance would differ so widely if all of our assumptions are valid and ($\mu_1 = \mu_2$). The F ratio is designed to test this question. (H_o: ${\sigma_1}^2 = {\sigma_2}^2$)

$$F(df_{BG}, df_{WG}) = \frac{\text{Between Groups estimate of } \sigma_y^2}{\text{Within Groups estimate of } \sigma_y^2} = \frac{MS_{WG}}{MS_{BG}} \quad \text{(B.6)}$$

$F(1, 10) = 192 = 10.67 (p = .0085)$

The degrees of freedom for the two estimates of variance in B.6 are df_{BG} = k-1 = 2-1 = 1, and $df_{WG} = (n_1 + n_2 - k) = (6 + 6 - 2) = 10$. Notice that these are exactly the same F ratio and degrees of freedom that we calculated earlier when we converted the t-test to an F-test.

If the null hypothesis and assumptions were true, such that independent random samples were drawn from two normally distributed populations with equal means and equal variances, then it would be very surprising indeed

($p<.01$) to find that these two estimates of the common population variance would differ so widely.

We conclude that the null hypothesis and assumptions are not likely all to be true. If we are confident that our assumptions are OK, then we reject the null hypothesis (H_0: $\mu_1 = \mu_2 = \ldots = \mu_k$).

More than two groups: One-way ANOVA

The extension to more than two groups is now easy. B.5 and B.3 can be used directly to calculate the between-groups and within-groups estimates of the population variance, and B.6 can be used to test them for equality. If the between-groups estimate is significantly larger than the within-groups estimate, we conclude that the population means are unlikely to be equal, or that an assumption of the test has been violated.

Assumptions of the test. We can expect our calculated level of statistical significance (the p value from the F distribution) to be accurate only if the assumptions required for the test procedure have been satisfied. Recall the assumptions:

1) observations were randomly and independently chosen from the populations;

2) population distributions are normal for each group; and

3) population variances are equal for all groups.

If the sampling was not independent and random, the results of the F-test may be completely spurious. No statistical procedure will allow strong generalizations to a population if random sampling is not used. Fortunately, the sampling procedure is generally under the control of the researcher, so faulty sampling as an explanation for a surprisingly large F usually can be ruled out.

Perhaps the best approach to identify serious departures from normality in the shape of the population distributions is to plot the sample distributions and apply the "intraocular trauma test." Extreme departures from normality, especially strong skew or outliers, will be apparent. Admittedly, some practice is needed to calibrate your eyeballs, but a plot is likely to be more useful than summary statistics alone for identifying problems in your data. Distributions with isolated extreme scores (e.g., three or more standard deviations away from the mean) typically cause more serious problems than smoothly skewed distributions.

There are several ways to deal with extreme scores. Transformations may be useful to reduce the effects of extreme scores (and reduce skew). Sometimes an outlier is caused by an error in coding that can be corrected. Be especially alert for missing data codes that accidentally are used as legitimate data. Sometimes outliers are legitimate scores from cases that are qualitatively different from the population of interest. Such cases should be removed and treated separately. They may be very interesting and important cases, so they should not routinely be ignored. Recent years have seen the development of a number of "robust" methods that are less sensitive to extreme scores. With Winsorized data, some number (g) of scores in each tail of the distribution are set equal to the next most extreme score (the g+1st score from the end). With trimmed data, some proportion of the scores from each tail are discarded. A popular level of trimming is 15% from each end. Hampel and biweight procedures retain all data but give less weight to scores farther from the mean.

Equality of variance can be tested, but there are compelling arguments against using the test to decide whether or not to use ANOVA. First, ANOVA is little affected by small to moderate departures from homogeneity of variance, especially if the sample sizes are equal or nearly equal. Second, the tests of homogeneity are more powerful for larger samples than for smaller samples, but ANOVA is less affected by heterogeneity when the samples are larger. This leads to the awkward situation where the tests of homogeneity are most likely to detect a violation of homogeneity when it least matters. Third, several of the most commonly used tests of homogeneity are inaccurate for non-normal distributions. This includes placeCityBartlett's test, F max, and Cochran's C (see Kirk for a discussion of these tests). Levene's test of homogeneity of variance is less sensitive to departures from normality. addressStreetBox (1953) characterized testing for homogeneity before using ANOVA as sending a rowboat out into the ocean to see if it is calm enough for an ocean liner.

Unequal within-group variances for the different populations is a problem for ANOVA (and the t-test) only when three conditions simultaneously exist – I call this the "triple whammy":

1) the variances are quite unequal (say a 2:1 ratio or greater); 2) the samples are quite unequal in size (say a 2:1 ratio or greater), and 3) at least one sample is small (say 10 or fewer cases). In this situation, ANOVA is too liberal (gives false significance) when the smallest samples are taken from the populations with the largest variance. Conversely, ANOVA is too conservative (fails to detect differences among means) when the smallest samples are taken from the populations with the smallest variance (see Boneau, 1960). Many

statistical packages, including SPSS, provide tests of equality of variance in ANOVA and also ANOVA tests that do not assume equal variance.

If you suspect that an assumption of ANOVA has been violated in a way that compromises the test, it is prudent to supplement the regular analyses with procedures that are robust to the suspected violation of the assumption. If both approaches yield the same conclusions, report the results from the standard test and note that the results were confirmed with the robust procedure. If the results differ, considerable caution is warranted, and the more conservative test is probably appropriate.

Statistical Significance, Practical Significance, and Non-Significance

Failure to reject the null hypothesis does not mean that the null hypothesis is true (it almost certainly is false). On the other hand, if we reject the null hypothesis, we have not necessarily found a practical or important effect. It is important to examine plots of the data, and to report means and variances, not just p values from significance tests.

Appendix C

Jacobians

In this appendix, the detailed formulas for Jacobians and their determinants for each of the 3 tested kinematics of chapter 4 are presented. The Jacobian matrices are calculated using the DaMa Robotics Symbolic Toolbox for Matlab [Bellicoso].

C.1 Denavit-Hartenberg Parameters

In order to calculate the Jacobian matrix for each kinematics, local reference frames were first associated to each solid body acoording to the Denavit-Hartenberg (DH) convention. These reference frames are shown in Fig. 4.2. The DH parameters for each kinematics are as follows:

For the YP end effector kinematics, the DH parameters are:

$joint$	a	α	d	$theta$	P/R
1	0.00	$\pi/2$	0.00	θ_1	R
2	0.00	$\pi/2$	0.00	θ_2	R
3	0.00	0.00	0.00	θ_3	R
4	0.00	$\pi/2$	d_4	$\pi/2$	P
5	0.00	$\pi/2$	0.00	θ_5	R
6	-0.01	$-\pi/2$	0.00	θ_6	R

For the YPR end effector kinematics, the DH parameters are:

$joint$	a	α	d	$theta$	P/R
1	0.00	$\pi/2$	0.00	θ_1	R
2	0.00	$\pi/2$	0.00	θ_2	R
3	0.00	0.00	0.00	θ_3	R
4	0.00	$\pi/2$	d_4	$\pi/2$	P
5	0.00	$\pi/2$	0.00	θ_5	R
6	0.00	$\pi/2$	0.00	θ_6	R
7	0.00	0.00	-0.01	θ_7	R

For the YR end effector kinematics, the DH parameters are:

$joint$	a	α	d	θ	P/R
1	0.00	$\pi/2$	0.00	θ_1	R
2	0.00	$\pi/2$	0.00	θ_2	R
3	0.00	0.00	0.00	θ_3	R
4	0.00	$\pi/2$	d_4	$\pi/2$	P
5	0.00	$-\pi/2$	0.00	θ_5	R
6	0.00	0.00	-0.01	θ_6	R

The Jacobian for the YP kinematics is $J = {}^0_7 J_{YP}$ with:

$$
\begin{aligned}
J_{11} &= -\cos\theta_6\,(\cos\theta_5\,(\cos\theta_1\,\cos\theta_3 + \cos\theta_2\,\sin\theta_1\,\sin\theta_3) - \sin\theta_1\,\sin\theta_2\,\sin\theta_5) - \sin\theta_6\,(\cos\theta_1\,\sin\theta_3 - \cos\theta_2\,\cos\theta_3\,\sin\theta_1) - \mathrm{d}_4\,\sin\theta_1\,\sin\theta_2\\
J_{12} &= \cos\theta_1\,\mathrm{d}_4\,\cos\theta_2 - \cos\theta_6\,(\cos\theta_2\,\sin\theta_5 + \cos\theta_5\,\sin\theta_2\,\sin\theta_3) + \cos\theta_3\,\sin\theta_2\,\sin\theta_6)\\
J_{13} &= \cos\theta_1\,\cos\theta_2\,\sin\theta_3\,\sin\theta_6 - \cos\theta_3\,\sin\theta_1\,\sin\theta_6 + \cos\theta_5\,\cos\theta_6\,\sin\theta_1\,\sin\theta_3 + \cos\theta_1\,\cos\theta_2\,\cos\theta_3\,\cos\theta_5\,\cos\theta_6\\
J_{14} &= \cos\theta_1\,\sin\theta_2\\
J_{15} &= -\cos\theta_6\,(\cos\theta_1\,\cos\theta_5\,\sin\theta_2 - \cos\theta_3\,\sin\theta_1\,\sin\theta_5 + \cos\theta_1\,\cos\theta_2\,\sin\theta_3\,\sin\theta_5)\\
J_{16} &= \cos\theta_3\,\cos\theta_5\,\sin\theta_1\,\sin\theta_6 - \cos\theta_1\,\cos\theta_2\,\cos\theta_3\,\cos\theta_6 - \cos\theta_6\,\sin\theta_1\,\sin\theta_3 + \cos\theta_1\,\sin\theta_2\,\sin\theta_5\,\sin\theta_6 - \cos\theta_1\,\cos\theta_2\,\cos\theta_5\,\sin\theta_3\,\sin\theta_6\\
J_{21} &= \mathrm{d}_4\,\cos\theta_1\,\sin\theta_2 - \sin\theta_6\,(\sin\theta_1\,\sin\theta_3 + \cos\theta_1\,\cos\theta_2\,\cos\theta_3) - \cos\theta_6\,(\cos\theta_5\,(\cos\theta_3\,\sin\theta_1 - \cos\theta_1\,\cos\theta_2\,\sin\theta_3) +\\
&\quad \cos\theta_1\,\sin\theta_2\,\sin\theta_5)\\
J_{22} &= \sin\theta_1\,\mathrm{d}_4\,\cos\theta_2 - \cos\theta_6\,(\cos\theta_2\,\sin\theta_5 +\\
&\quad \cos\theta_5\,\sin\theta_2\,\sin\theta_3) + \cos\theta_3\,\sin\theta_2\,\sin\theta_6)\\
J_{23} &= \cos\theta_1\,\cos\theta_3\,\sin\theta_6 - \cos\theta_1\,\cos\theta_5\,\cos\theta_6\,\sin\theta_3 + \cos\theta_2\,\sin\theta_1\,\sin\theta_3\,\sin\theta_6 + \cos\theta_2\,\cos\theta_3\,\cos\theta_5\,\cos\theta_6\,\sin\theta_1\\
J_{24} &= \sin\theta_1\,\sin\theta_2\\
J_{25} &= -\cos\theta_6\,(\cos\theta_5\,\sin\theta_1\,\sin\theta_2 + \cos\theta_1\,\cos\theta_3\,\sin\theta_5 + \cos\theta_2\,\sin\theta_1\,\sin\theta_3\,\sin\theta_5)\\
J_{26} &= \cos\theta_1\,\cos\theta_6\,\sin\theta_3 - \cos\theta_2\,\cos\theta_3\,\cos\theta_6\,\sin\theta_1 - \cos\theta_1\,\cos\theta_3\,\cos\theta_5\,\sin\theta_6 + \sin\theta_1\,\sin\theta_2\,\sin\theta_5\,\sin\theta_6 - \cos\theta_2\,\cos\theta_5\,\sin\theta_1\,\sin\theta_3\,\sin\theta_6\\
J_{31} &= 0\\
J_{32} &= \mathrm{d}_4\,\sin\theta_2 - \cos\theta_6\,\sin\theta_2\,\sin\theta_5 - \cos\theta_2\,\cos\theta_3\,\sin\theta_6 + \cos\theta_2\,\cos\theta_5\,\cos\theta_6\,\sin\theta_3\\
J_{33} &= \sin\theta_2\,(\sin\theta_3\,\sin\theta_6 + \cos\theta_3\,\cos\theta_5\,\cos\theta_6)\\
J_{34} &= -\cos\theta_2\\
J_{35} &= \cos\theta_6\,(\cos\theta_2\,\cos\theta_5 - \sin\theta_2\,\sin\theta_3\,\sin\theta_5)\\
J_{36} &= -\cos\theta_2\,\sin\theta_5\,\sin\theta_6 - \cos\theta_3\,\cos\theta_6\,\sin\theta_2 - \cos\theta_5\,\sin\theta_2\,\sin\theta_3\,\sin\theta_6\\
J_{41} &= 0\\
J_{42} &= \sin\theta_1\\
J_{43} &= \cos\theta_1\,\sin\theta_2\\
J_{44} &= 0\\
J_{45} &= \sin\theta_1\,\sin\theta_3 + \cos\theta_1\,\cos\theta_2\,\cos\theta_3\\
J_{46} &= \sin\theta_5\,(\cos\theta_3\,\sin\theta_1 - \cos\theta_1\,\cos\theta_2\,\sin\theta_3) - \cos\theta_1\,\cos\theta_5\,\sin\theta_2\\
J_{51} &= 0\\
J_{52} &= -\cos\theta_1\\
J_{53} &= \sin\theta_1\,\sin\theta_2\\
J_{54} &= 0\\
J_{55} &= \cos\theta_2\,\cos\theta_3\,\sin\theta_1 - \cos\theta_1\,\sin\theta_3\\
J_{56} &= -\sin\theta_5\,(\cos\theta_1\,\cos\theta_3 + \cos\theta_2\,\sin\theta_1\,\sin\theta_3) - \cos\theta_5\,\sin\theta_1\,\sin\theta_2\\
J_{61} &= 1\\
J_{62} &= 0\\
J_{63} &= -\cos\theta_2\\
J_{64} &= 0\\
J_{65} &= \cos\theta_3\,\sin\theta_2\\
J_{66} &= \cos\theta_3\,\sin\theta_2
\end{aligned}
$$

Its determinant is:

$$|{}^0_6 J_{YP}| = -{\mathrm{d}_4}^2\,\sin\theta_5$$

To find the singular configurations, the equation $|{}^0_7 J_{YP}| = 0$ has to be solved which gives:

$$\mathrm{d}_4 = 0$$

$$\sin\theta_5 \; = 0 \rightarrow \theta_5 = 0 or \pi$$

The Jacobian for the YPR kinematics is $J =^{0}_{7} J_{YPR}$ with:

$$
\begin{aligned}
J_{11} &= \cos\theta_6\ (\cos\theta_1\ \sin\theta_3 - \cos\theta_2\ \cos\theta_3\ \sin\theta_1) - \sin\theta_6\ (\cos\theta_5\ (\cos\theta_1\ \cos\theta_3 + \cos\theta_2\ \sin\theta_1\ \sin\theta_3) - \sin\theta_1\ \sin\theta_2\ \sin\theta_5) - \mathrm{d}_4\ \sin\theta_1\ \sin\theta_2 \\
J_{12} &= -\cos\theta_1\ (\sin\theta_6\ (\cos\theta_2\ \sin\theta_5 + \cos\theta_5\ \sin\theta_2\ \sin\theta_3) - \mathrm{d}_4\ \cos\theta_2 + \cos\theta_3\ \cos\theta_6\ \sin\theta_2) \\
J_{13} &= \cos\theta_3\ \cos\theta_6\ \sin\theta_1 - \cos\theta_1\ \cos\theta_2\ \cos\theta_6\ \sin\theta_3 + \cos\theta_5\ \sin\theta_1\ \sin\theta_3\ \sin\theta_6 + \cos\theta_1\ \cos\theta_2\ \cos\theta_3\ \cos\theta_5\ \sin\theta_6 \\
J_{14} &= \cos\theta_1\ \sin\theta_2 \\
J_{15} &= -\sin\theta_6\ (\cos\theta_1\ \cos\theta_5\ \sin\theta_2 - \cos\theta_3\ \sin\theta_1\ \sin\theta_5 + \cos\theta_1\ \cos\theta_2\ \sin\theta_3\ \sin\theta_5) \\
J_{16} &= \cos\theta_1\ \cos\theta_2\ \cos\theta_5\ \cos\theta_6\ \sin\theta_3 - \cos\theta_1\ \cos\theta_2\ \cos\theta_3\ \sin\theta_6 - \cos\theta_3\ \cos\theta_5\ \cos\theta_6\ \sin\theta_1 - \cos\theta_1\ \cos\theta_6\ \sin\theta_2\ \sin\theta_5 - \sin\theta_1\ \sin\theta_3\ \sin\theta_6 \\
J_{21} &= \cos\theta_6\ (\sin\theta_1\ \sin\theta_3 + \cos\theta_1\ \cos\theta_2\ \cos\theta_3) - \sin\theta_6\ (\cos\theta_5\ (\cos\theta_3\ \sin\theta_1 - \cos\theta_1\ \cos\theta_2\ \sin\theta_3) + \cos\theta_1\ \sin\theta_2\ \sin\theta_5) + \mathrm{d}_4\ \cos\theta_1\ \sin\theta_2 \\
J_{22} &= -\sin\theta_1\ (\sin\theta_6\ (\cos\theta_2\ \sin\theta_5 + \cos\theta_5\ \sin\theta_2\ \sin\theta_3) - \mathrm{d}_4\ \cos\theta_2 + \cos\theta_3\ \cos\theta_6\ \sin\theta_2) \\
J_{23} &= \cos\theta_2\ \cos\theta_3\ \cos\theta_5\ \sin\theta_1\ \sin\theta_6 - \cos\theta_2\ \cos\theta_6\ \sin\theta_1\ \sin\theta_3 - \cos\theta_1\ \cos\theta_5\ \sin\theta_3\ \sin\theta_6 - \cos\theta_1\ \cos\theta_3\ \cos\theta_6 \\
J_{24} &= \sin\theta_1\ \sin\theta_2 \\
J_{25} &= -\sin\theta_6\ (\cos\theta_5\ \sin\theta_1\ \sin\theta_2 + \cos\theta_1\ \cos\theta_3\ \sin\theta_5 + \cos\theta_2\ \sin\theta_1\ \sin\theta_3\ \sin\theta_5) \\
J_{26} &= \cos\theta_1\ \sin\theta_3\ \sin\theta_6 + \cos\theta_1\ \cos\theta_3\ \cos\theta_5\ \cos\theta_6 - \cos\theta_2\ \cos\theta_3\ \sin\theta_1\ \sin\theta_6 - \cos\theta_6\ \sin\theta_1\ \sin\theta_2\ \sin\theta_5 + \cos\theta_2\ \cos\theta_5\ \cos\theta_6\ \sin\theta_1\ \sin\theta_3 \\
J_{31} &= 0 \\
J_{32} &= \mathrm{d}_4\ \sin\theta_2 - \sin\theta_2\ \sin\theta_5\ \sin\theta_6 + \cos\theta_2\ \cos\theta_3\ \cos\theta_6 + \cos\theta_2\ \cos\theta_5\ \sin\theta_3\ \sin\theta_6 \\
J_{33} &= -\sin\theta_2\ (\cos\theta_6\ \sin\theta_3 - \cos\theta_3\ \cos\theta_5\ \sin\theta_6) \\
J_{34} &= -\cos\theta_2 \\
J_{35} &= \sin\theta_6\ (\cos\theta_2\ \cos\theta_5 - \sin\theta_2\ \sin\theta_3\ \sin\theta_5) \\
J_{36} &= \cos\theta_2\ \cos\theta_6\ \sin\theta_5 - \cos\theta_3\ \sin\theta_2\ \sin\theta_6 + \cos\theta_5\ \cos\theta_6\ \sin\theta_2\ \sin\theta_3 \\
J_{41} &= 0 \\
J_{42} &= \sin\theta_1 \\
J_{43} &= \cos\theta_1\ \sin\theta_2 \\
J_{44} &= 0 \\
J_{45} &= \sin\theta_1\ \sin\theta_3 + \cos\theta_1\ \cos\theta_2\ \cos\theta_3 \\
J_{46} &= \sin\theta_5\ (\cos\theta_3\ \sin\theta_1 - \cos\theta_1\ \cos\theta_2\ \sin\theta_3) - \cos\theta_1\ \cos\theta_5\ \sin\theta_2 \\
J_{51} &= 0 \\
J_{52} &= -\cos\theta_1 \\
J_{53} &= \sin\theta_1\ \sin\theta_2 \\
J_{54} &= 0 \\
J_{55} &= \cos\theta_2\ \cos\theta_3\ \sin\theta_1 - \cos\theta_1\ \sin\theta_3 \\
J_{56} &= -\sin\theta_5\ (\cos\theta_1\ \cos\theta_3 + \cos\theta_2\ \sin\theta_1\ \sin\theta_3) - \cos\theta_5\ \sin\theta_1\ \sin\theta_2 \\
J_{61} &= 1 \\
J_{62} &= 0 \\
J_{63} &= -\cos\theta_2 \\
J_{64} &= 0 \\
J_{65} &= \cos\theta_3\ \sin\theta_2 \\
J_{66} &= \cos\theta_2\ \cos\theta_5 - \sin\theta_2\ \sin\theta_3\ \sin\theta_5
\end{aligned}
$$

For the YPR kinematics which is a 7 DOF redundant kinematics, joint displacement conditions leading to singularities can be identified by:

- determining the joint-displacement conditions for one 6-joint SCM; followed by
- checking the determinants of the other 6-joint SCMs
  - to see if all $|J_i|$ are driven to zero implying a singularity, or
  - to determine further joint-displacement conditions required to cause $|J_i| = 0$ for all i.

Applying this procedure for all potential singularities of the original 6-joint SCM will identify all potential joint-displacement conditions causing singularity of the complete Jacobian matrix, i.e. all singularities causing a loss of one DOF will be identified.

The determinants of the seven 6-joint SCMs are:

$|J_1| = 0$

$|J_2| = 0$

$|J_3| = \mathrm{d}_4{}^2\ \sin\theta_6$

$|J_4| = 0$

$|J_5| = -{d_4}^2 \cos\theta_6 \sin\theta_5$

$|J_6| = -{d_4}^2 \cos\theta_5 \sin\theta_6$

$|J_7| = -{d_4}^2 \sin\theta_5$

All the 7 determinants are 0 for:

$$d_4 = 0$$

$$\sin\theta_5 = 0 \; and \; \sin\theta_6 = 0 \rightarrow \theta_5 = 0 \; or \; \pi \; and \; \theta_6 = 0 \; or \; \pi$$

The Jacobian for the YR kinematics is $J = {}^0_7 J_{YR}$ with:

$$
\begin{aligned}
J_{11} &= \sin\theta_5 (\cos\theta_1 \cos\theta_3 + \cos\theta_2 \sin\theta_1 \sin\theta_3) + \cos\theta_5 \sin\theta_1 \sin\theta_2 - d_4 \sin\theta_1 \sin\theta_2 \\
J_{12} &= \cos\theta_1 (d_4 \cos\theta_2 - \cos\theta_2 \cos\theta_5 + \sin\theta_2 \sin\theta_3 \sin\theta_5) \\
J_{13} &= -\sin\theta_5 (\sin\theta_1 \sin\theta_3 + \cos\theta_1 \cos\theta_2 \cos\theta_3) \\
J_{14} &= \cos\theta_1 \sin\theta_2 \\
J_{15} &= \cos\theta_1 \sin\theta_2 \sin\theta_5 + \cos\theta_3 \cos\theta_5 \sin\theta_1 - \cos\theta_1 \cos\theta_2 \cos\theta_5 \sin\theta_3 \\
J_{16} &= 0 \\
J_{21} &= \sin\theta_5 (\cos\theta_3 \sin\theta_1 - \cos\theta_1 \cos\theta_2 \sin\theta_3) + d_4 \cos\theta_1 \sin\theta_2 - \cos\theta_1 \cos\theta_5 \sin\theta_2 \\
J_{22} &= \sin\theta_1 (d_4 \cos\theta_2 - \cos\theta_2 \cos\theta_5 + \sin\theta_2 \sin\theta_3 \sin\theta_5) \\
J_{23} &= \sin\theta_5 (\cos\theta_1 \sin\theta_3 - \cos\theta_2 \cos\theta_3 \sin\theta_1) \\
J_{24} &= \sin\theta_1 \sin\theta_2 \\
J_{25} &= \sin\theta_1 \sin\theta_2 \sin\theta_5 - \cos\theta_1 \cos\theta_3 \cos\theta_5 - \cos\theta_2 \cos\theta_5 \sin\theta_1 \sin\theta_3 \\
J_{26} &= 0 \\
J_{31} &= 0 \\
J_{32} &= d_4 \sin\theta_2 - \cos\theta_5 \sin\theta_2 - \cos\theta_2 \sin\theta_3 \sin\theta_5 \\
J_{33} &= -\cos\theta_3 \sin\theta_2 \sin\theta_5 \\
J_{34} &= -\cos\theta_2 \\
J_{35} &= -\cos\theta_2 \sin\theta_5 - \cos\theta_5 \sin\theta_2 \sin\theta_3 \\
J_{36} &= 0 \\
J_{41} &= 0 \\
J_{42} &= \sin\theta_1 \\
J_{43} &= \cos\theta_1 \sin\theta_2 \\
J_{44} &= 0 \\
J_{45} &= \sin\theta_1 \sin\theta_3 + \cos\theta_1 \cos\theta_2 \cos\theta_3 \\
J_{46} &= \cos\theta_1 \cos\theta_5 \sin\theta_2 - \sin\theta_5 (\cos\theta_3 \sin\theta_1 - \cos\theta_1 \cos\theta_2 \sin\theta_3) \\
J_{51} &= 0 \\
J_{52} &= -\cos\theta_1 \\
J_{53} &= \sin\theta_1 \sin\theta_2 \\
J_{54} &= 0 \\
J_{55} &= \cos\theta_2 \cos\theta_3 \sin\theta_1 - \cos\theta_1 \sin\theta_3 \\
J_{56} &= \sin\theta_5 (\cos\theta_1 \cos\theta_3 + \cos\theta_2 \sin\theta_1 \sin\theta_3) + \cos\theta_5 \sin\theta_1 \sin\theta_2 \\
J_{61} &= 1 \\
J_{62} &= 0 \\
J_{63} &= -\cos\theta_2 \\
J_{64} &= 0 \\
J_{65} &= \cos\theta_3 \sin\theta_2 \\
J_{66} &= \sin\theta_2 \sin\theta_3 \sin\theta_5 - \cos\theta_2 \cos\theta_5
\end{aligned}
$$

Its determinant is:

$|{}^0_6 J_{YR}| = {d_4}^2 \sin\theta_5$

Thus, singularities occur when:

$$d_4 = 0$$

$$\sin\theta_5 \; = 0 \rightarrow \theta_5 = 0 \; or \; \pi$$

Appendix D

RULA Calculations

This appendix explains how the real-time Rapid Upper Limb Assesment (RULA) ergonomic score is calculated during a laparoscopic surgery exercise on the virtual reality simulator, based on the acquisition of the positions of anatomical landmarks using a CodaMotion 3D locator.

RULA is a method for rapid ergonomic assessment of an activity performed using the upper limb. An integer score of 1 to 7 quantifies the risk associated with the activity (1 or 2 indicate a temperorily acceptable posture, 7 requires immediate stop of the activity). The global score is calculated from the angles of the upper limb, the overall posture of the trunk and neck, the muscular load and the evolution of the posture over time (static posture is not favorable).

The general posture of the trunk and neck, and the muscular load vary little during laparoscopic surgery, and this part of the calculation is done only once for the duration of experiment. On the contrary, the arm is constantly in motion and the component of the RULA score related to the arm must be calculated in real-time. For this, the elevation angles of the arm, elbow flexion, flexion and ulnar deviation of the wrist and the angle of pronation are calculated from the positions of CodaMotion markers placed on anatomical landmarks of the arm's segments. Other factors such as the elevation of the shoulder affect this calculation as well.

The angle calculations are essentially calculations of angles between lines, planes or a mix of this, calculated from scholar products (direction vector of a line or normal to a plane). However, these lines and planes are not defined directly by the CodaMotion markers. The axis/rotation center of the upper limb segments, must be calculated based on their positions.

The end points of hand and forearm longitudinal axis are known directly from marker positions: the forearm axis connects the middle of the segment joining the 2 markers on the elbow and the middle of the segment joining the 2 markers of the wrist. Hand axis goes from this last point to the marker placed on hand.

The arm axis joins the elbow to the center of rotation of the shoulder. The center of rotation of the shoulder is calculated before the actual trial during a

short calibration exercise: with the arm stretched, the hand moves about the shoulder, keeping a marker of the wrist on the surface of a sphere. A least square approximation of the points gives the center of the sphere. The relative position of this point to the marker on the shoulder is considered constant and from now on, the center of rotation is only a translation of that marker. The center of rotation is calculated in a local coordinate system associated to the trunk, so that the movements of the trunk during the calibration does not affect the calculations of center of rotation.

The local coordinate system has one axis defined by the 2 markers on the shoulders and one axis defined as vertical to the floor during an initial calibration of CodaMotion. The third axis is the vector product of these 2 vectors and is perpendicular to the trunk. The origin of this system is defined as being between the shoulders and on the floor.

Calibration

Marker positions are saved at a frequency of 10 Hz during an exercise. Post treatment of these positions is done in Matlab to calculate the upper limb angles. We will denote:

$ACmin_b, ACmaj_b$ Acromio Claviculare articulation (major and minor shoulder markers)

LE_b Lateral Epicondyle (elbow marker, radius and thumb side)

ME_b Medial Epicondyle (elbow marker, ulna and small finger side)

RS_b Radial Styloid (wrist marker, radius side)

US_b Ulnar Styloid (wrist marker, ulna side)

MC_b Middle MetaCarpal extremity (marqueur main, base du majeur)

The _b suffix means that these positions are in the CodaMotion's fixed coordinate system.

Definition of the instantaneous coordinate system of the tronc

The midpoint of the segment joining the 2 shoulder markers at rest is defined as the origin. The Z axis is defined perpendicular to the tronc and coming out.

$z_{origin} = 0$

$x_{origin} = (fracx_{ACmaj_b} + x_{ACmin_b}2$

$y_{origin} = (fracy_{ACmaj_b} + y_{ACmin_b}2$

All the positions are then translated from the CodaMotion's fixed coordinates to the tronc's instantaneous coordinates:

$ACmin = ACmin_b - origin$

$ACmaj = ACmaj_b - origin$

$LE = LE_b - origin$

$ME = ME_b - origin$

$RS = RS_b - origin$

$US = US_b - origin$

$MC = MC_b - origin$

The positions without the suffix _b are in the tronc's coordinates. They are then rotated from the CodaMotion's fixed coordinates to the tronc's instantaneous coordinates. The rotation matrix is:

$Z_{tronc} = (0\ 0\ 1)^t$

$Y_{tronc} = \frac{1}{norm(Y_{tronc})}.(x_{ACmin}\ - x_{ACmaj}.y_{ACmin} - y_{ACmaj}\ 0)^t$

$X_{tronc} = Y_{tronc} \times X_{tronc}$

$R = (X^t_{tronc}\ Y^t_{tronc}\ Z^t_{tronc})$

$ACmin = R.ACmin$

$ACmaj = R.ACmaj$

$LE = R.LE$

$ME = R.ME$

$RS = R.RS$

$US = R.US$

$MC = R.MC$

Calculating the shoulder's rotation center center

The rotation center is calculated using one of the wrist markers and the least square methode for fitting the positions of this marker on a sphere while moving the ourstretched arm.

Note that during angular movements of the arm, shoulder elevation changes. We must therefore take into account the instantaneous displacement

of the rotation center. Assuming a constant distance between the rotation center and the shoulder marker, and assuming further that the shoulder at rest is in its lowest position, the instant elevation in the shoulder marker compared to its rest position $ACmaj_{minZ}$ must be subtracted from the Z coordinate of each point of the RS marker.

$z_{ME} = z_{ME} - (z_{ACmaj} - z_{ACmaj_{minZ}}))$

In the above formula, ME will be replaced with LE if LE is used for calculating the rotation center.

Calibration of initial angles

The initial angles are calculated with the arm stretched along the body.

$z_{GH} = z_{GH} + (ACmaj(j,3) - ACmaj_{minZ})$

(GlenoHumeral rotation center or shoulder's rotation center)

$EC = LE + ME/2$

$WC = RS + US/2$

$vect_{bras} = (EC - GH)/norm(EC - GH)$

$vect_{avant\ bras} = (WC - EC)/norm(WC - EC)$

$elbow\ flexion = acos(vect_{bras}.vect_{avant\ bras})$

$segment_{marqueurs\ poignet} = (US - RS)/norm(US - RS)$

$vect_{main} = (MC - WC)/norm(MC - WC)$

$normale_{main} = segment_{marqueurs\ poignet} \times vect_{main}/norm(segment_{marqueurs\ poignet} \times vect_{main})$

$wrist\ flexion = acos(vect_{avant\ bras}.normale_{main})$

$wrist\ deviation = acos(segment_{marqueurs\ poignet}.vect_{main})$

$pronosupination = acos((0\ \ -1\ 0).segment_{marqueurs\ poignet})$

$residu_{elbow\ flexion} = mean(elbow\ flexion)$

$residu_{wrist\ flexion} = 90 - mean(wrist\ flexion)$

$residu_{wrist\ deviation} = mean(wrist\ deviation) - 90$

$residu_{pronosupination} = 90 - mean(pronosupination)$

Calculating average lengths during calibration:

$dist_{ACmin\ ACmaj} = norm(ACmin - ACmaj)$

$dist_{LE\ ME} = norm(LE - ME)$

$dist_{RS\ US} = norm(RS - US)$

$dist_{MC\ WC} = norm(MC - (RS + US)/2)$

Calculating the RULA score for the arm

Supposing that the type of instrument used in the exercises on the simulator does not affect the position of the tronc, the legs or the neck, the only interesting RULA score here is the score of the major arm, holding the manipulating instrument.

Calculating instantanieaous angles of the arm

Arm Elevation

$arm\ elevation = acos((0\ 0\ -1)^t.vect - bras)$

Shoulder Elevation

$shoulder\ elevation = ACmaj - ACmaj_{minZ}$

Elbow Flexion

$elbow\ \ flexion\ \ =\ \ acos(vect_{bras}.vect_{avant\ bras})/(|bras| * |avant\ \ bras|) - residu_{elbow\ \ flexion}$

Wrist Flexion

$wrist\ flexion = 90 - arccos(vect_{avant\ bras}.normale_{main})/(|vect_{avant\ bras}| * |normale_{main}|) - residu_{wrist\ \ flexion}$

Wrist Deviation

$wrist\ deviation = -90 + arccos(segment_{marqueurs\ poignet}.normal_{main})/(|segment_{marqueurs_poignet}| * residu_{wrist\ \ deviation}$

Prono-supination

$pronosupination = 90 - arccos(segment_{marqueurs\ poignet}.normale_{plan\ bras})/(|segment_{marqueurs\ poignet}|$
$residu_{pronosupination}$

RULA Arm Score

The RULA score for major arm is calculated from the Table A of RULA calculations tables (see App. E).

Neck and Tronc Score (supposed constant)

From the RULA score table:

Neck score = 1 (from 0 10) Tronc score = 1 (right without lateral flexion or torsion) Legs score = 1 (standing in equilibrium)

As a result:

global tronc score = 1

Global RULA score

Global RULA score = global tronc score (1) + Upper Body Mucle Use Score (1, statistics) + Force/load Score (0, charge ¡ 2kg) + RULA Arm Score + Arm Mucle Use Score (1, repetitive mouvements);

Appendix E

RULA Score Table

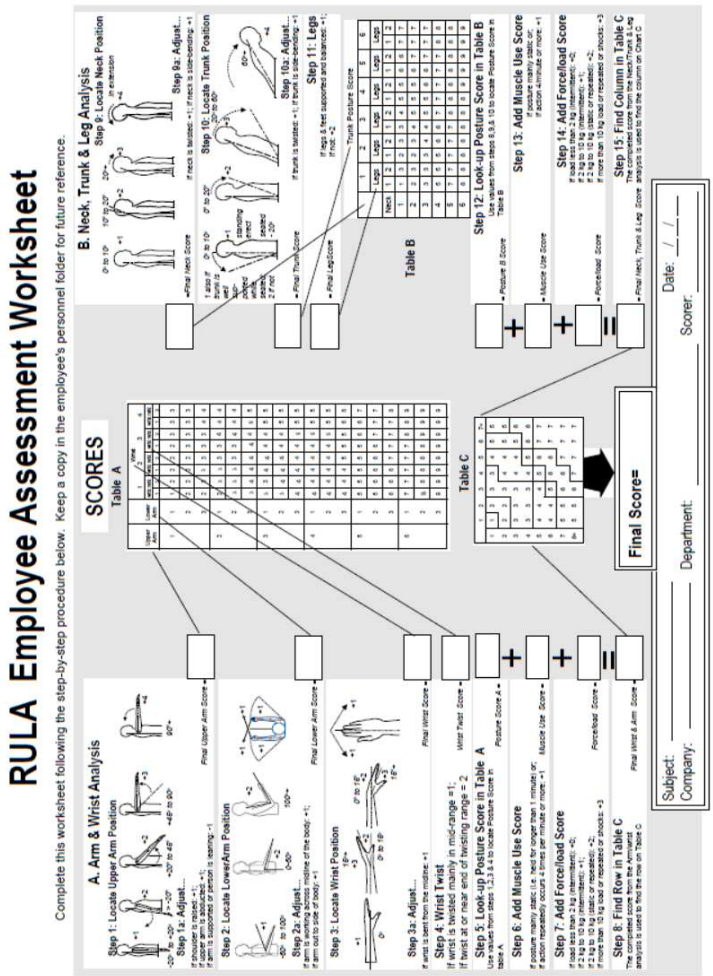

Appendix F

Participants in the Ergonomics Evaluation Tests

Group	*Name*	*Male / Female*	*Right-Handed / Left-Handed*	*Experience in laparoscopy*	*Experience in surgical robotics*	*Video games*	*Instruments order*
Students	Participant01	Female	Right-Handed	0	0		Test interrupted
Students	Participant02	Male	Left-Handed	0	0		Test interrupted
Students	Participant03	Male	Right-Handed	0	0	+++	Fixed, Free Joint
Students	Participant04	Male	Right-Handed	0	0	+++	Free Joint,Fixed
Students	Participant05	Male	Right-Handed	0	0	+++	Fixed, Free Joint
Students	Participant06	Male	Right-Handed	0	0	++	Free Joint,Fixed
Students	Participant07	Male	Right-Handed	0	0	+++	Fixed, Free Joint
Students	Participant08	Male	Right-Handed	0	0	++	Free Joint,Fixed
Surgeons	Participant09	Male	Right-Handed	+++	AESOP	0	Fixed, Free Joint
Surgeons	Participant10	Female	Right-Handed	+++	AESOP	0	Free Joint, Fixed
Surgeons	Participant11	Male	Left-Handed	+++	AESOP	+	Fixed, Free Joint
Surgeons	Participant12	Male	Right-Handed	+++	AESOP	0	Free Joint, Fixed
Surgeons	Participant13	Male	Right-Handed	+	Da Vinci +++	0	Fixed, Free Joint
Surgeons	Participant14	Female	Right-Handed	+++	AESOP	0	Free Joint, Fixed
Surgeons	Participant15	Male	Right-Handed	++	Da Vinci +-	+++	Fixed, Free Joint
Surgeons	Participant16	Female	Right-Handed	+	Simulateurs +-	0	Free Joint, Fixed
Surgeons	Participant17	Male	Right-Handed	+	Simulateurs +	+	Fixed, Free Joint
Surgeons	Participant18	Male	Right-Handed	++	Da Vinci +++	+	Free Joint, Fixed

Bibliography

[Ahmed 2004] S. Ahmed, G. B. Hanna and A. Cuschieri. *Optimal Angle Between Instrument Shaft and Handle for Laparoscopic Bowel Suturing.* Archives of Surgery, vol. 139, pages 89–92, 2004. 79

[Ballantyne 2004] G.H. Ballantyne, J. Marescaux and P.C. Giulianotti. Primer of robotic and telerobotic surgery. Lippincott Williams & Wilkins, 2004. 5

[Baron 2007] T.H. Baron. *Natural orifice transluminal endoscopic surgery.* The British Journal of Surgery, vol. 94, pages 1–2, January 2007. 15

[Bellicoso] D. Bellicoso and M. Caputano. Dama robotics symbolic toolbox for matlab. http://www.damarob.altervista.org. 125

[Berguer 1997] R. Berguer, G. T. Rab, H. Abu-Ghaida, A. Alarcon and J. Chung. *A comparison of surgeons posture during laparoscopic and open surgical procedures.* Surgical Endoscopy, vol. 11, pages 139–142, 1997. 79

[Berguer 1998] R. Berguer. *Surgical technology and the ergonomics of laparoscopic instruments.* Surgical Endoscopy, vol. 12, pages 458–462, 1998. 79

[Berguer 1999] R. Berguer, D. L. Forkey and W. D. Smith. *Ergonomic problems associated with laparoscopic surgery.* Surgical Endoscopy, vol. 13, pages 466–468, 1999. 79

[Berguer 2001] R. Berguer, W. Smith and Y. Chung. *Performing laparoscopic surgery is significantly more stressful for the surgeon than open surgery.* Surgical Endoscopy, vol. 15, pages 1204–1207, 2001. 79

[Berguer 2006] R. Berguer. *Ergonomics in Laparoscopic Surgery.* The Sages Manual, pages 454–464, 2006. 56, 68, 79, 81

[Brown 2004] Jeffrey D. Brown, Jacob Rosen, Lily Chang, Mika N. Sinanan and Blake Hannaford. *J.D. Brown- Quantifying Surgeon Grasping Mechanics in Laparoscopy Quantifying Surgeon Grasping Mechanics in Laparoscopy Using the Blue DRAGON System*, 2004. 27

[Bruyns 2002] C. Bruyns and M. Ottensmeyer. *Measurements of Soft-Tissue Mechanical Properties to Support Development of a Physically Based Virtual Animal Model.* Proceedings of MICCAI '02, pages 282–289, 2002. 58

[Buess 1989] G. Buess, A. Melzer and A. Cuschieri. *Instruments for endoscopic surgery.* Operative manual of endoscopic surgery - Springer-Verlag, pp. 15, 1989. 4

[Cao 1996] C. G. L. Cao, C. L. Mackenzie and S. Payandeh. *Task And Motion Analyses In Endoscopic Surgery.* Proceedings of the 5th Annual Symposium on Haptic Interfaces for Virtual Environment and Teleoperator Systems, pages 583–590, 1996. 39, 82

[Chedmail 1990] P. Chedmail and M. Gautier. *Optimum choice of robot actuators.* Journal of engineering for industry, vol. 112, no. 4, pages 361–367, 1990. 67

[Chen 1996] E. J. Chen, J. Novakofski, W. K. Jenkins and W. D. O'Brien Jr. *Young's modulus measurements of soft tissues with application to elasticity imaging.* Ultrasonics, Ferroelectrics and Frequency Control, IEEE Transactions on, vol. 43, no. 1, pages 191–194, Jan 1996. 58

[Cho 2010] Min-Soo Cho, Byung Min, Young-Ki Hong and Woo-Jung Lee. *Single-site versus conventional laparoscopic appendectomy: comparison of short-term operative outcomes.* Surgical Endoscopy, pages 1–5, 2010. 20

[Cuschieri 1995] A. Cuschieri. *Whither minimal access surgery: tribulations and expectations.* American Journal of Surgery, vol. 169, pages 9–19, 1995. 56, 68, 79, 81

[Dakin 2003] G.F. Dakin and M. Gagner. *Comparison of laparoscopic skills performance between standard instruments and two surgical robotic systems.* Surgical Endoscopy, vol. 17, no. 4, pages 574–579, 2003. 69

[Dario 2000] P. Dario, M. C. Carrozza, M. Marcacci, S. D'Attanasio, B. Magnani, O. Tonet and G. Megali. *A novel mechatronic tool for computer-assisted arthroscopy.* IEEE Trans. Inform. Technol. Biomed., vol. 4, pages 15–29, January 2000. 22

[Dario 2003] P. Dario, B. Hannaford and A. Menciassi. *Smart surgical tools and augmenting devices.* IEEE Transactions on Robotics and Automation, vol. 19, no. 5, pages 782–792, October 2003. 13, 22

[D'Attanasio 2002] S. D'Attanasio, O. Tonet, G. Megali, M. C. Carrozza and P. Dario. *A semi-authomatic hand-held mechatronic endoscope with collision avoidance capabilities.* Proceedings of IEEE International Conference on Robotics and Automation, pages 1586–1591, 2002. 22

[De Sars 2010] V. De Sars, S. Haliyo and J. Szewczyk. *A practical approach to the design and control of active endoscopes.* Mechatronics, vol. 20, no. 2, pages 251 – 264, 2010. 22

[De 2007] S. De, J. Rosen, A. Dagan, B. Hannaford, P. Swanson and M. Sinanan. *Assessment of Tissue Damage due to Mechanical Stresses.* The International Journal of Robotics Research, vol. 26, no. 11–12, pages 1159–1171, 2007. 58

[Delignieres 1987] S. Delignieres. *The morphology choice of robots.* 1987. 67

[Derossis 1998] A. M. Derossis, G. M. Fried, M. Abrahamowicz, H. H. Sigman, J. S. Barkun and J. L. Meakins. *Development of a model for training and evaluation of laparoscopic skills.* American Journal of Surgery, vol. 175, pages 482–487, 1998. 39, 82

[DiMartino 2004] Allison DiMartino, Kathryn Doné, Timothy Judkins, Jonathan Morse, Jennifer Melander, Dmitry Oleynikov and M. Susan Hallbeck. *Ergonomic Laparoscopic Tool Handle Design.* PROCEEDINGS of the HUMAN FACTORS AND ERGONOMICS SOCIETY 48th ANNUAL MEETING, pages 1354–1358, 2004. 17

[Doné 2003] Kathryn Doné, Shinya Takahashi, Andrew Nickel, Xuedong Ding and Susan Hallbeck. *How should trackball directional movement intuitively relate to an end effector?* PROCEEDINGS of the HUMAN FACTORS AND ERGONOMICS SOCIETY 47th ANNUAL MEETING, pages 1122–1125, 2003. 17

[Emam 2001] T. Emam, T. Frank, G. Hanna and A. Cuschieri. *Influence of handle design on the surgeon's upper limb movements, muscle recruitment, and fatigue during endoscopic suturing.* Surgical Endoscopy, vol. 15, pages 667–672, 2001. 79

[Feldman 2004] L. S. Feldman, S. E. Hagarty, G. Ghitulescu, D. Stanbridge and G.M. Fried. *Relationship between objective assessment of technical skills and subjective in-training evaluations in surgical residents.* Journal of the American College of Surgeons, vol. 198, pages 105–110, 2004. 39

[Feng 2008] C. Feng, J. W. Rozenblit and A. Hamilton. *Fuzzy Logic-Based Performance Assessment in the Virtual, Assistive Surgical Trainer (VAST).* Proceedings of the 15th Annual IEEE International Conference and Workshop on the Engineering of Computer Based Systems, pages 203–209, 2008. 87

[Gallagher 2001] Anthony G. Gallagher, Karen Richie, Neil McClure and Jim McGuigan. *Objective Psychomotor Skills Assessment of Experienced, Junior, and Novice Laparoscopists with Virtual Reality.* World Journal of Surgery, vol. 25, no. 11, pages 1478–1483, November 2001. 58

[Gielen 1997] C.C.A.M. Gielen, E.J. Vrijenhoek, T. Flash and S.F.W. Neggers. *Arm Position Constraints During Pointing and Reaching in 3-D Space.* The Journal of Neurophysiology, vol. 78, no. 2, pages 660–673, 1997. 63

[Gopura 2009] R.A.R.C. Gopura and K. Kiguchi. *Mechanical designs of active upper-limb exoskeleton robots: State-of-the-art and design difficulties.* In IEEE International Conference onRehabilitation Robotics, ICORR 2009., pages 178–187, 2009. 86

[Gossot 2001] D. Gossot and G. Lange. *Deflectable and rotatable endoscopic instrument with intuitive control.* Minimally Invasive Therapy & Allied Technologies, vol. 10, no. 6, pages 295–299, 2001. 16

[Guthart 2000] G.S. Guthart and J.K. Jr. Salisbury. *The Intuitive telesurgery system: overview and application.* Proceedings of IEEE International Conference on Robotics and Automation, vol. 1, pages 618–621, 2000. viii, 54

[Hallbeck 2005] M. S. Hallbeck, D. Oleynikov, K. Doné, T. Judkins, A. DiMartino, J. Morse and L. N. Verner. *Ergonomic handle and articulating laparoscopic tool.* United States Patent Application # US 2005/0187575 A1, August 2005. 17, 50, 109

[Hance 2005] J. Hance, R. Aggarwal, K. Moorthy, Y. Munz, S. Undre and A. Darzi. *Assessment of psychomotor skills acquisition during laparoscopic cholecystectomy courses.* American Journal of Surgery, vol. 190, pages 507–511, 2005. 39

[Hashizume 2002] M. Hashizume, M. Shimada, M. Tomikawa, Y. Ikeda, I. Takahashi, R. Abe, F. Koga, N. Gotoh, K. Konishi, S. Maehara

and K. Sugimachi. *Early experiences of endoscopic procedures in general surgery assisted by a computer-enhanced surgical system.* Surgical endoscopy, vol. 16, no. 8, pages 1187–1191, August 2002. 5

[Hassan Zahraee 2010] A. Hassan Zahraee, J. K. Paik, J. Szewczyk and G. Morel. *Towards the Development of a Hand-Held Surgical Robot for Laparoscopy.* IEEE/ASME Transactions on Mechatronics, vol. 15, no. 6, pages 853–861, 2010. 110

[Hinman 2007] C. D. Hinman and D. J. Danitz. *Tool with rotation lock.* United States Patent Application # US 2007/0287993 A1, December 2007. vii, 15, 17, 50

[Horgan 2009] S. Horgan, J. Cullen, M. Talamini, Y. Mintz, A. Ferreres, G. Jacobsen, B. Sandler, J. Bosia, T. Savides, D. Easter, M. Savu, S. Ramamoorthy, E. Whitcomb, S. Agarwal, E. Lukacz, G. Dominguez and P. Ferraina. *Natural orifice surgery: initial clinical experience.* Surgical Endoscopy, vol. 23, pages 1512–1518, 2009. 18

[Hubens 2003] G. Hubens, H. Coveliers, L. Balliu, M. Ruppert and W. Vaneerdeweg. *A performance study comparing manual and robotically assisted laparoscopic surgery using the da Vinci system.* Surgical Endoscopy, vol. 17, no. 10, pages 1595–1599, 2003. 5

[Jinno 2002] Makoto Jinno, Nobuto Matsuhira, Takamitsu Sunaoshi, Takehiro Hato, Toyomi Miyagawa, Yasuhide Morikawa, Toshiharu Furukawa, Soji Ozawa, Masaki Kitajima and Kazuo Nakazawa. *Development of a Master Slave Combined Manipulator for Laparoscopic Surgery.* In Takeyoshi Dohi and Ron Kikinis, editeurs, Medical Image Computing and Computer-Assisted Intervention MICCAI 2002, volume 2488 of *Lecture Notes in Computer Science*, pages 52–59. Springer Berlin / Heidelberg, 2002. vii, viii, 5, 24, 26, 49, 57

[Jinno 2008] M. Jinno, T. Sunaoshi and S. Omori. *Manipulator and control method therefor.* United States Patent Application # US 2008/0245175 A1, Terumo Kabushiki Kaisha, Tokyo (JP) and Kabushiki Kaisha Toshiba, Tokyo (JP), October 2008. vii, 9

[Kersten 1994] D. Kersten, P. Mamassian and D.C. Knill. *Moving Cast Shadows and the Perception of Relative Depth.* 1994. 41

[Khalil 2002] W. Khalil and E. Dombre. Modelisation, identification and control of robots. Hermes Penton Science, London, 2002. 67

[Kode 2007] V.R.C. Kode and M.C. Cavusoglu. *Design and Characterization of a Novel Hybrid Actuator Using Shape Memory Alloy and DC Micromotor for Minimally Invasive Surgery Applications*. Mechatronics, IEEE/ASME Transactions on, vol. 12, no. 4, pages 455–464, Aug. 2007. 103

[Kundhal 2009] Pavi Kundhal and Teodor Grantcharov. *Psychomotor performance measured in a virtual environment correlates with technical skills in the operating room*. Surgical Endoscopy, vol. 23, pages 645–649, 2009. 33

[Lai 2000] F. Lai and R.D. Howe. *Evaluating control modes for constrained robotic surgery*. Proceedings of IEEE International Conference on Robotics and Automation, vol. 1, pages 603–609, April 2000. vii, 4, 49

[Law 2004] Benjamin Law, M. Stella Atkins, A. E. Kirkpatrick and Alan J. Lomax. *Eye gaze patterns differentiate novice and experts in a virtual laparoscopic surgery training environment*. In ETRA '04: Proceedings of the 2004 symposium on Eye tracking research & applications, pages 41–48, New York, NY, USA, 2004. ACM. 58

[Lee 2009] W. Lee and A. Chamorro. *Surgical Instrument*. United States Patent # US 7615067 B2, Cambridge Endoscopic Devices, Inc., Framingham, MA (US), November 2009. 18

[Ma 2003] N. Ma and G. SONG. *Control of shape memory alloy actuator using pulse width modulation*. Smart materials and structures, vol. 12, no. 5, pages 712–719, 2003. 102

[Maithel 2006] S. Maithel, R. Sierra, J. Korndorffer, P. Neumann, S. Dawson, M. Callery, D. Jones and D. Scott. *Construct and face validity of MIST-VR, Endotower, and CELTS*. Surgical Endoscopy, vol. 20, pages 104–112, 2006. 33

[Marczyk 2008] S. Marczyk. *Surgical instrument with articulating tool assembly*. United States Patent Application # US 2008/0083811 A1, April 2008. 19

[Martin 1997] J. A. Martin, G. Regehr, R. Reznick, H. Macrae, J. Murnaghan, C. Hutchison and M. Brown. *Objective structured assessment of technical skill (OSATS) for surgical residents*. vol. 84, no. 2, pages 273–278, 1997. 33

[Matern 1999] U. Matern and P. Waller. *Instruments for minimally invasive surgery: principles of ergonomic handles.* Surgical Endoscopy, vol. 13, pages 174–182, 1999. viii, 80

[Mathis 2007] Kellie L. Mathis and Douglas A. Wiegmann. *Construct Validation of a Laparoscopic Surgical Simulator.* Simulation In Healthcare, vol. 2, pages 178–182, 2007. 31

[McAtamney 1993] L. McAtamney and E. N. Corlett. *RULA: a survey method for the investigation of work-related upper limb disorders.* Applied Ergonomics, vol. 24, pages 91–99, 1993. 84

[Med 2009] Mosby's Medical Dictionary, 8th Ed., 2009. 32

[Melzer 1997] A. Melzer, K. Kipfmüller and B. Halfar. *Deflectable endoscopic instrument system DENIS.* Surgical Endoscopy, vol. 11, pages 1045–1051, 1997. 16

[México 2004] Querétaro México and Toshiyuki Hino. *Development of a Miniature Robot Finger with a Variable Stiffness Mechanism using Shape Memory.* International Simposium on Robotics and Automation, August 2004. 102

[Mishra 2008] S. K. Mishra, A. Ganpule, A. Kurien, V. Muthu and M. R. Desai. *Task completion time: Objective tool for assessment of technical skills in laparoscopic simulator for urology trainees.* Indian J Urol., vol. 24, no. 1, pages 35–38, Jan–Mar 2008. 69

[Najmaldin 1998] A. Najmaldin and P. Guillou. A guide to laparoscopic surgery. Blackwell Science, Oxford, 1998. 2, 3

[Nakamura 2000] Ryoichi Nakamura, Etsuko Kobayashi, Ken Masamune, Ichiro Sakuma, Takeyoshi Dohi, Naoki Yahagi, Takayuki Tsuji, Daijo Hashimoto, Mitsuo Shimada and Makoto Hashizume. *Multi-DOF Forceps Manipulator System for Laparoscopic Surgery.* In Scott Delp, Anthony DiGoia and Branislav Jaramaz, editeurs, Medical Image Computing and Computer-Assisted Intervention MICCAI 2000, volume 1935 of *Lecture Notes in Computer Science.* Springer Berlin / Heidelberg, 2000. vii, 23

[Nakamura 2001] Ryoichi Nakamura, Takeshi Oura, Etsuko Kobayashi, Ichiro Sakuma, Takeyoshi Dohi, Naoki Yahagi, Takayuki Tsuji, Mitsuo Shimada and Makoto Hashizume. *Multi-DOF Forceps Manipulator System for Laparoscopic Surgery Mechanism Miniaturized & Evaluation*

of New Interface -. In Wiro Niessen and Max Viergever, editeurs, Medical Image Computing and Computer-Assisted Intervention MICCAI 2001, volume 2208 of *Lecture Notes in Computer Science*, pages 606–613. Springer Berlin / Heidelberg, 2001. vii, 24

[Nguyen 2001] N. T. Nguyen, H. S. Ho, W.D. Smith, C. Philipps, C. Lewis, R.M.D. Vera and R. Berguer. *An ergonomic evaluation of surgeons' axial skeletal and upper extremity movements during laparoscopic and open surgery.* The American Journal of Surgery, vol. 182, pages 720–724, 2001. 79

[Oleynikov 2006] D. Oleynikov, B. Solomon and M. S. Hallbeck. *Effect of Visual Feedback on Surgical Performance Using the da Vinci Surgical System.* Journal of Laparoendoscopic & Advanced Surgical Techniques, vol. 16, no. 5, 2006. 58

[Peirs 2002] J. Peirs, H. Van Brussel, D. Reynaerts and G. De Gersem. *A Flexible Distal Tip with Two Degrees of Freedom for Enhanced Dexterity in Endoscopic Robot Surgery.* The 13th Micromechanics Europe Workshop, pages 271–274, 2002. 102

[Person 2001] J. Person, A. Hodgson and A. Nagy. *Automated high frequency posture sampling for ergonomic assessment of laparoscopic surgery.* Surgical Endoscopy, vol. 15, pages 997–1003, 2001. 79, 84

[Piccigallo 2008] Marco Piccigallo, Francesco Focacci, Oliver Tonet, Giuseppe Megali, Claudio Quaglia and Paolo Dario. *Hand-held robotic instrument for dextrous laparoscopic interventions.* The international journal of medical robotics + computer assisted surgery : MRCAS, vol. 4, no. 4, pages 331–338, 2008. vii, 27, 28

[Podhorodeski 1989] R. P. Podhorodeski. New approaches for the solution of inverse instantaneous kinematic problems and of contact forces in multiple contact grasping. Ph.D. Dissertation, University of Toronto, 1989. 73

[Podhorodeski 2000] R. P. Podhorodeski, S. B. Nokleby and J. D. Wittchen. *Resolving velocity-degenerate configurations (singularities) of redundant manipulators.* In DETC2000 Proceedings, ASME International Design Engineering Technical Conference and Computers and Information in Engineering Conference series, pages 1–10. ASME, Sep 2000. 73

[Rao 2004] G.V. Rao, M.J. Mansard, P.K. Ravula1, P. Rebala1, R.R. Dama and D.N. Reddy. *Single-port surgery: Current applications and limitations*. Asian Journal of Endoscopic Surgery, vol. 2, pages 56–64, 2004. 15

[Ravi 2004] P. Kiran Ravi, P. Delaney Conor, A.J. Senagore, B.L. Millward and V.W. Fazio. *Operative Blood loss and use of Blood products after laparoscopic and conventional open colorectal operations*. Archives of surgery, vol. 139, no. 1, pages 39–42, 2004. 3

[Raybourn 2010] James H. Raybourn, Abhay Rane and Chandru P. Sundaram. *Laparoendoscopic Single-site Surgery for Nephrectomy as a Feasible Alternative to Traditional Laparoscopy*. Urology, vol. 75, pages 100–103, January 2010. 18

[Reilly 2008] Michael Reilly. *A Wii warm-up hones surgical skills*. The New Scientist, vol. 197, no. 2639, page 24, January 2008. 58

[Reuters 2007] Reuters. *Novare Announces Completion of 100th Single Port Laparoscopic Procedure Using Real-Hand*. http://www.reuters.com/article/idUS189926+18-Dec-2007+PRN20071218, December 2007. 18

[Richards 2000] C. Richards, J. Rosen, B. Hannaford, C. Pellegrini and M. Sinanan. *Skills evaluation in minimally invasive surgery using force/torque signatures*. Surgical Endoscopy, vol. 14, pages 791–798, 2000. 27

[Röse 2006] Andreas Röse, T. A. Kern, D. Eicher, B. Schemmer and Helmut F. Schlaak. *INKOMAN - An intracorporal manipulator for minimally invasive surgery*, January 2006. vii, 26, 27

[Röse 2009a] A. Röse, C. Wohlleber, S. Kassner, H.F. Schlaak and R. Werthschutzky. *A novel piezoelectric driven laparoscopic instrument with multiple degree of freedom parallel kinematic structure*. pages 2162–2167, oct. 2009. 26

[Röse 2009b] Andreas Röse and H. F. Schlaak. *A parallel kinematic mechanism for highly flexible laparoscopic instruments*. In Jos Sloten, Pascal Verdonck, Marc Nyssen and Jens Haueisen, editeurs, 4th European Conference of the International Federation for Medical and Biological Engineering, volume 2 of *IFMBE Proceedings*, pages 903–906. Springer Berlin Heidelberg, 2009. 27

[Rosen 2002a] J. Rosen, J. D. Brown, M. Barreca, L. Chang, B. Hannaford and B. Sinanan. *The Blue DRAGON - A System for Monitoring the Kinematics and the Dynamics of Endoscopic Tools in Minimally Invasive Surgery for Objective Laparoscopic Skill Assessment.* In Studies in Health Technology and Informatics - Medicine Meets Virtual Reality, volume 85, pages 412–418. IOS Press, 2002. 58

[Rosen 2002b] J. Rosen, J. D. Brown, M. Barreca, L. Chang, B. Hannaford and B. Sinanan. *The Blue DRAGON - A System for Monitoring the Kinematics and the Dynamics of Endoscopic Tools in Minimally Invasive Surgery for Objective Laparoscopic Skill Assessment.* vol. 85, pages 412–418, 2002. 103

[Rosen 2006] J. Rosen, J. Brown, L. Chang and B. Hannaford. *Generalized approach for modeling minimally invasive surgery as a stochastic process using a discrete markov model.* IEEE Transactions in Biomedical Engineering, vol. 53, no. 3, pages 399–413, 2006. 58

[Rosser 2007] J. C. Rosser, P. J. Lynch, L. Cuddihy, J. Gentile D. A. Klonsky and R. Merrell. *The Impact of Video Games on Training Surgeons in the 21st Century.* Archives of Surgery, vol. 142, no. 2, pages 181–186, 2007. 58

[Salkini 2010] M.W. Salkini, C.R. Doarn, N. Kiehl, T.J. Broderick, J.F. Donovan and K. Gaitonde. *The Role of Haptic Feedback in Laparoscopic Training Using the LapMentor II.* vol. 24, no. 1, 2010. 33

[Satava 2003] R.M. Satava, A. Cuschieri and J. Hamdorf. *Metrics for objective Assessment.* Surgical Endoscopy, vol. 17, pages 220–226, 2003. 85

[Schijven 2002] M. Schijven, J. Jakimowicz and C. Schot. *The Advanced Dundee Endoscopic Psychomotor Tester (ADEPT) objectifying subjective psychomotor test performance.* Surgical Endoscopy, vol. 16, pages 943–948, 2002. 39

[Schijven 2003] M. Schijven and J. Jakimowicz. *Construct validity: Experts and novices performing on the Xitact LS500 laparoscopy simulator.* Surgical endoscopy, vol. 17, pages 803–810, 2003. 33

[Schneider 2003] A. Schneider, C. Altgassen, H. Hertel, R. Tozzi and C. Koehler. *Advantages of Laparoscopy.* International Journal of Gynecological Cancer, vol. 13, page 121, 2003. 3

[Schwarz 2005] K. M. Schwarz, M. O. Schurr and G. F. Buesz. *Surgical instrument for minimally invasive surgical interventions*. United States Patent # US 6,913,613 B2, Tuebingen Scientific Surgical Products GmbH, Tuebingen (DE), July 2005. 18

[Shussman 2010] Noam Shussman, Avraham Schlager, Ram Elazary, Abed Khalaileh, Andrei Keidar, Mark Talamini, Santiago Horgan, Avraham Rivkind and Yoav Mintz. *Single-incision laparoscopic cholecystectomy: lessons learned for success*. Surgical Endoscopy, pages 1–4, 2010. 20

[Soechting 1995] J.F. Soechting, C.A. Buneo, U. Herrmann and M. Flanders. *Moving effortlessly in three dimensions: does Donders' law apply to arm movement?* Journal of Neuroscience, vol. 15, pages 621–6280, 1995. 63

[Staniisic 2000] M. M. Staniisic. Advances in robot kinematics. Kluwer Academic Publishers, Norwell, MA, USA, 2000. 73

[Stolzenburg 2010] J.U. Stolzenburg, P. Kallidonis, M.A. Oh, N. Ghulam, M. Do, T. Haefner, A. Dietel, H. Till, G. Sakellaropoulos and E.N. Liatsikos. *Comparative Assessment of Laparoscopic Single-Site Surgery Instruments to Conventional Laparoscopic in Laboratory Setting*. Journal of Endourology, vol. 24, pages 239–245, February 2010. 20

[Suzuki 2005] Takashi Suzuki, Youichi Katayama, Etsuko Kobayashi and Ichiro Sakuma. *Compact Forceps Manipulator Using Friction Wheel Mechanism and Gimbals Mechanism for Laparoscopic Surgery*. In James Duncan and Guido Gerig, editeurs, Medical Image Computing and Computer-Assisted Intervention MICCAI 2005, volume 3750 of *Lecture Notes in Computer Science*, pages 81–88. Springer Berlin / Heidelberg, 2005. 24

[Tendick 1997] F. Tendick and M. C. Cavusoglu. *Human-machine interfaces for minimally invasive surgery*. Proc. of the 19th Annual International Conference of the IEEE Engineering in Medicine and Biology Society, pages 2771–2776, 1997. 80

[Tonet 2006] Oliver Tonet, Francesco Focacci, Marco Piccigallo, Filippo Cavallo, Miyuki Uematsu, Giuseppe Megali and Paolo Dario. *Comparison of Control Modes of a Hand-Held Robot for Laparoscopic Surgery*. In Rasmus Larsen, Mads Nielsen and Jon Sporring, editeurs, Medical Image Computing and Computer-Assisted Intervention MICCAI 2006, Lecture Notes in Computer Science, pages 429–436. Springer Berlin / Heidelberg, 2006. 49

[Torres Bermudez 2009] J. Torres Bermudez, G. Buess, M. Waseda, I. Gacek, F. Becerra Garcia, G. Manukyan and N. Inaky. *Laparoscopic intracorporal colorectal sutured anastomosis using the Radius Surgical System in a phantom model.* Surgical Endoscopy, vol. 23, pages 1624–1632, 2009. 19

[Tuijthof 2003] G.J.M. Tuijthof, S.J.M.P. van Engelen, J.L. Herder, R.H.M. Goossens, C.J. Snijders and C.N. van Dijk. *Ergonomic handle for an arthroscopic cutter.* Minimally Invasive Therapy & Allied Technologies, vol. 12, no. 1-2, pages 82–90, 2003. 16, 17

[Van Dongen 2007] K. Van Dongen, E. Tournoij, D. van der Zee, M. Schijven and I. Broeders. *Construct validity of the LapSim: Can the LapSim virtual reality simulator distinguish between novices and experts?* Surgical Endoscopy, vol. 21, pages 1413–1417, 2007. 33

[Vereczkei 2004] A. Vereczkei, H. Feussner, T. Negele, F. Fritzsche, T. Seitz, H. Bubb and O. P. Horvath. *Ergonomic assessment of the static stress confronted by surgeons during laparoscopic cholecystectomy.* Surgical Endoscopy, vol. 18, pages 1118–1122, 2004. 79

[Wauben 2006] L. Wauben, M. van Veelen, D. Gossot and R. Goossens. *Application of ergonomic guidelines during minimally invasive surgery: a questionnaire survey of 284 surgeons.* Surgical Endoscopy, vol. 20, pages 1268–1274, 2006. 79

[Website 2007] Novare Surgical Website. *Single Port Surgery.* http://www.novaresurgical.com/physicians/single-port-surgery, 2007. vii, 16, 18

[Whitney 1969] D. E. Whitney. *Resolved Motion Rate Control of Manipulators and Human Prostheses.* IEEE Transactions on Man Machine Systems, vol. 10, no. 2, pages 47–53, 1969. 73

[Wong 2010] Kenneth K.Y. Wong, Patrick H.Y. Chung, Lawrence C.L. Lan, Ivy H.Y. Chan and Paul K.H. Tam. *The first report of a single-port laparoscopic nephrectomy in a child.* Hong Kong Medical Journal, vol. 16, April 2010. 18

[Yamaguchi 2007] Shohei Yamaguchi, Kozo Konishi, Takefumi Yasunaga, Daisuke Yoshida, Nao Kinjo, Kiichiro Kobayashi, Satoshi Ieiri, Ken Okazaki, Hideaki Nakashima, Kazuo Tanoue, Yoshihiko Maehara and Makoto Hashizume. *Construct validity for eyehand coordination skill*

on a virtual reality laparoscopic surgical simulator. Surgical Endoscopy, vol. 21, pages 2253–2257, 2007. 32

[Yamashita 2003] H. Yamashita, D. Kim, N. Hata and T. Dohi. *Multi-slider linkage mechanism for endoscopic forceps manipulator*. Proceedings of IEEE/RSJ International Conference on Intelligent Robots and Systems, vol. 3, pages 2577–2582, 2003. vii, 24, 25

[Yamashita 2004] Hiromasa Yamashita, Nobuhiko Hata, Makoto Hashizume and Takeyoshi Dohi. *Handheld Laparoscopic Forceps Manipulator Using Multi-slider Linkage Mechanisms*. In Christian Barillot, David R. Haynor and Pierre Hellier, editeurs, Medical Image Computing and Computer-Assisted Intervention MICCAI 2004, volume 3217 of *Lecture Notes in Computer Science*, pages 121–128. Springer Berlin / Heidelberg, 2004. 24

List of Publications

Patent

1. A. Hassan Zahraee and J. Szewczyk. *Surgical instrument specially for peritoneal surgery.* Patent Application in France no. FR 1055254, submitted in July 2010.

Journal Papers

1. A. Hassan Zahraee, J.K. Paik, J. Szewcyzk and G. Morel. *Towards the Development of a Hand-Held Surgical Robot for Laparoscopy.* IEEE/ASME Transactions on Mechatronics, Vol. 15, no. 6, pp. 853-861, Dec. 2010.

2. J.F. Menudet, A. Hassan-Zahraee, B. Solano, J. Szewczyk, B. Herman, C. Rotinat, C. Vidal and B. Gayet. *ID2U Project: Single use dexterous surgical instrument.* IRBM, Vol. 32, no. 3, pp. 169-171, June 2011.

Conference Papers

1. A. Hassan Zahraee, J. Szewczyk and G. Morel. *Evaluating Control Modes for Hand-Held Robotic Surgical Instrument Using Virtual Reality Simulator.* IEEE/ASME International Conference on Advanced Intelligent Mechatronics (AIM'09), Jul. 14-17, 2009, Singapore, pp. 1946 - 1951.

2. A. Hassan Zahraee, J. Szewczyk and G. Morel. *Simulation for Optimal Design of Surgical Robots.* Annual International Conference of the IEEE Engineering in Medicine and Biology Society, Sep. 2-6, 2009, Minneapolis, Minnesota, USA. EMBC 2009. pp. 273-279.

3. A. Hassan Zahraee, J.K. Paik, J. Szewcyzk and G. Morel. *Robotic Hand-Held Surgical Device : Evaluation of End-Effector's Kinematics and Development of Proof-of-Concept Prototypes.* International Conference on Medical Image Computing and Computer Assisted Intervention (MICCAI'10), Sep. 20-24, 2010, Beijing, China. Lecture Notes in Computer Science, 2010, Volume 6363/2010, pp. 432-439, Springer Berlin / Heidelberg.

4. A. Hassan Zahraee, B. Herman and J. Szewczyk. *Mechatronic Design of a Hand-Held Instrument with Active Trocar for Laparoscopy.* IEEE International Conference on Robotics & Automation (ICRA'11), May 9-13, 2011, Shanghai, China.

5. B. Herman, A. Hassan Zahraee, J. Szewczyk., G. Morel, C. Bourdin, J.L. Vercher and B. Gayet. *Ergonomic and gesture performance of robotized instruments for laparoscopic surgery.* IEEE/RSJ International Conference on Intelligent Robots and Systems (IROS2011), September 25-30, 2011, San Francisco, CA.